ASSESSING THE IMPACT OF CLIMATE-INDUCED VEGETATION CHANGES ON SOIL ORGANIC MATTER COMPOSITION

A Thesis Submitted to the College of Graduate Studies and Research
in Partial Fulfillment of the Requirements
for the Degree of Master of Science
in the Department of Soil Science
University of Saskatchewan
Saskatoon, SK, Canada

By
Kendra Nicole Purton

PERMISSION TO USE

In presenting this thesis in partial fulfillment of the requirements for a Postgraduate degree from the University of Saskatchewan, I agree that the Libraries of this University may make it freely available for inspection. I further agree that permission for copying of this thesis in any manner, in whole or in part, for scholarly purposes may be granted by the professor or professors who supervised my thesis work or, in their absence, by the Head of the Department or the Dean of the College in which my thesis work was done. It is understood that any copying, publication, or use of this thesis or parts thereof for financial gain shall not be allowed without my written permission. It is also understood that due recognition shall be given to me and to the University of Saskatchewan in any scholarly use that may be made of any material in my thesis. Requests for permission to copy or to make other uses of materials in this thesis, in whole or part, should be addressed to:

Head, Department of Soil Science
College of Agriculture and Bioresources
University of Saskatchewan
51 Campus Dr.
Saskatoon, SK
Canada, S7N 5A8

DISCLAIMER

Reference in this thesis to any commercial product, process, or service by trade name, trademark, manufacturer, or otherwise, does not constitute or imply its endorsement, recommendation, or favoring by the University of Saskatchewan. The views and opinions of the author expressed herein do not state or reflect those of the University of Saskatchewan, and shall not be used for advertising or product endorsement purposes.

ABSTRACT

Despite the importance of soil organic matter (SOM) in C storage and provision of ecosystem services, the magnitude and direction of the response of SOM to climate change remains debated. Particularly contested is the role of biochemical recalcitrance in determining the biological stability of SOM, which in turn, may also vary with climate. Employing a climosequence study design controlling for confounding pedogenic factors, the research described in this thesis aimed to uncover the response of both SOM chemistry and SOM biological stability to changes in climate and associated land use shifts at the grassland-forest ecotone in west-central Saskatchewan. Characterization of SOM chemistry was achieved using two advanced analytical techniques: X-ray absorption near edge structure (XANES) spectroscopy and pyrolysis-field ionization mass spectrometry (Py-FIMS). Agreements between XANES and Py-FIMS revealed only minor differences in SOM chemistry resulting from a 0.7 °C mean annual temperature (MAT) gradient and associated broad differences in land use, but revealed a clear influence of depth within soil profiles. In contrast, long-term aerobic incubations revealed that biological stability of SOM varied with both climate and climate-induced differences in land use, but was not largely influenced by depth. Together, these findings suggest a decoupling of SOM chemistry and its biological stability, indicating that factors other than biochemical recalcitrance are the primary drivers of SOM persistence in these soils.

ACKNOWLEDGEMENTS

I am immensely grateful for the support and encouragement from my supervisors, Drs. Dan Pennock and Fran Walley, as well as their financial support and guidance throughout my M.Sc. program. I would like to thank my advisory committee, Drs. Derek Peak and Angela Bedard-Haughn, for their helpful input and direction during this project. Many thanks also to Dr. Sylvie Quideau for her contributions as an external examiner.

Much of the work in this thesis would not have been possible without the help from everyone in the Soil Genesis and Soil Agronomy/Fertility Lab groups. Special thanks to Jeremy Kiss, Thuan Ha, and Javan Fisher for their extraordinary efforts in field sampling. I am especially grateful for the opportunity to classify soils in the field with Dr. Pennock and Kent Watson. Many thanks to everyone who assisted with laboratory analysis, and all those who provided much needed support in completing synchrotron work.

I am extremely thankful for the helpful input of Prof. Dr. Leinweber, his support of my visit to Universität Rostock, and his financial support for Py-FIMS work. Thanks to the Soil Science research group at Universität Rostock, and particularly members of the Mass Spectrometry Laboratory, Kai-Uwe Eckhardt and Rolf Beese, for Py-FIMS data collection and their technical expertise. I would also like to thank Tom Regier, Jay Dynes, and David Chevrier for their support with synchrotron work. Special thanks to Adam Gillespie, for guidance concerning XANES processing and analysis.

To all the friends I have made throughout my time in the department, thank you for making the days in the department so enjoyable. Thank you to my parents, Bob and Debbie, and my brother, Brendon, for encouraging and supporting me in all my undertakings. Finally, to Javan, thank you for sharing every step of this journey with me.

Financial support was provided by the Natural Sciences and Engineering Research Council (NSERC). Travel to Rostock, Germany was funded by the NSERC Michael Smith Foreign Study Supplement. Research described in this thesis was performed at the Canadian Light Source (CLS), which is supported by the Canadian Foundation for Innovation, NSERC, the University of Saskatchewan, the Government of Saskatchewan, Western Economic Diversification Canada, the National Research Council Canada, and the Canadian Institutes of Health Research.

To Javan:

Your unfailing support makes everything possible.

Thank you my love.

TABLE OF CONTENTS

LIST OF TABLES

LIST OF FIGURES

LIST OF ABBREVIATIONS

CLS	Canadian Light Source
CO_2	Carbon dioxide
DOM	Dissolved organic matter
GC-MS	Gas chromatography-mass spectrometry
GHG	Greenhouse gas
MAP	Mean annual precipitation
MAT	Mean annual temperature
MIT	Mineralization-immobilization turnover
m/z	Mass-to-charge ratio
NEXAFS	Near-edge X-ray absorption fine structure
NMR	Nuclear magnetic resonance
NMS	Non-metric multidimensional scaling
OC	Organic C
OM	Organic matter
PCA	Principal component analysis
PFY	Partial fluorescence yield
Py-FIMS	Pyrolysis-field ionization mass spectrometry
RDA	Redundancy analysis
SGM	Spherical grating monochromator
SOC	Soil organic carbon
SOM	Soil organic matter
SON	Soil organic nitrogen
TC	Total C
TFY	Total fluorescence yield
TII	Total ion intensity
TN	Total N
XANES	X-ray absorption near edge structure
XAS	X-ray absorption spectroscopy

1. INTRODUCTION

As the largest actively cycling terrestrial C pool—containing approximately 1500 to 2000 Pg C in the top 1 m (Amundson, 2001; Janzen, 2004)—soil organic matter (SOM) has the potential to alter atmospheric carbon dioxide (CO_2) concentrations and thus affect climate change. However, the direction and magnitude of the response of soil organic carbon (SOC) to changes in climate remains uncertain (Davidson and Janssens, 2006; Janssens and Vicca, 2010) due to the complex dynamics of controls on SOM persistence (Davidson and Janssens, 2006). Current models of SOM dynamics (e.g., CENTURY, RothC) partition SOM and litter inputs into multiple pools with different decomposition rates and emphasize the importance of biochemical recalcitrance in controlling SOM turnover (Kleber and Johnson, 2010; Gärdenäs et al., 2011; Dungait et al., 2012). However, recent evidence suggests biochemical recalcitrance may not be an important determinant of SOM persistence (Marschner et al., 2008; Kleber, 2010; Schmidt et al., 2011; Dungait et al., 2012). As such, current climate change models are predicated on limited and outdated knowledge of SOM, hindering our ability to accurately predict changes in SOC stocks.

Soils are much more than a medium for C sequestration, contributing to the provision of numerous ecosystem services (Janzen, 2004). Given the magnitude of observed and forecasted global changes caused by elevated greenhouse gas (GHG) concentrations (IPCC, 2013, 2014), a key challenge humanity must meet centers on anticipating how climate change will impact ecosystem functioning (Janzen et al., 2011). Indeed, many of the benefits derived from high SOM contents are accrued from its decomposition, and as such, at fixed inputs of OM there is a tradeoff between climate change mitigation and soil productivity (Janzen, 2006). Consequently, climate change mitigation strategies aimed at enhancing stocks of stable SOC pools (Six et al., 2002; Krull et al., 2003; Goh, 2011), including those suggesting increasing inputs of biochemically recalcitrant compounds (Lorenz et al., 2007), will impact soil productivity. Likewise, climate change and associated land use shifts may lead to the residual enrichment of

stable SOM (Dalias et al., 2001; Paré et al., 2006; Hilli et al., 2008), potentially leaving us with predominantly inert SOC and a reduction in other ecosystem services.

Clearly, there is a need to evaluate both the chemical quality of SOM pools, and to examine how these pools—and their functioning—will change in a warming climate. Specifically, does SOM chemistry and decomposition vary with climate and climate-induced land use changes? In addition, are SOM chemistry and its biological stability related, and if so, in what manner? The goal of this thesis was to explore these questions by examining changes in SOM chemistry and mineralization along a pedogenically defensible climosequence at the grassland-forest boundary in west-central Saskatchewan, Canada, with the aim of enhancing knowledge regarding the potential effects of climate change on SOM dynamics.

This thesis is organized in six chapters, beginning with an introduction (Chapter 1) and a literature review (Chapter 2). The following two chapters are written as stand-alone manuscripts for publication, with a preface linking the objectives of each manuscript to the overarching goal of the thesis. Chapter 3 characterizes differences in SOM chemistry that occur with latitude along a climosequence, with the aim of relating these differences to climate, and climate-induced differences in land use. Chapter 4 builds on the previous chapter by describing changes in the biological stability of SOM along the same climosequence, and attempts to reconcile differences in biological stability with differences in SOM chemistry. Furthermore, it aims to link the biochemical recalcitrance of SOM to its decomposition by investigating changes in SOM chemistry during a laboratory incubation. Finally, Chapter 5 synthesizes findings from the two research chapters (Chapters 3-4), providing an overall conclusion for the thesis, and is followed by a list of references (Chapter 6).

2. LITERATURE REVIEW

2.1 Soil Organic Matter Chemistry

Despite the important role of SOM as a C storage pool and a provider of numerous other ecological services, a large fraction of SOM remains "molecularly uncharacterized" (Hedges et al., 2000). Traditional concepts of SOM chemistry, arising from early and widespread adoption of alkaline extractions to characterize SOM, proposed that over time, humification processes led to the formation of large polymeric macromolecules (Kleber and Johnson, 2010). This classical perception of old SOM as complex implies that the biochemical properties of SOM determine its stability (e.g., Waksman, 1936, and references therein). While the ubiquitous operation of humification processes has been questioned (Piccolo, 2001; Sutton and Sposito, 2005; Wershaw, 2004, 1986), this biochemically-focused viewpoint of SOM has endured. Contemporary concepts of SOM turnover include SOM chemistry as a driver of persistence (e.g., Sollins et al., 1996; Krull et al., 2003; von Lützow et al., 2006), and compartment-based models of SOM cycling are largely based on concepts of biochemical recalcitrance (Kleber and Johnson, 2010; Gärdenäs et al., 2011; Dungait et al., 2012), highlighting the need to more completely characterize SOM chemistry. Additionally, understanding changes in SOM chemistry may be vital to our understanding of the effect of ecological shifts on soil functioning, as molecular level characterization of SOM may be sensitive to changes not observed by other measures of the function and status of soils (Simpson and Simpson, 2012). Thus, to make significant advances in predicting effects of climate and land use changes on soil functioning and soil C storage, we must first understand the chemical nature of SOM.

2.1.1 Plant litter and microbial inputs

Soil organic matter comprises all material containing organic C (OC) in soils. From a pedogenic perspective, plant litter and the microbial biomass represent primary and secondary parent materials of SOM, respectively (Kögel-Knabner, 2002). As such, relatively

undecomposed SOM contains a greater proportion of plant-derived constituents, while degraded SOM—having been processed by the microbial biomass—is characterized by microbially-derived compounds (Grandy and Neff, 2008), and is enriched in peptides and SON (Knicker, 2011). Contributions from plant litter primarily include polysaccharides and lignin (Kögel-Knabner, 2002). Fungal cell walls are comprised predominately of polysaccharides and proteins (Rogers et al., 1980; Wessels and Sietsma, 1981; Peberdy, 1990), while carbohydrates and amino acids dominate bacterial inputs (Rogers et al., 1980; Koch, 1990).

2.1.2 Transformations of soil organic matter chemistry during decomposition

While it is well-known that SOM constituents exist as a continuum from untransformed biomolecules to highly altered products (Schaumann and Thiele-Bruhn, 2011), the drivers of SOM chemical transformations during decomposition are disputed. Three main hypotheses have been put forward (Wickings et al., 2012). First, the current paradigm of litter decomposition, termed the 'Chemical Convergence Hypothesis' (Wickings et al., 2012), suggests that a single decomposer 'funnel' exists (Grandy and Neff, 2008; Fierer et al., 2009), resulting from a shared set of physiological constraints and biochemical pathways (McGill, 2007), which lead to the chemical convergence of SOM. Decomposition thus follows a predictable pattern, beginning with the loss of relatively labile plant-derived compounds (e.g., water soluble compounds), followed by the degradation of more biochemically recalcitrant plant-derived compounds (e.g., cellulose and hemicellulose; Berg and Mcclaugherty, 2014), and culminating in the accumulation of microbially-derived compounds (Grandy and Neff, 2008). Due to concomitant physical breakdown of plant particulate OM as decomposition proceeds, trends that occur in SOM chemistry during degradation are also evident across soil particle sizes (Grandy and Neff, 2008). Second, the 'Initial Litter Quality Hypothesis' (Wickings et al., 2012) proposes that differences in initial litter quality persist throughout decomposition. Chemical characteristics of litter can be inherited by SOM (Angers and Mehuys, 1990; Otto and Simpson, 2005, 2006; Filley et al., 2008; Stewart et al., 2011; Urbanová et al., 2014), and may endure despite changes in land use (Sleutel et al., 2008, 2011; Dümig et al., 2009; Pisani et al., 2013). Finally, the 'Decomposer Control Hypothesis' (Wickings et al., 2012) suggests that functionally distinct decomposer communities lead to differences in litter chemistry during decomposition (Sinsabaugh et al., 2002; Šnajdr et al., 2011). However, these hypothesized controls on SOM chemistry during decomposition are not mutually exclusive, and recent studies have found evidence supporting multiple controls on

SOM chemistry during decomposition (Wickings et al., 2012; Wallenstein et al., 2013; Parsons et al., 2014). As such, SOM chemistry may reflect the relative state of decay of OM, differences in initial litter inputs, differences in decomposer communities, or a combination of these controls.

2.1.3 Land use and climatic effects on soil organic matter chemistry

Clearly, climate-induced changes in land use will alter initial litter inputs; according to the 'Initial Litter Quality Hypothesis' (Wickings et al., 2012), such alterations may persist as litter is decomposed and incorporated into SOM. Grass and forest litter—the initial source materials of SOM—are chemically distinct (e.g., Otto and Simpson, 2005, 2006; Marín-Spiotta et al., 2008). Higher ratios of suberin-to-cutin in grassland soils indicate a predominance of root-derived inputs whereas leaf-derived inputs dominate in aspen soils at the grassland-forest ecotone of Alberta (Otto and Simpson, 2006). This finding is particularly important, as root-derived SOM typically has a longer residence time than shoot-derived SOM (Rasse et al., 2005). Additionally, compared to grasslands, woodland litter inputs and non-aggregated particulate OM may be enriched in cutin and suberin-derived fatty acids relative to lignin (Filley et al., 2008).

Conversions from native land uses to pasture, cropland, or tree plantations typically led to differences in the molecular nature of SOM (Fernandez et al., 2012; Pisani et al., 2013; Yannikos et al., 2014). For example, findings from studies comparing paired cultivated and grassland soils suggest that cultivation leads to the residual enrichment of heterocyclic-N (Schnitzer et al., 2006; Leinweber et al., 2009b; Gillespie et al., 2011). Notably, differences in SOM chemistry between land uses may be specific to different soil size fractions (Guggenberger et al., 1995) or may be difficult to deconvolute from changes in SOM chemistry caused by concurrent shifts in the microbial community (Yannikos et al., 2014), often observed to occur with land use differences (e.g., Cookson et al., 2007; Steenwerth and Jackson, 2002).

Likewise, climate may alter the molecular nature of SOM, as microbial decomposition is influenced by temperature and moisture (Davidson and Janssens, 2006). According to the 'Chemical Convergence Hypothesis' (Wickings et al., 2012), the chemistry of all SOM should be approaching a uniform quality, with any differences in SOM chemistry reflecting differences in the relative state of decomposition. We expect SOM decomposition to increase in warmer climates as rates of enzyme-mediated reactions increase with temperature (Conant et al., 2011), but concurrent increases in water-limitation may limit decomposition (Davidson and Janssens,

2006). Preferential decomposition of labile SOM constituents may lead to the residual accumulation of more recalcitrant SOM at sites with higher mean annual temperatures (MAT; Hilli et al., 2008).

Consistent with these expectations, Feng et al. (2008) found carbohydrates—considered to be relatively labile—were depleted and lignin degradation was accelerated with soil warming. Additionally, leaf-derived cuticular C increased with soil warming (Feng et al., 2008). However, while findings suggest carbohydrates increase with mean annual precipitation (MAP; Amelung et al., 1997; Dalmolin et al., 2006), a lack of consensus regarding the effect of climate on other SOM constituents (Amelung et al., 1997, 1999a; b, 2006; Sjögersten et al., 2003; Glaser and Amelung, 2003; Djukic et al., 2010; Xu et al., 2010), has hindered our understanding of how climate change will alter SOM chemistry. Furthermore, like differences in land use, effects of climatic differences on SOM chemistry may be confounded by simultaneous shifts in microbial community composition, which have been observed to occur in soil warming treatments (Zogg et al., 1997; Frey et al., 2008).

2.1.4 Analytical tools to assess soil organic matter chemistry: X-ray absorption near edge structure and pyrolysis-field ionization mass spectrometry

Many challenges remain in elucidating the nature of changes in SOM chemistry that may occur with climate change. Particularly, the use of disparate analytical techniques make generalizations regarding the effect of climate and land use on SOM chemistry difficult, and corroboration from multiple analytical techniques has been recommended (Leinweber et al., 2009a, 2013). Recently, XANES and Py-FIMS have been used successfully as complementary techniques to examine the effects of soil fractionation (Gillespie et al., 2009; Leinweber et al., 2010), heat from vegetation burning (Kiersch et al., 2012b), soil leachate depth (Kruse et al., 2010), landscape position (Gillespie et al., 2011), and land use (Leinweber et al., 2009b; Kruse et al., 2010; Gillespie et al., 2011; Yannikos et al., 2014) on SOM chemistry, but have yet to be applied to the examination of climate change effects on SOM chemistry.

X-ray absorption near-edge structure—also known as near-edge X-ray absorption fine structure (NEXAFS)—is a type of X-ray absorption spectroscopy (XAS). This element-specific technique probes the electronic structure of molecules, providing information on the bonding environment of the target atom (Stöhr, 1992). In XAS, the energy of the incoming X-ray is scanned through the absorption edge of the element of interest (Lombi and Susini, 2009). In the

case of *K*-edge XANES, this excitation is targeted at core electrons in the 1s orbital. When the X-ray energy is near the absorption edge, these electrons are excited to unoccupied orbitals (Lombi and Susini, 2009). For atoms to return to their ground state, electrons from higher energy levels must fill the vacancies left by the excitation of the core electrons, and the difference in energy between the two electron levels is emitted as fluorescence or as Auger electrons (Lombi and Susini, 2009). The energy of the features in the resultant XANES spectrum thus provides information on the chemical bonding environment of the absorber atom.

Though XANES has only recently been applied to the characterization of SOM (Vairavamurthy and Wang, 2002), its application has been largely successful. A wide variety of reference spectra have been published for SOM constituents commonly found in soils at both the N (Leinweber et al., 2007, 2010) and C *K*-edges (Myneni, 2002; Urquhart and Ade, 2002; Dhez et al., 2003; Cooney and Urquhart, 2004; Hardie et al., 2007; Solomon et al., 2009; Kruse et al., 2011). Additionally, XANES analysis of SOM chemistry has been applied in diverse contexts: describing soils from different land uses (Leinweber et al., 2009b; Gillespie et al., 2011; Yannikos et al., 2014), investigating effects of burning (Lehmann et al., 2005; Kiersch et al., 2012a), and describing variability within profiles (Gillespie et al., 2014b) and aggregates (Lehmann et al., 2005, 2008; Schumacher et al., 2005).

However, while the application of XANES to SOM characterization has been largely successful, the technique also has limitations. For example, due to significant overlap of some resonances (Leinweber et al., 2007) only a few functional groups can be unambiguously distinguished in complex substances such as whole soils (Leinweber et al., 2013). Additionally, various SOM moieties have different X-ray absorption cross-sections (Stöhr, 1992), prohibiting the comparison of features within a single spectrum, and soft X-rays used in C and N *K*-edge XANES are inherently surface-sensitive (Sham and Rivers, 2002). Furthermore, measurements may have non-linear backgrounds (Regier, 2012) and be distorted by self-absorption effects (de Groot et al., 1994). Finally, the application of C and N *K*-edge XANES to the examination of SOM is limited due to low concentrations of these elements in soils, where relevant signals can be partially masked by interference from the mineral matrix (Kinyangi et al., 2006). Clearly, such limitations stress the need for multiple methods to obtain a more comprehensive understanding of SOM chemistry.

Pyrolysis-field ionization mass spectrometry is a powerful technique combining temperature-resolved pyrolysis with soft ionization. During analyses, thermal energy cleaves chemical bonds within a sample, and the resulting pyrolyzates are identified with high sensitivity and specificity using mass spectrometry (Schulten, 1996). The field ionization technique results in the formation of ionic molecules that have undergone little or no fragmentation (Schulten, 1987; Schulten and Leinweber, 1996), thereby providing insight into the composition of the original sample (Leinweber et al., 2009a). The results obtained from Py-FIMS are rich, yielding a high resolution mass-spectrometric 'fingerprint' of the ion intensities of molecules with different mass-to-charge ratios (*m/z*) as well as thermal information provided by step-wise heating of samples. The former is sensitive to minor differences in SOM composition while the latter provides information on resistance to microbial decomposition (Leinweber et al., 2008) as well as the strength and type of bonds present (Schulten and Leinweber, 1999; Sleutel et al., 2011). As such, Py-FIMS, particularly when coupled with complementary techniques such as XANES, can provide important insight into SOM composition.

Pyrolysis-field ionization mass spectrometry has been successfully applied to describe whole soils (e.g., Hempfling et al., 1988; Schnitzer and Schulten, 1992; Wilcken et al., 1997; Gillespie et al., 2009, 2011; Kiersch et al., 2012b), as well as to relate SOM thermal stability and chemical composition to SOM decomposition (Leinweber et al., 2008). In addition, Py-FIMS has been used to investigate OM composition in different sources of litter (Kögel et al., 1988; Leinweber et al., 2013), different soil types (Leinweber et al., 2009a, 2013; Thiele-Bruhn et al., 2014), and different soil fractions (Leinweber and Schulten, 1995; Schulten and Leinweber, 1999; Leinweber et al., 2010). The application of Py-FIMS has been successfully used to assess the effects of vegetation burning (Kiersch et al., 2012a), different land uses (Schnitzer et al., 2006; Leinweber et al., 2009b; Kruse et al., 2010; Yannikos et al., 2014), and different land use histories (Sleutel et al., 2008, 2011) on OM chemistry.

Like XANES, Py-FIMS suffers from some analytical limitations. The sensitivity of Py-FIMS is limited due to the soft nature of field ionization required to reduce fragmentation (Schulten, 1996; Schulten and Leinweber, 1996). Additionally, although the step-wise heating process utilized in Py-FIMS transfers less energy to samples than flash-pyrolysis methods, there is nevertheless a possibility for pyrolytic formation of heterocyclic-N artifacts (Leinweber et al., 2013), which must be corrected for in analysis (Kruse et al., 2011). Furthermore, the quantitative

data derived from the assignment of Py-FIMS marker signals represent only an approximation, as many selected biomarkers overlap with signals from other compounds (Schnitzer and Schulten, 1992; Schulten, 1996).

2.2 Persistence of Soil Organic Matter—A Changing Paradigm

As early as the 1800's, conflicting observations of the decomposability of SOM (Waksman, 1936) led to the widespread attribution of differences in SOM persistence to differences in biochemical recalcitrance, as no other mechanisms for SOM stabilization were yet known (Kleber and Johnson, 2010). Both organo-mineral interactions and spatial inaccessibility were later recognized as important stabilization mechanisms, though biochemical recalcitrance was still considered a key determinant of SOM persistence (Stevenson, 1994; Christensen, 1996; Sollins et al., 1996; Krull et al., 2003), being well-aligned with traditional concepts of humification leading to large, complex macromolecules (Kononova, 1961). However, recent structural models depict SOM as supramolecular assemblies of partial degradation products held together by non-covalent bonds (Piccolo, 2001; Sutton and Sposito, 2005; Wershaw, 2004, 1986) rather than as large macromolecules (Kononova, 1961; Stevenson, 1994), implying that complex, biochemically recalcitrant humification products do not exist in abundance in natural environments. Furthermore, partial degradation products of plant litter that are generally assumed to be biochemically recalcitrant (e.g., lignin, lipids) may not be stable relative to the bulk SOM (Amelung et al., 2008; Marschner et al., 2008; Dungait et al., 2012). Together, these findings have led many to doubt the importance of biochemical recalcitrance in determining SOM turnover (Marschner et al., 2008; Kleber, 2010; Schmidt et al., 2011; Dungait et al., 2012). Current concepts of SOM stabilization mechanisms continue to recognize the role of biochemical recalcitrance and its effect of selective preservation, but note that organo-mineral interactions and spatial inaccessibility may exert greater influence on SOM stabilization (von Lützow et al., 2006). The relevance of biochemical recalcitrance may be limited to early stages of decomposition (von Lützow et al., 2006), and may only lead to short-term stabilization of SOM (von Lützow et al., 2008).

However, this changing paradigm of controls on SOM persistence has not yet been incorporated into models of C turnover. Given the large amount of C stored in SOM (~2000 Pg C) relative to the atmosphere (~785 Pg C; Janzen, 2004), soils have a significant potential to

influence climate change feedbacks. As such, assumptions regarding SOM persistence are key determinants in model-based estimates of the magnitude and direction of the response of SOM to climate change (Jones and Falloon, 2009). Models of SOM cycling often represent SOM as compartmental, with each pool having a different turnover time (e.g., CENTURY, RothC; Smith and Falloon, 2000). As such, both biochemically recalcitrant SOM and protected SOM may be partitioned into a common pool represented by a single decomposition rate (Davidson and Janssens, 2006). While compartmental models often incorporate clay content as a control on SOC turnover, transfers of SOC from fast-cycling pools to pools with longer turnover times are treated as a consequence of out-dated concepts of humification processes and resulting increases in biochemical recalcitrance (Kleber and Johnson, 2010; Gärdenäs et al., 2011). However, the response and potential feedback of biochemically recalcitrant SOM and protected SOM to climatic changes may be markedly different (Davidson and Janssens, 2006; Kleber and Johnson, 2010), emphasizing the need to further our understanding regarding controls on SOM persistence.

2.2.1 Biochemical recalcitrance: linking form and function

Biochemical recalcitrance—though variously defined (Kleber, 2010)—is used here to mean refractory due to intrinsic molecular structure (Sollins et al., 1996). While both highly aromatic molecules, such as lignin, as well as highly aliphatic molecules, such as lipids and waxes, may be refractory (Derenne and Largeau, 2001), molecular properties such as size, polarity, and bonding influence persistence (von Lützow et al., 2006). Biochemically recalcitrant compounds are thought to be selectively preserved (Kalbitz et al., 2003a) as the microbial biomass preferentially degrade more labile compounds (Trinsoutrot et al., 2000).

Observed discrepancies between molecular structure and turnover times of SOM (e.g., Amelung et al., 2008; Marschner et al., 2008) have led to controversy surrounding the role of biochemical recalcitrance in SOM stabilization (Kleber, 2010; Schmidt et al., 2011; Dungait et al., 2012). Compounds perceived as biochemically recalcitrant may not be stabilized in the long term (e.g., lignin), or their persistence may be controlled by other stabilization mechanisms influenced by chemical composition. For example, the hydrophobicity of lipids (Bachmann et al., 2008) may reduce microbial accessibility (von Lützow et al., 2006). Conversely, compounds traditionally described as relatively labile such as microbially-derived peptides and proteins may persist for long times (Knicker, 2004; Miltner et al., 2009) and are ubiquitous in soils (Knicker et

al., 1993; Knicker and Kögel-Knabner, 1998; Schulten and Schnitzer, 1998; Rillig et al., 2007; Olk, 2008).

Such inconsistencies between a compound's perceived and observed stability clearly highlight the problematic nature of terms such as 'labile' or 'biochemical recalcitrance'. While such terms may be appropriate in describing the degradability of compounds in relatively simple systems, they may be unsuitable for describing the decomposition of OM in complex systems such as soils. Indeed, the observed persistence of a compound in soils may be attributable to a variety of disparate mechanisms including microbial resynthesis and biomass recycling, microbial processing of old SOM, or the simultaneous operation of other stabilization mechanisms (von Lützow et al., 2006). As such, despite the term 'biochemical recalcitrance' denoting resistance to degradation, its role in SOM stabilization may be only minor or easily obscured. Confusion arising from the prevalence of such ill-defined terms are exacerbated by the common use of operational definitions of recalcitrance (Kleber, 2010). Nevertheless, throughout this thesis, the terms 'labile' and 'biochemically recalcitrant' are used to relate our findings to traditional concepts of SOM degradation.

In light of the controversy surrounding biochemical recalcitrance, current concepts of its importance in SOM stabilization have shifted. Though previously believed to control SOM stabilization in the long-term (Krull et al., 2003), present views suggest that the biochemical recalcitrance of plant-derived and microbially-processed compounds contribute to SOM stabilization only in the short-term (<10 y turnover times), while charred OM and, potentially, humic substances lead to long-term SOM stabilization (>100 y turnover times; von Lützow et al., 2008). Additionally, biochemical recalcitrance may determine persistence in the absence of other stabilization mechanisms (Kalbitz et al., 2003b). As such, recent research continues to link SOM chemistry to its persistence. Gillespie et al. (2014b) found strong relationships between cumulative C mineralization and ratios of carboxylic acids:ketones, carbohydrates:ketones, and phenols:ketones as measured using C *K*-edge XANES, highlighting the use of ketone as a biomarker of microbially-transformed SOM (Gillespie et al., 2014a) that may persist in soils. In agreement with the notion that root-derived SOM inputs are relatively stable (Rasse et al., 2005), Heumann et al. (2011) found N mineralization rates to be negatively correlated with the proportion of sterols and suberins in sandy arable soils of NW Germany. Leinweber et al. (2008) found relationships between SOM mineralization and specific chemical constituents, though

these were modified by factors such as land management. While the recent paradigm shift suggests a purely molecular characterization of SOM is insufficient to describe its persistence, SOM chemistry clearly remains a determinant of SOM turnover, both by conferring biochemical recalcitrance as well as by influencing the operation of other stabilization mechanisms.

2.2.2 Interactions with surfaces and metal ions

Organo-mineral interactions can increase SOM persistence and can occur via six mechanisms: ligand exchange, cation bridges, anion bridges, anion exchange, cation exchange, van der Waals interactions, and hydrophobic effects (Arnarson and Keil, 2000; Feng et al., 2005). The relative dominance of these mechanisms may vary with environmental conditions (Arnarson and Keil, 2000; Mikutta et al., 2007), and may be zonal due to the tendency of amphiphilic OM fragments to self-assemble into layered structures when in contact with mineral surfaces (Kleber et al., 2007). Interactions between OM and mineral soil surfaces is greatest for clay-sized particles (von Lützow et al., 2006) and increases with specific surface area (Saggar et al., 1996), suggesting that soil texture influences SOM stability. While a mechanistic understanding of how organo-mineral associations increase OM persistence is currently lacking, evidence suggests that desorption must occur prior to microbial decomposition of OM (Mikutta et al., 2007), and degradative microbial enzymes, in addition to OM, can be adsorbed by minerals (Demanèche et al., 2001), further inhibiting decomposition.

Biochemical quality modifies the strength and proclivity of organo-mineral interactions. Findings regarding the chemistry of SOM in organo-mineral interactions are conflicting, with some studies suggesting that aromatic compounds are preferentially and strongly sorbed to mineral surfaces (e.g., Kalbitz et al., 2005; Mikutta et al., 2007), while others suggest that aliphatic materials are preferentially sorbed (Wang and Xing, 2005). However, these contradictory observations may be resolvable as the selective sorption of different biochemical compounds can vary with clay mineralogy (Wattel-Koekkoek et al., 2001; Feng et al., 2005), suggesting that different SOM binding mechanisms operate in different clay minerals. For example, Feng et al. (2005) found more CH_2 groups—likely derived from cutin—sorbed to kaolinite, while peptides were more abundant on montmorillonite. Likewise, (Kalbitz et al., 2005) argue that increases in stability due to sorption may be greater for easily mineralizable dissolved organic matter (DOM) with high concentrations of carbohydrates than for poorly mineralizable DOM with high concentrations of aromatics.

In addition to stabilization via organo-mineral interactions, SOM can also be stabilized by complexation of metal ions such as Ca^{2+}, Mg^{2+}, Al^{3+}, Fe^{3+}, and heavy metals (von Lützow et al., 2006, 2008). Compared to uncomplexed DOM, Al-DOM precipitates and complexes can significantly reduce C mineralization (Schwesig et al., 2003; Scheel et al., 2007). However, like organo-mineral associations, affinities for metal complexation are thought to differ between various OM moieties, and the stability of the resulting complex may vary with the ions involved and with environmental conditions (Stevenson, 1994). Given the complexity involved, the effects of OM-metal complexation on OM stability are difficult to disentangle from changes in substrate quality, metal toxicity to microorganisms, effects of metals on extracellular enzymes, and the ability to form cation bridges (von Lützow et al., 2006).

2.2.3 Spatial inaccessibility

The spatial accessibility of SOM can be reduced via distance from preferential flow paths, aggregation, intercalation of OM within interlayer spaces of phyllosilicate minerals, hydrophobicity, and encapsulation within organic macromolecules (von Lützow et al., 2006). Subsoil OM is protected from decomposition due, in part, to reduced abundances and activities of microorganisms at depth (Taylor et al., 2002). Aggregation can compartmentalize microbes from substrate and decrease microbial activity by reducing diffusion of oxygen (Six et al., 2002). Land use can modify microbial accessibility, as evidenced by SOC losses of agricultural soils due to disruption of aggregates by tillage (Tisdall and Oades, 1982; Elliot, 1986; Six et al., 2000). Notably, the biochemical composition of aggregates may be distinct from that of total OM (Lehmann et al., 2008), and interior (i.e., protected) SOM may differ in chemistry from exterior SOM, being enriched in aliphatics (Kinyangi et al., 2006; Marín-Spiotta et al., 2008). As such, stabilization of SOM within aggregates may arise from both occlusion as well as biochemical recalcitrance. Intercalation of OM within the framework of phyllosilicates can occur in mineral soils (Theng et al., 1986; Leinweber and Schulten, 1995) and marine sediments (Kennedy et al., 2002), and may act to preferentially preserve aliphatics (Leinweber and Schulten, 1995). Intercalation is most likely to occur in acidic soils, where the pH-dependent negative charge of OM is suppressed, inhibiting repulsion from negatively charged interlayer surfaces (Theng et al., 1986). However, even in acidic soils the role of intercalation may be insignificant (e.g., Eusterhues et al., 2003). Soil hydrophobicity occurs when a layer of hydrophobic organic molecules coats a mineral surface (Doerr et al., 2000). This reduces microbial access to OM, and

may help promote aggregation (Piccolo and Mbagwu, 1999; Jandl et al., 2004). Finally, while encapsulation in organic macromolecules has been proposed (Knicker et al., 1996; Zang et al., 2000), there is currently little evidence to support the role of macromolecule encapsulation in SOM stabilization (von Lützow et al., 2006).

2.2.4 Determining soil organic matter persistence: long-term aerobic incubations

Long-term aerobic incubations are commonly used in measurements of the biologically active fractions of SOC and SON (Curtin and Campbell, 2008; Hopkins, 2008). While not analogous measurements, potentially mineralizable N and readily mineralizable C both reflect the size of the labile pool of SOM that can be mineralized by the indigenous microbial biomass under optimum conditions (Haynes, 2005). Notably, the CO_2 evolved during incubations to estimate readily mineralizable C reflects the total metabolic activity of soil microorganisms, while inorganic N leached during incubations to estimate potentially mineralizable N reflects the balance of N mineralization-immobilization turnover (MIT; Haynes, 2005). When readily mineralizable C and potentially mineralizable N are expressed on a per unit mass SOC or SON basis, these measures reflect the degradability of SOM in a soil (Baldock and Broos, 2011), and as such are highly relevant to predictions of future SOM stocks in a changing climate. Additionally, despite recent shifts in our understanding of plant N utilization (Schimel and Bennett, 2004), measures of net N mineralization provide an indication of the supply of plant-available N (Baldock and Broos, 2011), and may thereby indicate changes in ecosystem functioning due to climate and land use changes.

3. WILL CHANGES IN CLIMATE AND LAND USE AFFECT SOIL ORGANIC MATTER COMPOSITION? EVIDENCE FROM AN ECOTONAL CLIMOSEQUENCE[1]

3.1 Preface

While many studies have focused directly on predicting changes to SOM pools resulting from climate change and shifts in land use, less research has focused on examining changes in the drivers of SOM persistence in this same context. This study considers the broader impacts of climatic change at the grassland-forest ecotone in Saskatchewan, examining changes in one driver of SOM persistence resulting from differences in climate and land use. The biochemistry of SOM has the potential to lead to SOM stabilization through inherent biochemical recalcitrance as well as by affecting organo-mineral association and accessibility. By examining changes to one of the dominant controls of SOM decomposition, research findings from this study have widespread applicability for the prediction of SOM persistence under plausible climate change scenarios.

[1] This manuscript is currently in review for publication in Geoderma. Coauthors include Dan Pennock, Peter Leinweber, and Fran Walley, all of whom provided invaluable contributions to the funding of research, assistance in facilitation of laboratory analyses and data interpretation, as well as editing this manuscript. Both Dan Pennock and Fran Walley conceptualized the study design.

3.2 Abstract

As the largest actively cycling pool of terrestrial C, the response of SOM to climate change may greatly affect global C cycling and climate change feedbacks. Despite the influence of SOM chemistry on decomposition, uncertainty exists regarding the response of SOM chemistry to climate change and associated land use shifts. Here, we adopt a climosequence approach, using latitude along a uniform glacial till deposit at the grassland-forest ecotone in central Canada as a surrogate for the effects of climate change on SOM chemistry. Additionally, we evaluate differences in SOM chemistry from paired native grassland, native trembling aspen (*Populus tremuloides*) forest, and cultivated soil profiles to investigate the effects of likely climate-induced land use alterations.

The combination of C and N *K*-edge XANES with Py-FIMS techniques revealed only modest differences in surface SOM chemistry related to land use and latitude. Greater variation was apparent in the vertical stratification of SOM constituents from soil depth profiles. These findings indicate that pedon-scale processes have greater control over SOM chemistry than do processes operating on landscape (e.g., land use) and regional (e.g., climate) scales, and that SOM chemistry is largely unresponsive to climatic change on the magnitude of the MAT gradient under study (~0.7 °C) and associated land use shifts.

3.3 Introduction

From 1880 to 2012, global MAT increased by 0.85 °C and continues to rise, largely due to increasing atmospheric CO_2 concentrations (IPCC, 2013). Soils have the capacity to strongly influence atmospheric CO_2 as they represent the largest actively cycling pool of terrestrial C (Janzen, 2004). However, the direction and magnitude of the response of SOC to climate change remains uncertain (Davidson and Janssens, 2006; Janssens and Vicca, 2010) due to the complexity of dynamics controlling SOM decomposition (Davidson and Janssens, 2006). The importance of SOM chemistry in defining persistence, though recently brought into question (Schmidt et al., 2011), may remain an important control on SOM turnover (Conant et al., 2011). However, despite influencing future SOC stocks, interactions of SOM chemistry with climate change and associated land use shifts have yet to be fully explored.

Paleorecords of rapid forest-to-grassland conversions at the prairie-forest ecotone in central Canada suggest that this region is particularly sensitive to environmental change

(Williams et al., 2009). By 2020, this region is predicted to experience a 2 °C increase in MAT relative to the 1961-1990 average (Sauchyn and Kulshreshtha, 2008), and concomitant increases in precipitation will be insufficient to offset increasing evapotranspiration (Hogg and Hurdle, 1995; Sauchyn and Kulshreshtha, 2008; Barrow, 2009). As trembling aspen, an important boreal forest species, is moisture-limited in this region (Hogg and Hurdle, 1995), future drying trends may trigger abrupt vegetation shifts (Williams et al., 2009). Additionally, ongoing agricultural conversion of native forests in the region (Fitzsimmons, 2002) may increase as food demand grows and warming trends continue. As SOM can inherit chemical characteristics of plant inputs (Filley et al., 2008; Stewart et al., 2011), vegetation shifts and agricultural conversion at the prairie-forest ecotone may alter SOM chemistry.

Land use change will not only modify plant inputs at the soil surface, but may also affect subsoil SOM chemistry. Though deep SOM comprises an important global C storage pool, relatively little is known about its chemistry (Rumpel and Kögel-Knabner, 2011). Land use can affect SOM chemistry and its vertical distribution by modifying plant inputs (Otto and Simpson, 2005, 2006) and their distributions (Jackson et al., 1996; Jobbágy and Jackson, 2000), as well as through processes such as tillage-induced admixing of soil. As increased labile C inputs to subsoils may stimulate degradation of previously unavailable SOM (Fontaine et al., 2007), climate-induced land use changes at the prairie-forest ecotone may affect subsoil SOM chemistry and its decomposition.

The effects of climate and land use change on SOM chemistry represents a knowledge gap in our understanding of SOM dynamics. Climatic effects on SOM chemistry have been examined using latitudinal gradients (e.g., Amelung et al., 1997, 1999a; 1999b, 2006; Glaser and Amelung, 2003; Kawahigashi et al., 2004), elevation gradients (e.g., Dalmolin et al., 2006; Djukic et al., 2010) and soil warming experiments (e.g., Sjögersten et al., 2003). Despite these efforts, no consensus has emerged, though findings suggest that soil carbohydrates increase with precipitation (Amelung et al., 1997; Dalmolin et al., 2006). Studies of land use effects have focused on surface SOM chemistry, and indicate that cultivation leads to enrichment of heterocyclic-N (Schnitzer et al., 2006; Leinweber et al., 2009b; Gillespie et al., 2011); other land uses are less commonly studied (e.g., Fernandez et al., 2012; Pisani et al., 2013). While studies of soil depth profiles suggest that aliphatic compounds increase with depth in forest soils (Rumpel et al., 2002; Sjögersten et al., 2003; Spielvogel et al., 2008), findings from grassland

profiles are conflicting (Dalmolin et al., 2006; Feng and Simpson, 2007) and comparisons of subsoils across land uses are lacking.

Accordingly, the analysis of SOM chemistry along a pedogenically defensible climosequence using multiple analytical techniques represents a unique opportunity to isolate effects of climate and land use. Previous studies have combined gas chromatography-mass spectroscopy (GC-MS) with nuclear magnetic resonance (NMR) (e.g., Schnitzer et al., 2006; Pisani et al., 2013), NMR and Py-FIMS (e.g., Kogel-Knabner et al., 1988; Wilcken et al., 1997), and other methods (e.g., Amelung et al., 1997; Kiem et al., 2000; Jokic et al., 2003; Solomon et al., 2005; Jandl et al., 2005; Djukic et al., 2010; Gillespie et al., 2013) to characterize SOM. Here, we combine synchrotron-based C and N *K*-edge XANES, and Py-FIMS to analyze SOM chemistry. These techniques have been used to examine effects of soil fractionation (Gillespie et al., 2009; Leinweber et al., 2010), vegetation burning (Kiersch et al., 2012a), soil leachate depth (Kruse et al., 2010), landscape position (Gillespie et al., 2011), and land use (Leinweber et al., 2009b; Kruse et al., 2010; Gillespie et al., 2011; Yannikos et al., 2014) on SOM composition. These methods provide complementary information on SOM chemistry, as XANES is element specific and probes functional group chemistry and bonding environments (Stöhr, 1992; Myneni, 2002), while Py-FIMS identifies nominal masses, providing a thermally-resolved mass spectroscopic "fingerprint" (Schnitzer and Schulten, 1992; Leinweber et al., 2009a). Ours is the first study to apply these advanced techniques to soils from a climosequence study design that controls for confounding pedogenic factors.

Here, we explore the effects of climate change and associated land use shifts on SOM composition by characterizing native grassland, native trembling aspen, and cultivated soils along a climosequence in Saskatchewan, Canada. We utilize changes in SOM chemistry that occur with latitude as a surrogate for climate change effects and examine the impacts of associated land use shifts on surface SOM. Furthermore, we examine soil depth profiles to 20 cm depth to elucidate land use effects on subsoil SOM chemistry and its vertical distribution.

3.4 Materials and Methods

3.4.1 Sites and sampling design

Twelve locations (denoted 1-12, south to north) located on a uniform glacial till deposit ('Ice-Stream 1' described by Ó Cofaigh et al., 2009) were selected to comprise a 46-km

climosequence across the prairie-forest ecotone in west-central Saskatchewan (Fig. 3.1). From south to north along the climosequence, MAT decreases from 0.9°C to 0.2°C, and MAP increases from 418 to 443 mm (Hijmans et al., 2005). Here, the prairie-forest boundary was static (from 10-6 ka and 2-0 ka) or in a period of forest encroachment (from 6-2 ka) during the past 10,000 years (Williams et al., 2009). As such, native aspen forest (n = 12), cultivated (n = 12), and where available, native grassland (n = 4) sites were sampled at each location. In the summer of 2012, the top 5 cm of mineral soil was collected from a midslope position at each site. At location 3 sites, soils were collected in 5 cm increments to 20 cm; organic materials were sampled separately. All pedons were classified according to the Canadian System of Soil Classification (Soil Classification Working Group, 1998).

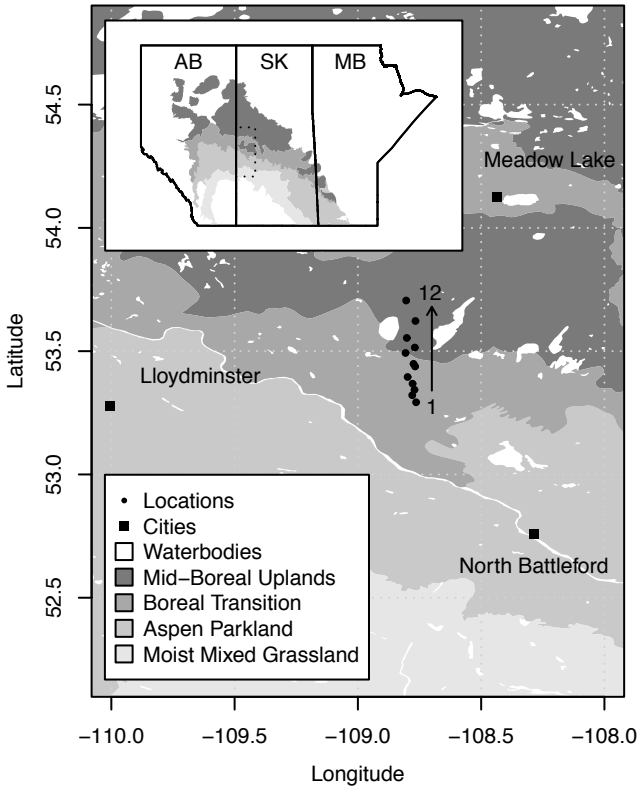

Fig. 3.1 Map depicting study area. Points indicate locations 1 through 12. The inset map depicts the location of the study area in the Canadian Prairies.

3.4.2 Soil properties

Samples were air-dried and ground for analyses. Total C (TC) and total N (TN) were determined by combustion using a LECO CR-12 (LECO Corp, St. Joseph, MI) and a LECO CNS-2000 (LECO Corp, St. Joseph, MI), respectively. Particle size distributions were determined using the modified pipette method after removal of OM with 30% H_2O_2 (Indorante et al., 1990). Soil pH was measured in $CaCl_2$ (Hendershot et al., 2008).

3.4.3 Carbon and N K-edge X-ray absorption near edge structure spectroscopy

Prior to XANES analysis, subsamples of each soil were pulverized using a ball-mill and ~1 mg of each sample was rehydrated in deionized H_2O and air-dried on Si wafers freshly coated with Au. Wafers were affixed to sample plates using conductive C tape (SGE, Toronto, ON, Canada). Carbon and N *K*-edge XANES spectra were measured at the spherical grating monochromator (SGM) beamline 11ID-1 at the Canadian Light Source (CLS, Saskatoon, SK, Canada). At these edges, the beamline delivers 10^{11} photons s^{-1} with a resolving power (E/ΔE) greater than 10^4 (Regier et al., 2007a; b). The exit slit was set at 25 μm. Spectra were collected in fast-scanning mode, which continuously scans the monochromator energy while acquiring signal from the detectors. Each scan was collected for 20 s (e.g., Gillespie et al., 2013, 2014) from a fresh location to reduce beam-induced radiation damage (Leinweber et al., 2007). Total fluorescence yield (TFY) spectra of location 3 soil profile samples were collected in May 2013 using a two-stage micro channel plate detector. Partial fluorescence yield (PFY) spectra of climosequence surface soils were recorded in July 2013 using a silicon drift detector. The 1s → $\pi^*_{C=O}$ transition at 288.6 eV (Kim et al., 2003) of citric acid was used for calibration at the C *K*-edge. For calibration at the N *K*-edge, the 1s → π^* vibrational manifold of N_2 gas evolved from $(NH_4)_2SO_4$ at 400.8 eV was used (Gillespie et al., 2008).

A minimum of twenty scans were averaged and normalized to the incident flux using scans of an Au coated Si wafer. Measurements of the incident flux at the C *K*-edge were scaled and offset prior to normalization to mitigate the effect of flux attenuation by C contamination on beam optics (Watts et al., 2006). Spectra were background corrected with a linear regression fit through the pre-edge region and normalized to an edge jump of unity using custom macros (Gillespie et al., 2014b; a) in IGOR Pro (ver. 6.2, WaveMetrics Inc., Lake Oswego, OR, USA) and Athena (ver. 0.8.56, Ravel and Newville, 2005) software packages. Features at the C and N

K-edges were assigned according to the literature (Myneni, 2002; Urquhart and Ade, 2002; Dhez et al., 2003; Cooney and Urquhart, 2004; Hardie et al., 2007; Leinweber et al., 2007; Solomon et al., 2009; Kruse et al., 2011).

Curve-fitting followed by non-metric multidimensional scaling (NMS) analysis was used to visualize differences between spectra (Gillespie et al., 2011). As NMS aims to preserve the ordering relationship among objects, it is suitable for semi-quantitative data such as XANES peak heights. Briefly, after fitting a background arctangent function ($f(x) = a_1 * \text{atan}[(x - a_2) * a_3] + a_4$; Rovezzi et al., 2009) Gaussian curves were fit to assigned spectral features using the Fityk software package (version 1.2.1, Wojdyr, 2010). Curve parameters were constrained to ensure equal width of all $1s \rightarrow \pi^*$ features. The NMS ordination was performed on Bray-Curtis distances of C and N *K*-edge peak heights (Gillespie et al., 2014a) using package "vegan" (Oksanen et al., 2013) of the R software program (ver. 3.0.2, R Core Team, 2013). An assessment of stress vs. dimensionality determined the number of dimensions of the final ordination (Legendre and Legendre, 2012). Significant relationships between environmental variables and ordination scores were determined by permutation tests. Due to their extreme influence on the ordination, litter samples were omitted from analysis and carboxyl:ketone ratios were treated as an environmental variable.

3.4.4 Pyrolysis-field ionization mass spectrometry

About 5 milligrams of each air-dried and pulverized sample was pyrolyzed in the ion source (emitter: 4.7 kV, counter electrode -5.5 kV) of a double-focusing Finnigan MAT 95. Samples were heated in a vacuum of 10^{-4} Pa from 50 °C to 650 °C, in 10 °C steps over 15 minutes. Between magnetic scans the emitter was flash heated to avoid residues of pyrolysis products. Sixty-five spectra were recorded for the mass range 15 to 900 *m/z*. Total ion intensities (TII) were referred to 1 mg of the sample. Volatile matter was calculated as mass loss in percentage of sample weight. Marker signals (*m/z*) were assigned to relevant substance groups according to Hempfling et al. (1988), Schnitzer and Schulten (1992), Schulten and Leinweber (1996), van Bochove et al. (1996), and Leinweber et al. (2009a, 2013). Thermostability, a predictor for microbial decomposition (Leinweber et al., 2008), was calculated by dividing mass loss of SOM at high temperatures (400 – 650 °C) by mass loss over the whole temperature range (50 – 650 °C).

Data from climosequence surface soils were subject to redundancy analysis (RDA), a canonical multivariate technique combining multiple linear regression and principal component analysis (PCA) to explicitly explore relationships between response and explanatory variables (Legendre and Legendre, 2012). The ordination was performed on a covariance matrix of Py-FIMS *m/z* signals using latitude as the constraining variable. Additionally, PCA – an eigenvector based multidimensional analysis – was performed on Py-FIMS *m/z* signals of location 3 soils to explore differences between land use depth profiles. Ordinations were performed in package "vegan" (Oksanen et al., 2013) of the R software program (ver. 3.0.2, R Core Team, 2013). Permutation tests revealed significant relationships between compound classes, environmental variables, and ordination scores.

3.4.5 Statistics

Statistical analyses were conducted using R (ver. 3.0.2, R Core Team, 2013). Normality and homogeneity of variance were assessed using Shapiro-Wilk's test and Levene's test, respectively. Non-normally distributed data were transformed using the Box-Cox procedure. Linear regression was performed to determine relationships between response variables and latitude. Univariate ANOVA and Tukey's HSD tests were used to assess differences between land uses, using mixed-effects models where appropriate.

3.5 Results

3.5.1 Climosequence surface soils

3.5.1.1 General soil characteristics

Our study design aimed to control for confounding pedogenic factors by sampling soils located on a uniform glacial till deposit. This was achieved for all sites except at location 1, where the forest site had higher silt content than other sites (Table 3.1). This incongruity may be attributed to the genesis of this soil on the margins of the glacial ice stream upon which the climosequence is located ('Ice-Stream 1' in Ó Cofaigh et al., 2009). All other sites had similar textures, confirming their genesis on the same parent material. Additionally, clay content decreased with latitude ($p < 0.001$; $r = -0.62$), consistent with the north-to-south flow of the ice-stream (Ó Cofaigh et al., 2009).

Table 3.1 Locations and properties of climosequence surface soils assessed for SOM chemistry.

Land use	Location	Latitude	Longitude	TC	OC	TN	OC:TN	pH	Sand	Silt	Clay	— Soil classification —		
		°N	°W	— g kg^{-1} —					— % —			Canadian†	WRB‡	USDA§
Grassland	1	53.293	108.760	49.7	43.8	4.2	10.3	5.7	49	26	25	O.BLC	CH-cc	C.Haplocryoll
Grassland	2	53.321	108.777	44.5	39.0	4.2	9.2	7.0	69	12	19	CA.BLC	CL-ha	T.Calcicryoll
Grassland	3	53.341	108.764	45.6	45.4	4.1	11.0	6.1	69	17	15	O.BLC	CH-cc	C.Haplocryoll
Grassland	6	53.438	108.765	29.6	25.2	2.5	9.9	7.0	81	6	13	O.BLC	CH-cc	C.Haplocryoll
Forest	1	53.293	108.763	52.3	53.2	4.3	12.4	6.3	31	57	12	O.LG	GL-ha.lv	T.Cryaqualf
Forest	2	53.319	108.776	63.8	55.8	5.4	10.4	5.4	64	17	19	D.GL	LV-ct-hu	T.Haplocryalf
Forest	3	53.341	108.765	57.6	55.9	4.2	13.2	4.9	63	19	18	D.GL	LV-ct-hu	T.Haplocryalf
Forest	6	53.438	108.764	78.9	71.3	4.8	14.9	5.2	56	31	13	BR.GL	LV-ct-ap	T.Haplocryalf
Forest	8	53.489	108.809	30.9	32.1	2.1	15.3	5.5	65	20	15	D.GL	LV-ct-hu	T.Haplocryalf
Forest	12	53.707	108.805	6.1	5.9	0.4	14.9	4.9	67	28	5	D.GL	LV-ct-hu	T.Haplocryalf
Cultivated	1	53.292	108.770	43.3	36.8	4.0	9.3	6.7	57	26	17	O.BLC	CH-cc	C.Haplocryoll
Cultivated	2	53.324	108.786	30.2	27.3	2.9	9.5	7.2	66	21	13	CA.BLC	CL-ha	T.Calcicryoll
Cultivated	3	53.347	108.782	41.5	24.9	3.0	8.3	4.7	64	23	14	O.BLC	CH-cc	C.Haplocryoll
Cultivated	6	53.438	108.773	57.4	60.7	5.4	11.3	6.1	53	30	18	O.BLC	CH-cc	C.Haplocryoll
Cultivated	8	53.496	108.806	23.9	20.4	2.2	9.1	5.3	58	30	11	O.BLC	CH-cc	C.Haplocryoll
Cultivated	9	53.600	108.783	23.3	21.6	2.4	9.0	6.3	56	21	23	D.GL	LV-ct-hu	T.Haplocryalf
Cultivated	12	53.704	108.804	41.9	44.3	2.8	15.6	5.2	67	23	10	O.BLC	CH-cc	C.Haplocryoll

† Soil Classification Working Group (1998). O.BLC = Orthic Black Chernozem; CA.BLC = Calcarous Black Chernozem; O.LG = Orthic Luvic Gleysol; D.GL = Dark Gray Luvisol; BR.GL = Brunisolic Gray Luvisol.

‡ IUSS Working Group WRB (2014). CH-cc = Calcic Chernozem; CL-ha = Haplic Calcisol; GL-ha.lv = Haplic Luvic Gleysol; LV-ct-hu = Cutanic Luvisol (Humic); LV-ct-ap = Cutanic Luvisol (Abruptic).

§ Soil Survey Staff (2014). C = Calcic; T = Typic.

Other soil characteristics varied between land uses and across the climosequence (Table 3.1). While TC ($p < 0.01$; $r = -0.51$), OC ($p < 0.05$, $r = -0.45$), TN ($p < 0.001$, $r = -0.67$), and pH ($p < 0.05$, $r = -0.39$) were negatively correlated with latitude, log OC:TN ratios increased ($p < 0.01$, $r = 0.55$). Soil pH ($p < 0.01$; grassland: 6.4 ± 0.6; forest: 5.3 ± 0.5; cultivated: 6.0 ± 0.7) and OC:TN ratios ($p < 0.01$; grassland: 10.2 ± 0.7; forest: 13.4 ± 2.6; cultivated: 10.7 ± 2.1) differed between land uses (mean ± standard deviation).

3.5.1.2 Carbon and N *K*-edge X-ray absorption near edge structure

Three features dominate C *K*-edge XANES spectra and were tentatively assigned as: a) C=C in protonated/alkylated aromatics and alkenes at 285.5 eV (aromatic-C); b) aliphatic C in nitriles, carbonyl-C in ketones and aldehydes, and C bound in aromatic heterocycles (e.g., pyrrole, imidazole, and purine) at 286.5 eV (ketone); and c) carbonyl-C in carboxyl and amide at 288.5 eV (carboxyl) (Fig. 3.2; Table 3.2). While not prominent, a minor feature at 287.2 eV, assigned to aliphatic CH, CH_2, and CH_3 as well as aromatic C bound to hydroxyl and ether functional groups, was present and tended to increase with latitude, particularly in the cultivated soil (Fig. 3.2). Visually, proportions of the dominant peaks were similar regardless of land use or location; however, peak heights revealed differences. Forest soils had higher proportions of ketone than grassland soils ($p < 0.05$) and greater proportions of carboxyl than cultivated soils ($p < 0.05$). Carboxyl:ketone ratios tended to be lower in forest soils than in other land uses ($p < 0.10$). No trends across the latitudinal gradient were apparent.

Table 3.2 Carbon and N *K*-edge X-ray absorption near edge structure (XANES) peak heights of grassland, forest, and cultivated surface soils along climosequence.

Land use	Site	Aromatic-C	Ketone	Carboxyl	Carboxyl: ketone	Heterocyclic-N	Amide	Alkyl-N
				— Normalized absorbance (arbitrary units) —				
Grassland	1	0.20	0.13	0.58	4.52	0.06	0.45	0.28
Grassland	2	0.16	0.11	0.54	4.84	0.04	0.48	0.25
Grassland	3	0.17	0.13	0.60	4.64	0.05	0.46	0.26
Grassland	6	0.19	0.15	0.58	3.85	0.04	0.49	0.23
Forest	1	0.24	0.25	0.59	2.35	0.07	0.40	0.25
Forest	2	0.24	0.23	0.59	2.60	0.08	0.41	0.37
Forest	3	0.24	0.24	0.66	2.74	0.08	0.42	0.29
Forest	6	0.36	0.34	0.54	1.60	0.03	0.45	0.30
Forest	8	0.26	0.23	0.56	2.46	0.06	0.37	0.36
Forest	12	0.16	0.12	0.54	4.60	0.06	0.37	0.36
Cultivated	1	0.19	0.11	0.52	4.55	0.06	0.40	0.31
Cultivated	2	0.18	0.09	0.52	5.92	0.05	0.44	0.23
Cultivated	3	0.26	0.20	0.55	2.71	0.04	0.45	0.26
Cultivated	8	0.25	0.19	0.53	2.81	0.06	0.41	0.33
Cultivated	9	0.25	0.17	0.46	2.73	0.05	0.38	0.41
Cultivated	12	0.22	0.23	0.55	2.45	0.06	0.42	0.31
Summary statistics of surface soils by land use†								
Grassland		0.18 ± 0.02	0.13 ± 0.02 b	0.57 ± 0.02 ab	4.46 ± 0.43	0.04 ± 0.01	0.47 ± 0.02 a	0.31 ± 0.06
Forest		0.25 ± 0.06	0.23 ± 0.07 a	0.58 ± 0.05 a	2.73 ± 1.00	0.06 ± 0.02	0.40 ± 0.03 b	0.32 ± 0.05
Cultivated		0.23 ± 0.03	0.16 ± 0.05 ab	0.52 ± 0.03 b	3.53 ± 1.40	0.05 ± 0.01	0.42 ± 0.03 b	0.26 ± 0.02
ANOVA		ns	$p < 0.05$	$p < 0.05$	$p = 0.08$	ns	$p < 0.01$	ns

† Values are means of surface soils for each land use ± standard deviation; values with different lowercase letters are significantly different according to Tukey's HSD test ($p < 0.05$).

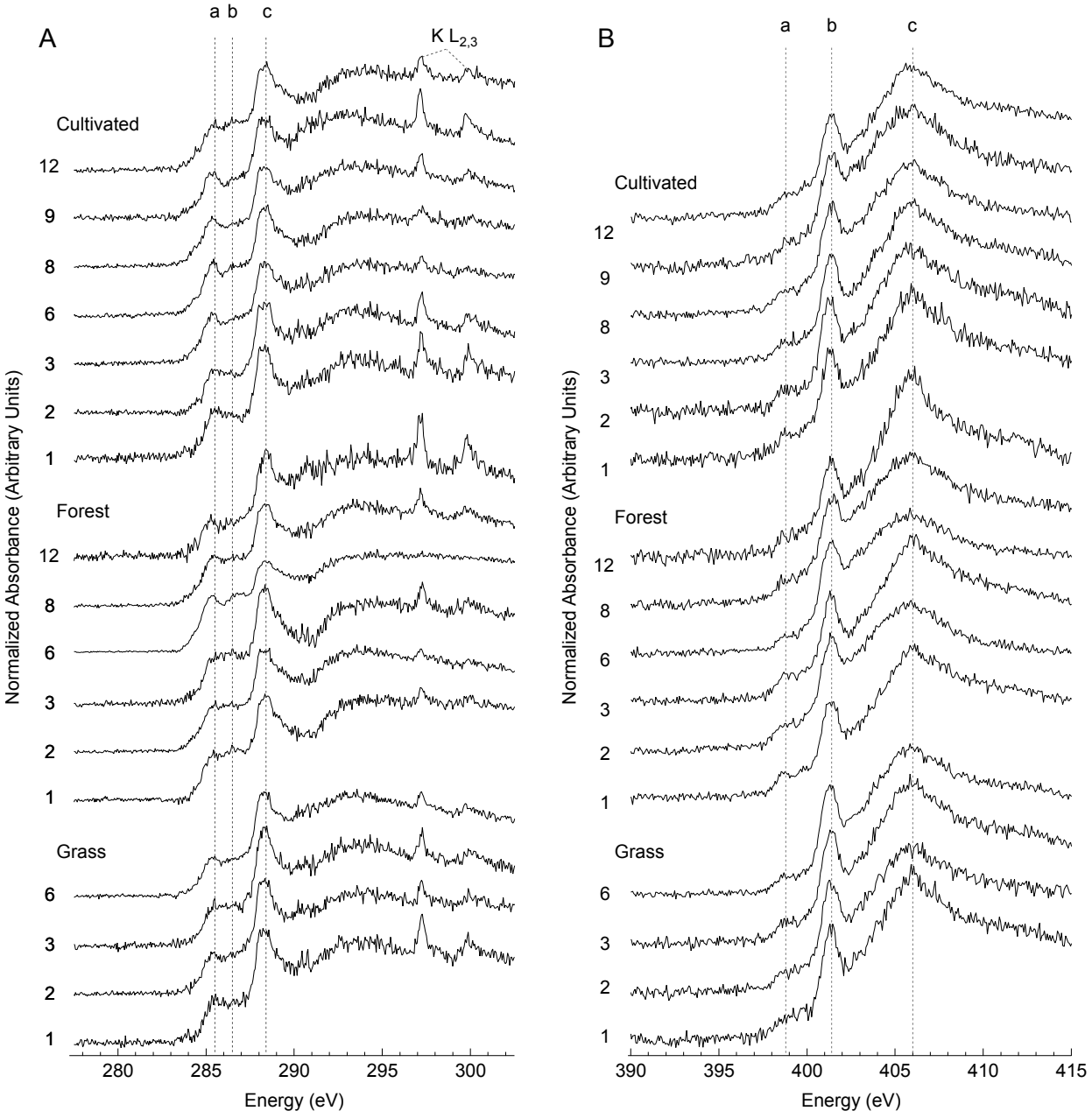

Fig. 3.2 (A) Carbon and (B) N *K*-edge X-ray absorption near edge structure (XANES) spectra of grassland, forest, and cultivated surface soils along climosequence. Location numbers are indicated to the left of each spectrum. Carbon features are assigned as (a) aromatic-C at 285.5 eV; (b) ketone at 286.5 eV; and (c) carboxyl at 288.5 eV. Nitrogen features are assigned as (a) heterocyclic-N at 398.8 eV; (b) amide at 401.4 eV; and (c) alkyl-N at 406 eV.

Dominant features at the N *K*-edge were tentatively assigned as: a) aromatic N in 6-membered rings (e.g., pyridine) at 398.8 eV (heterocyclic-N); b) amidic N with possible contributions from pyrrolic N at 401.4 eV (amide); and c) alkyl-N, inorganic NH_4^+, and the 1s → σ^* feature at 406.0 eV (alkyl-N) (Fig. 3.2b; Table 3.2). Like C spectra, proportions of N *K*-edge XANES features were similar across samples. While not significant, amide displayed a slight inverse trend with latitude ($p = 0.10$; $r = -0.43$), and was highest in grassland soils ($p < 0.01$). Alkyl-N increased with latitude ($p < 0.05$; $r = 0.57$), while variations in heterocyclic-N were not captured by land use or location.

3.5.1.3 Pyrolysis-field ionization mass spectrometry

Figure 3.3 depicts mass spectra and thermograms of forest surface soils from select locations along the climosequence. While some *m/z* signals ranged widely between samples (e.g., *m/z* 394, 396, 414 and 440), most spectra were dominated by signals from carbohydrates (e.g., *m/z* 60, 84, 96, 110, 126), lignin monomers (e.g., *m/z* 178, 192, 208), a homologous series of even-numbered fatty acids C_{16} – C_{26} (e.g., *m/z* 256, 284, 312, 340, 368, and 396), and a homologous series of alkenes C_{20} – C_{24} (e.g., *m/z* 280, 294, 308, 322, and 336).

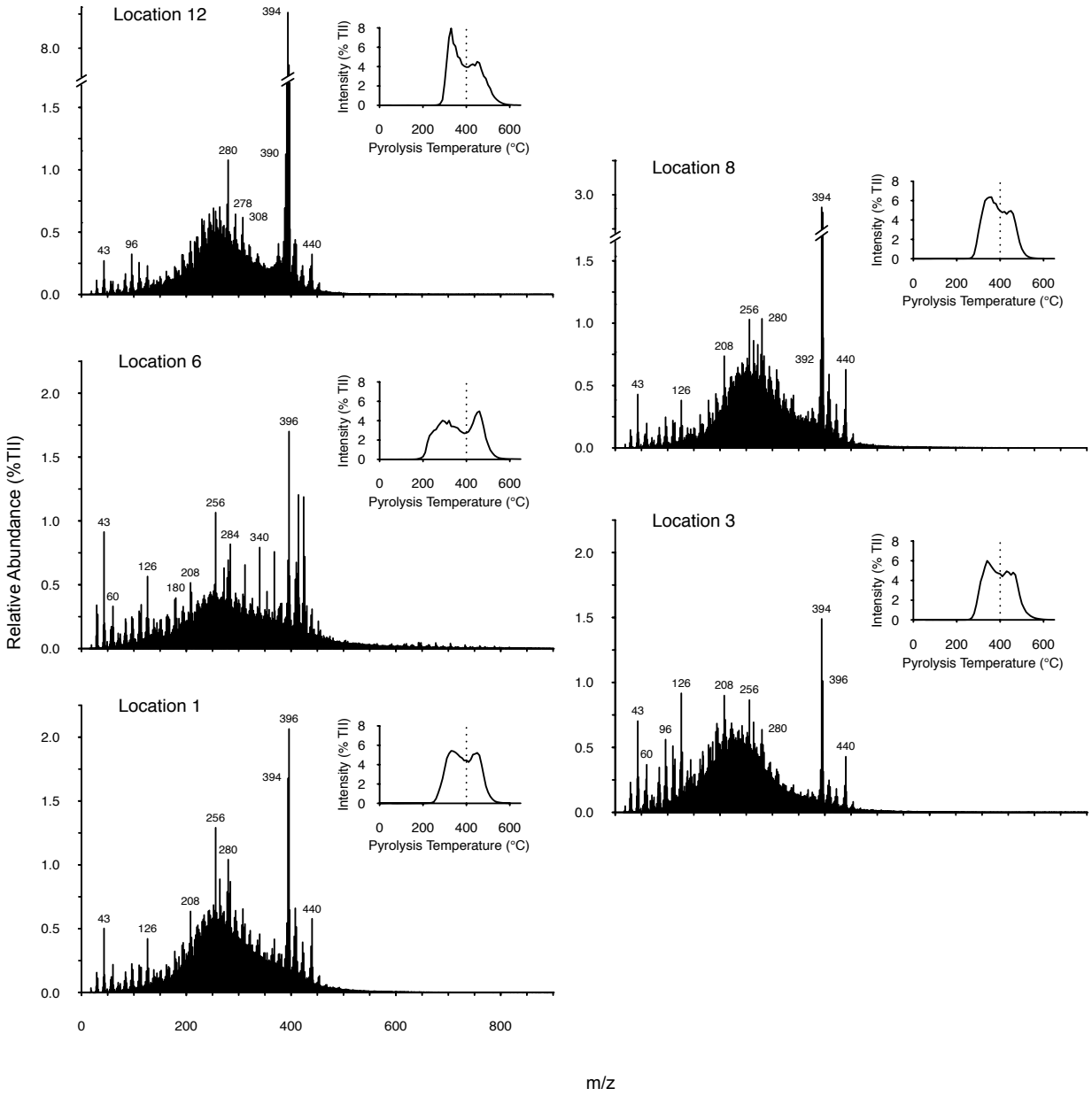

Fig. 3.3 Summed and averaged pyrolysis-field ionization mass spectrometry (Py-FIMS) mass spectra and thermograms of TII (inset) of forest surface soils from select locations along climosequence.

Relationships between *m/z* signals and latitude were explored using RDA. The ordination revealed that latitude captured 69.6% of the variation in forest surface soils (Fig. 3.4), represented primarily by *m/z* 394 and 396, which increased with latitude. Proportions of sterols and lipids were also positively correlated with latitude along the climosequence. In contrast, carbohydrates, phenols and lignin monomers, and amides had negative scores along the

constrained axis. Of the significantly correlated environmental variables, TC, TN, pH, and clay had negative scores along the constrained axis while sand and OC:TN ratios had positive scores along this axis. With the exception of the location 1, trends identified in the RDA are also apparent in Table 3.3, which additionally reveals a decrease in heterocyclic-N and nitriles with latitude.

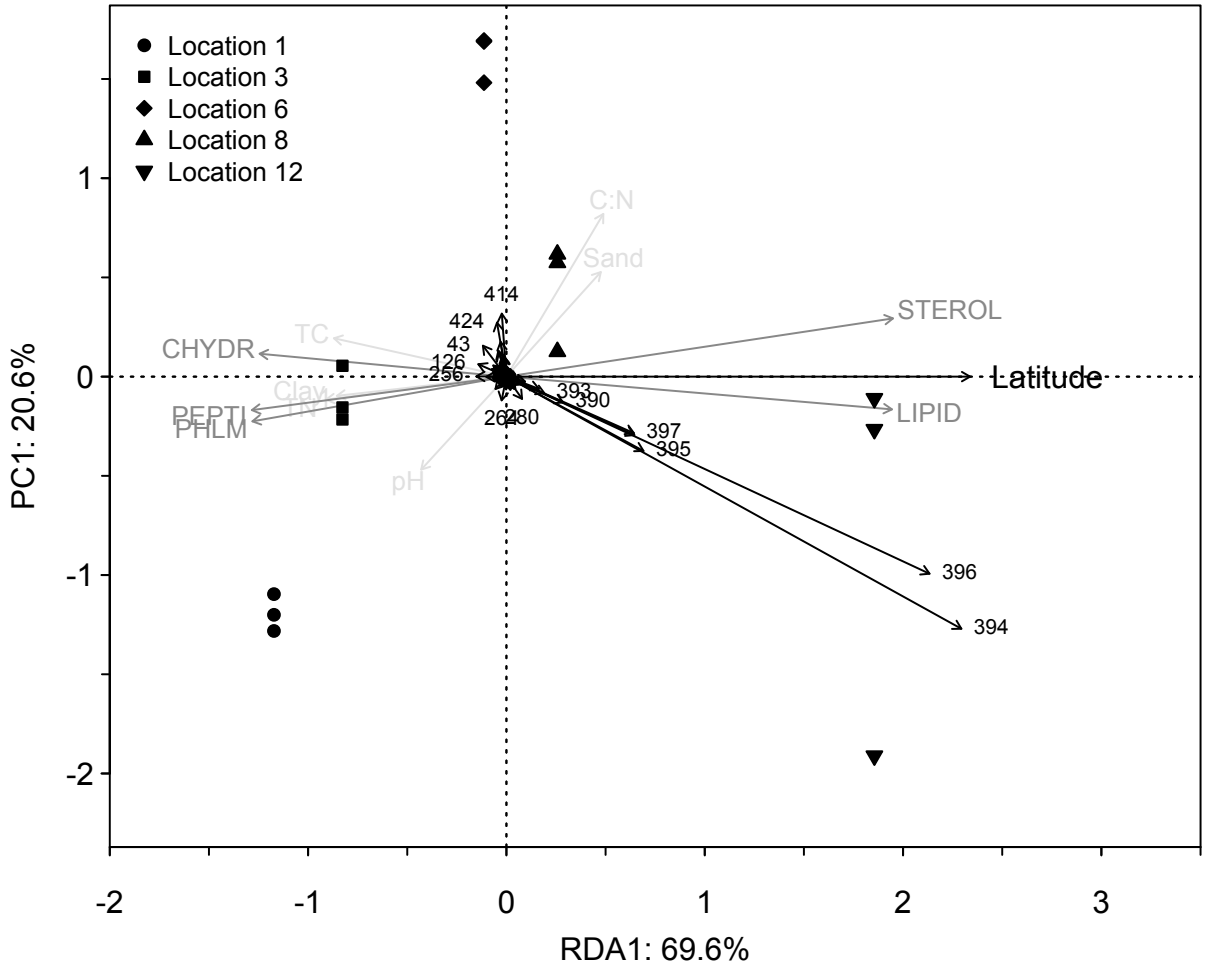

Fig. 3.4 Redundancy analysis (RDA) of pyrolysis-field ionization mass spectrometry (Py-FIMS) total ion intensities (TII) from forest surface soils along climosequence. Vectors directions and lengths indicate the strength of correlations between variables and the ordination. Black vectors correspond to *m/z* signals and latitude. Dark gray vectors indicate significant ($p < 0.05$) correlations between the ordination and Py-FIMS compound classes (scaled 2x for clarity). Light gray vectors indicate significant ($p < 0.05$) correlations between the ordination and environmental variables.

Table 3.3 Relative ion intensities (% TII) of pyrolysis-field ionization mass spectrometry (Py-FIMS) compound classes† from forest surface soils along climosequence.

Site	Latitude	CHYDR	PHLM	LDIM	LIPID	ALKYL	NCOMP	STEROL	PEPTI	SUBER	FATTY	VM	HEX:PENT
	°N	— % TII —										%	
1	53.293	2.5	4.9	2.8	7.5	8.3	0.9	8.0	2.7	0.3	5.6	18.0	2.8
3	53.341	5.3	8.9	1.9	5.9	9.9	2.1	4.4	4.8	0.2	2.4	8.0	2.9
6	53.438	3.5	5.5	2.6	5.7	6.6	1.2	8.8	3.1	0.6	8.3	46.5	2.2
8	53.489	2.5	5.1	2.7	9.0	8.6	0.8	9.9	2.7	0.2	4.7	14.0	2.7
12	53.707	2.0	3.8	2.9	13.1	7.4	0.7	23.4	2.1	0.2	7.2	5.4	2.9

† CHYDR = carbohydrates; PHLM = phenols and lignin monomers; LDIM = lignin dimers; LIPID = lipids, alkanes, alkenes, fatty acids and n-alkyl esters; ALKYL = alkylaromatics; NCOMP = heterocyclic nitrogen and nitriles; STEROL = sterols; PEPTI = amides (amino acids, peptides and amino sugars); SUBER = suberin; FATTY = free fatty acids; VM = volatile matter; HEX:PENT = hexose:pentose. Letters indicate significant differences according to Tukey's HSD test ($p < 0.05$) between different locations.

3.5.2 Soil depth profiles as affected by land use

3.5.2.1 General soil characteristics

Table 3.4 shows chemical and physical properties of location 3 soil profiles. Soil pH ($p < 0.01$; grassland: 6.2 ± 0.2; forest: 5.1 ± 0.3; cultivated: 4.7 ± 1.3; mean ± standard deviation) and OC:TN ratios ($p < 0.05$; grassland: 11.8 ± 1.0; forest: 11.5 ± 1.4; cultivated: 7.8 ± 2.1) differed between land uses. Total C ($p < 0.001$, $r = -0.91$), OC ($p < 0.001$, $r = -0.85$), and TN ($p < 0.001$, $r = -0.93$) decreased with depth.

Table 3.4 Properties of location 3 soil depth profiles.

Land use	Depth	Horizon†	TC	OC	TN	OC:TN	pH	Sand	Silt	Clay
	cm		— g kg^{-1} —					— % —		
Grassland	Litter	F	77.4	75.0	7.1	10.6	6.1	NA‡	NA	NA
Grassland	0–5	Ah	45.6	45.4	4.1	11.0	6.1	69	15	17
Grassland	5–10	Ah	24.7	24.4	2.1	11.4	6.1	68	15	17
Grassland	10–15	Ah/Bm	22.9	20.2	1.8	11.1	6.3	66	13	21
Grassland	15–20	Bm	13.4	13.3	1.0	13.0	6.5	75	5	21
Forest	Litter	LF	329.6	305.6	21.5	14.2	5.7	NA	NA	NA
Forest	0–5	Ah	57.6	55.9	4.2	13.2	4.9	63	19	18
Forest	5–10	Ah/Aej	24.6	23.3	2.1	11.2	5.0	63	21	16
Forest	10–15	Aej	11.5	11.0	1.1	9.6	5.0	61	28	11
Forest	15–20	Aej/Bt	7.9	8.2	0.7	11.1	5.5	61	26	14
Cultivated	0–5	Ap	41.5	24.9	3.0	8.3	4.7	64	23	14
Cultivated	5–10	Ap	21.4	23.4	2.4	9.7	4.7	61	25	14
Cultivated	10–15	Ap/Bt	13.1	12.1	1.5	7.9	3.1	52	29	19
Cultivated	15–20	Bt	4.6	4.4	0.9	4.8	6.3	45	34	22

† Soil Classification Working Group (1998).
‡ Particle size only determinable in mineral soils.

3.5.2.2 Carbon and N *K*-edge X-ray absorption near edge structure

Features in C *K*-edge spectra of location 3 profiles (Fig. 3.5a; Table 3.5) were the same as those previously assigned (Fig. 3.2a), though the energy of the aromatic-C feature was slightly lower. Proportions of aromatic-C ($p < 0.001$, $r = -0.82$) and ketone ($p < 0.001$, $r = 0.79$) decreased with depth, while carboxyl:ketone ratios increased with depth ($p < 0.01$, $r = 0.72$).

Dominant N *K*-edge spectral features of location 3 profiles (Fig. 3.5b; Table 3.5) were the same at those previously assigned (Fig. 3.2b). Proportions of heterocyclic-N ($p < 0.05$, $r = -0.56$) and amide ($p < 0.001$, $r = -0.86$) tended to decrease with depth. Amide was higher in the

grassland profile than cultivated and forest profiles ($p < 0.01$). While not significant, the grassland profile had higher a proportion of alkyl-N than the cultivated profile ($p < 0.10$).

Peak heights of XANES features were subject to NMS ordination to visualize differences in SOM chemistry between land use depth profiles (Fig. 3.6). The final stress of the two-dimensional ordination was 3.0. A linear regression of NMS distances on the original Bray-Curtis distances indicated a goodness of fit with an R^2 of 0.997. Samples were not separated by land use, however the ordination separated deep increments (e.g., 15 – 20 cm) from other samples along the first NMS axis. These soils were correlated with high proportions of alkyl-N, carboxyl, and high carboxyl:ketone ratios. In contrast, aromatic-C, ketone, and heterocyclic-N were correlated with surface soils. Of the significantly correlated environmental variables, sand content and OC:TN ratios had positive scores along the second NMS axis, while silt content had negative values along this axis.

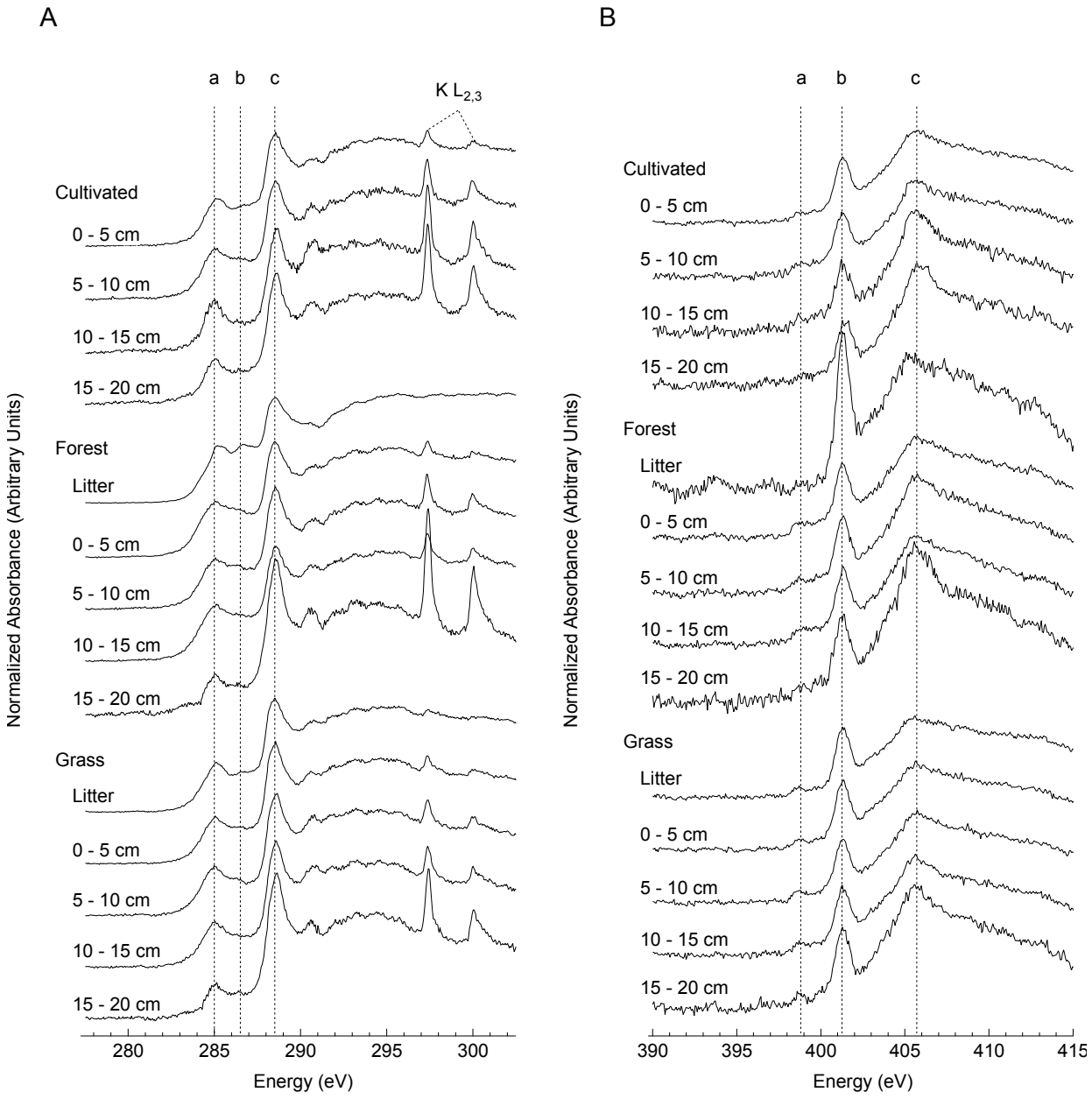

Fig. 3.5 (A) Carbon and (B) N *K*-edge X-ray absorption near edge structure (XANES) spectra of grassland, forest, and cultivated soil depth profiles from location 3. Depth increments (cm) are indicated above each spectrum. Carbon features are assigned as (a) aromatic-C at 285.0 eV; (b) ketone at 286.5 eV; and (c) carboxyl at 288.5 eV. Nitrogen features are assigned as (a) heterocyclic-N at 398.8 eV; (b) amide at 401.4 eV; and (c) alkyl-N at 405.5 eV.

Table 3.5 Carbon and N *K*-edge X-ray absorption near edge structure (XANES) peak heights of location 3 soil depth profiles.

Land use	Depth	Aromatic-C	Ketone	Carboxyl	Carboxyl: ketone	Heterocyclic-N	Amide	Alkyl-N
	cm	— Normalized absorbance (arbitrary units) —						
Grassland	Litter	0.24	0.15	0.52	3.51	0.04	0.46	0.18
Grassland	0–5	0.21	0.13	0.53	3.99	0.04	0.42	0.15
Grassland	5–10	0.22	0.12	0.50	4.05	0.04	0.36	0.17
Grassland	10–15	0.20	0.10	0.51	5.16	0.04	0.35	0.18
Grassland	15–20	0.11	0.04	0.56	13.08	0.03	0.33	0.16
Forest	Litter	0.33	0.30	0.57	1.89	–‡	0.51	0.26
Forest	0–5	0.26	0.20	0.51	2.55	0.05	0.36	0.18
Forest	5–10	0.22	0.16	0.51	3.23	0.03	0.33	0.16
Forest	10–15	0.26	0.18	0.48	2.66	0.04	0.32	0.13
Forest	15–20	0.10	0.03	0.50	18.39	0.02	0.29	0.22
Cultivated	0–5	0.23	0.15	0.53	3.47	0.03	0.37	0.18
Cultivated	5–10	0.22	0.13	0.48	3.59	0.04	0.34	0.20
Cultivated	10–15	0.19	0.05	0.42	9.03	0.03	0.27	0.24
Cultivated	15–20	0.15	0.06	0.46	7.20	0.01	0.29	0.23
Summary statistics of land use profiles†								
Grassland		0.19 ± 0.05	0.10 ± 0.04	0.53 ± 0.03	6.57 ± 4.37	0.04 ± 0.01	0.37 ± 0.04 a	0.17 ± 0.01
Forest		0.21 ± 0.07	0.14 ± 0.08	0.50 ± 0.01	6.71 ± 7.79	0.04 ± 0.01	0.32 ± 0.03 b	0.17 ± 0.04
Cultivated		0.20 ± 0.04	0.10 ± 0.05	0.47 ± 0.04	5.82 ± 2.75	0.03 ± 0.01	0.32 ± 0.05 b	0.21 ± 0.03
ANOVA		ns	ns	$p = 0.08$	ns	ns	$p < 0.01$	ns

† Values are means of mineral soil increments of each land use ± standard deviation; values with different lowercase letters are significantly different according to Tukey's HSD test ($p < 0.05$).

‡ Low signal to noise ratio prevented peak fitting.

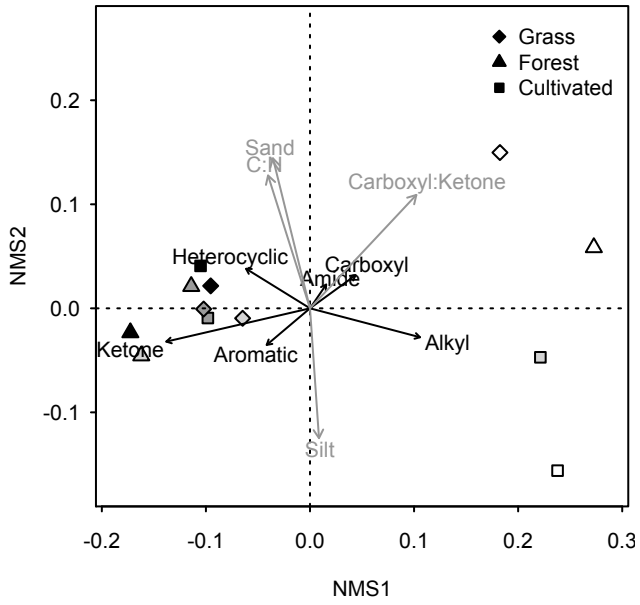

Fig. 3.6 Non-metric multidimensional scaling (NMS) analysis of C and N *K*-edge X-ray absorption near edge structure (XANES) peak heights from grassland, forest, and cultivated soil depth profiles from location 3. Vectors directions and lengths indicate the strength of the correlation between variables and the ordination. Black vectors correspond to XANES features used in the ordination. Gray vectors indicate significant (p < 0.05) correlations between the ordination and environmental variables (shown at ¼ scale for clarity). Symbol colors correspond to sample depth (cm): black = 0 – 5; dark gray = 5 – 10; light gray = 10 – 15; white = 15 – 20.

3.5.2.3 Pyrolysis-field ionization mass spectrometry

Mass spectra of surface soils and litter from different land uses at location 3 (Fig. 3.7), were dominated by similar *m/z* signals as those present in forest surface soils along the climosequence (Fig. 3.3). The PCA ordination (Fig. 3.8) separated samples by depth along the second PCA axis, while separation by land use was not discernable. Distinct features of the ordination are the large influence of *m/z* 394 and 396 to the forest soil 10 – 15 cm increment and increasing proportions of *m/z* 96 and 110 with depth. In most samples, SOM was primarily comprised of alkylaromatics, phenols and lignin monomers, and carbohydrates. Proportions of alkylaromatics ($p < 0.05$, $r = 0.60$), suberin ($p < 0.05$, $r = -0.63$; Fig. 3.8; Table 3.6), and thermostability ($p < 0.05$, $r = 0.62$; Fig. 3.9) varied with depth. While not significant, depth trends were also apparent in heterocyclic N ($p = 0.06$, $r = 0.56$) and log free fatty acids ($p = 0.09$, $r = -0.51$).

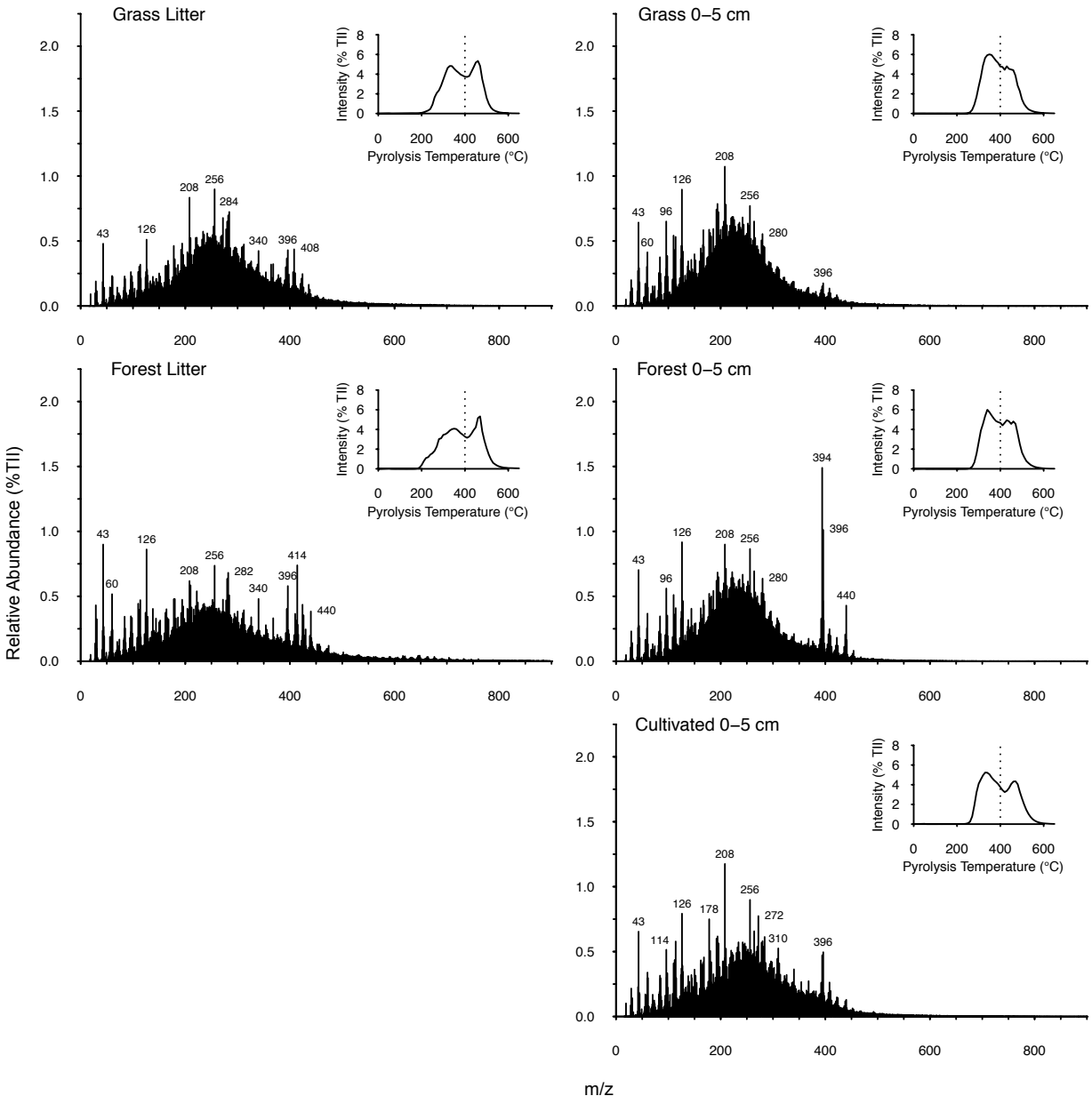

Fig. 3.7 Summed and averaged pyrolysis-field ionization mass spectrometry (Py-FIMS) mass spectra and thermograms of TII (inset) of litter and surface soils from grassland, forest, and cultivated soil depth profiles from location 3.

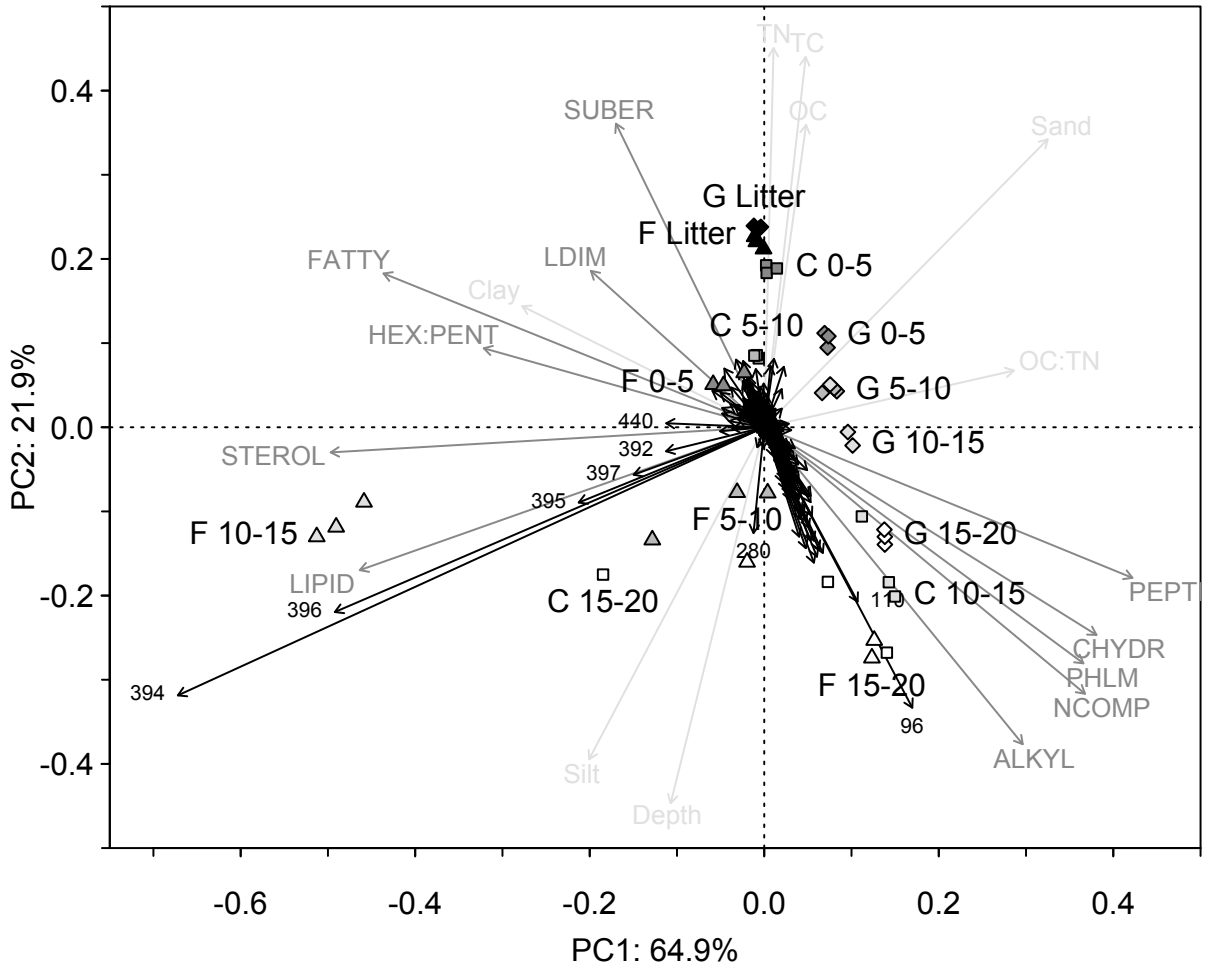

Fig. 3.8 Principal component analysis (PCA) of pyrolysis field ionization mass spectrometry (Py-FIMS) total ion intensities (TII) from grassland, forest, and cultivated soil depth profiles from location 3. Vectors directions and lengths indicate the strength of the correlation between variables and the ordination. Black vectors correspond to *m/z* signals. Dark gray vectors indicate significant ($p < 0.05$) correlations between the ordination and Py-FIMS compound classes (shown at ½ scale for clarity). Light gray vectors indicate significant ($p < 0.05$) correlations between the ordination and environmental variables (shown at ½ scale for clarity). Symbol labels indicate sample land use (G = grassland, F = forest, C = cultivated) and sample depth (cm).

Table 3.6 Relative ion intensities (% TII) of pyrolysis-field ionization mass spectrometry (Py-FIMS) compound classes† from location 3 soil depth profiles.

Land use	Depth	CHYDR	PHLM	LDIM	LIPID	ALKYL	NCOMP	STEROL	PEPTI	SUBER	FATTY	HEX: PENT
	cm	— % TII —										
Grassland	Litter	3.6	6.6	2.6	5.3	8.3	1.6	3.6	4.0	0.4	3.7	2.1
Grassland	0–5	5.8	10.2	1.6	4.5	10.5	2.5	1.5	5.6	0.1	1.7	2.3
Grassland	5–10	7.5	9.0	2.4	4.5	9.9	3.4	1.6	6.5	0.1	1.1	2.1
Grassland	10–15	6.7	8.8	2.8	5.1	10.7	3.1	1.2	5.9	0.1	0.6	2.1
Grassland	15–20	9.0	11.1	2.3	4.9	11.8	4.3	0.5	7.0	0.0	0.2	1.8
Forest	Litter	5.2	7.7	2.4	4.6	7.7	1.8	4.7	4.3	0.6	4.0	2.4
Forest	0–5	5.3	8.9	1.9	5.9	9.9	2.1	4.4	4.8	0.2	2.4	2.9
Forest	5–10	6.5	10.9	1.3	6.3	11.2	2.8	5.7	5.4	0.1	1.6	2.9
Forest	10–15	2.5	4.4	3.2	11.4	7.2	1.0	16.0	2.5	0.3	6.9	2.7
Forest	15–20	7.0	12.2	1.5	6.2	14.3	3.7	2.8	5.7	0.0	1.0	2.0
Cultivated	0–5	5.5	8.9	2.8	5.1	8.7	2.1	3.2	4.7	0.3	3.0	2.1
Cultivated	5–10	4.3	7.3	2.7	5.7	9.8	2.2	3.9	4.5	0.1	1.4	2.3
Cultivated	10–15	7.5	11.6	2.0	4.6	13.0	4.6	0.9	6.2	0.1	0.2	1.7
Cultivated	15–20	6.7	11.2	2.1	6.6	13.5	3.4	4.1	5.2	0.0	1.0	2.1

(continued on next page)

Table 3.6 - continued

Land use	CHYDR	PHLM	LDIM	LIPID	ALKYL	NCOMP	STEROL	PEPTI	SUBER	FATTY	HEX: PENT
	— % TII —										
Summary statistics of land use profiles‡											
Grassland	7.2 ± 1.3	9.8 ± 1.0	2.3 ± 0.5	4.7 ± 0.3 b	10.7 ± 0.8	3.3 ± 0.7	1.2 ± 0.5 b	6.3 ± 0.6	0.1 ± 0.0	0.9 ± 0.6	2.1 ± 0.2
Forest	5.4 ± 2.0	9.2 ± 3.3	1.9 ± 0.8	7.4 ± 2.5 a	10.7 ± 2.9	2.4 ± 1.1	7.1 ± 5.6 a	4.6 ± 1.4	0.1 ± 0.1	3.0 ± 2.5	2.6 ± 0.4
Cultivated	6.0 ± 1.5	9.8 ± 2.2	2.4 ± 0.5	5.5 ± 1.0 ab	11.3 ± 2.5	3.1 ± 1.2	3.0 ± 2.2 ab	5.2 ± 0.8	0.1 ± 0.1	1.4 ± 1.2	2.1 ± 0.3
ANOVA	ns	ns	ns	$p < 0.05$	ns	ns	$p < 0.05$	ns	ns	ns	$p = 0.05$

† CHYDR = carbohydrates; PHLM = phenols and lignin monomers; LDIM = lignin dimers; LIPID = lipids, alkanes, alkenes, fatty acids and n-alkyl esters; ALKYL = alkylaromatics; NCOMP = heterocyclic nitrogen and nitriles; STEROL = sterols; PEPTI = amides (amino acids, peptides and amino sugars); SUBER = suberin; FATTY = free fatty acids; HEX:PENT = hexose:pentose. Letters indicate significant differences according to Tukey's HSD test ($p < 0.05$) between different land uses at each depth.

‡ Values are means of mineral soil increments of each land use ± standard deviation; values with different lowercase letters are significantly different according to Tukey's HSD test ($p < 0.05$).

Differences between land use profiles were also apparent (Table 3.6). Forest soils were enriched in lipids ($p < 0.05$) and sterols ($p < 0.05$) relative to grassland and cultivated soils, decreasing in the order of forest > cultivated > grassland profiles. The forest profile also tended to have higher hexose:pentose ratios ($p = 0.05$). Thermostability tended to be lowest in the forest profile ($p = 0.07$; Fig. 3.9).

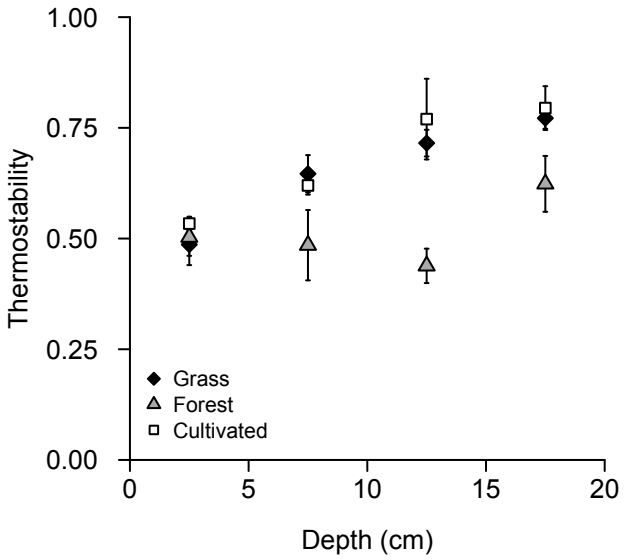

Fig. 3.9 Mean thermostability of organic matter in depth increments from grassland, forest, and cultivated soils from location 3. Arrows represent standard deviation.

3.6 Discussion

Generally, C and N *K*-edge XANES and Py-FIMS results agree with previous findings. Specifically, C *K*-edge XANES spectra (Figs. 3.2, 3.6) were dominated by carboxyl and displayed strong signals for aromatic-C (e.g., Jokic et al., 2003; Solomon et al., 2005; Lehmann et al., 2005, 2008; Schumacher et al., 2005; Gillespie et al., 2011, 2014; Kiersch et al., 2012a), while N *K*-edge XANES (Figs. 3.3, 3.7) displayed alkyl-N and heterocyclic-N features (e.g., Vairavamurthy and Wang, 2002; Gillespie et al., 2009, 2011, 2013; Leinweber et al., 2010; Kiersch et al., 2012b; Yannikos et al., 2014). The prominence of amide in N *K*-edge spectra is consistent with the notion that proteinaceous N is the dominant form of organic N in soils (Knicker and Kögel-Knabner, 1998; Schulten and Schnitzer, 1998; Olk, 2008). While Py-FIMS results typically fell within the range of reported values, forest soils (Tables 3.3, 3.6) had high

proportions of sterols and greater variability in the proportions of lipids, sterols, suberin, and fatty acids than commonly reported for Luvisols (Leinweber et al., 2009a; Thiele-Bruhn et al., 2014) and soils under poplar vegetation (Baum et al., 2013; Yannikos et al., 2014). In addition, all soils had low proportions of heterocyclic N and nitriles relative to soils from similar land uses and/or soil type (cf. Leinweber et al., 2009a; b; Gillespie et al., 2011; Heumann et al., 2011; Baum et al., 2013; Thiele-Bruhn et al., 2014; Yannikos et al., 2014). These differences are potentially attributable to differences in climate or management practices.

3.6.1 Effects of climate on surface soil organic matter chemistry

Predicted increases in temperature and moisture limitation in the region (Sauchyn and Kulshreshtha, 2008; Barrow, 2009) suggest that conditions at the northern end of the climosequence will become more similar to the current climate at its southern end, making reductions in latitude an ideal proxy for climate change. Despite a climatic gradient of ~0.7 °C MAT, we found SOM chemistry from soils along the climosequence to be remarkably similar, suggesting that climate change may have at most a modest effect on SOM chemistry. Only the alkyl-N XANES feature was significantly related to latitude. However, increases in alkyl-N did not occur consistently between sites (Table 3.2) nor were they large enough to be visually distinct in spectra (Fig. 3.2b). Indeed, differences in C and N *K*-edge XANES features across the climosequence were smaller than typically observed in soil spectra (cf. Gillespie et al., 2009, 2011, 2014; Kruse et al., 2010; Kiersch et al., 2012b; Yannikos et al., 2014). Trends in Py-FIMS compound classes were generally small, with differences across the climosequence having a similar or smaller magnitude to those reported (Leinweber et al., 2009a; Baum et al., 2013; Thiele-Bruhn et al., 2014; Yannikos et al., 2014), or were not strongly corroborated by C and N *K*-edge XANES (e.g., lipids, sterols, suberin, fatty acids; Table 3.3). Soils from different landscape positions at a single site (Gillespie et al., 2011) had greater variability in carbohydrates, lignin dimers, and heterocyclic-N and nitriles than found in the current study with sites located almost 50 km apart. These findings suggest that climatic effects on SOM chemistry may be insignificant compared to effects of other pedogenic factors that operate on a much smaller scale.

Though trends across the climosequence were minor, corroborating evidence from N *K*-edge XANES and Py-FIMS indicates that the proportion of N-containing compounds decreased

with latitude, and minor variations in C *K*-edge XANES may support observed increases in aliphatic and phenolic Py-FIMS compound classes with latitude. Decreases in the proportion of N-containing compounds with latitude suggest that SON is weakly related to MAT. This is consistent with findings that OC:TN ratios are negatively correlated to MAT (e.g., Barrett and Burke, 2000; Miller et al., 2004; Callesen et al., 2007; Homann et al., 2007) and positively correlated to MAP (e.g., Miller et al., 2004; Homann et al., 2007). Reductions in SON relative to SOC at the northern end of the climosequence are reflected in decreasing proportions of amides (Fig. 3.4; Table 3.3) and heterocyclic-N and nitriles (Table 3.3), as well as trends in OC:TN ratios (Table 3.1). Furthermore, increases in alkyl-N (Table 3.2) may reflect a residual enrichment of mineral-associated NH_4^+ (Kruse et al., 2011) as organic forms of N are reduced along this gradient. Location 1 forest soils are anomalous, with low proportions of N-containing compounds (Table 3.3), potentially caused by its fine soil texture relative to other sites along the transect (Table 3.1) due to its location on the boundary of the glacial deposit. Notably, while not a prominent spectral feature, minor increases in the feature at 287.2 eV (Fig. 3.2a)—representing changes in aliphatic- and phenolic-C—with increasing latitude may support the increases observed in associated Py-FIMS compound classes (Table 3.3), though variations are difficult to discern. As different soil size fractions are characterized by different proportions of plant- and microbially-derived compounds (Grandy and Neff, 2008), effects of texture on SOM chemistry may have obscured differences attributable to latitude, suggesting that minor changes in soil physical properties can overwhelm climatic effects.

While changes in SOM chemistry along the climosequence were modest, decreasing proportions of SON with latitude may result from differences in N inputs or degradation rates. Higher MATs at the southern end of the climosequence may enhance decomposition by increasing substrate availability (Curtin et al., 2012) and mineralization rates (Stanford et al., 1973), potentially leading to the relative enrichment of peptides and proteins during SOM maturation (Knicker, 2011). In contrast, decreases in SON with latitude may result from a decrease in microbial protein synthesis at the northern end of the climosequence. Nitrogen-limitation may restrict SOM degradation and lead to the relative enrichment of plant-derived compounds, potentially accompanied by increasing fungal dominance (Gillespie et al., 2014a). Indeed, lower proportions of phenols and lignin monomers relative to lignin dimers at northern locations along the transect (Table 3.3) may indicate less decomposition of lignin (Leinweber

and Schulten, 1995). Together with decreasing proportions of SON along the climosequence, this suggests a less decomposed state of SOM and increasing N-limitation. Additionally, increasing proportions of *m/z* 394 and 396 (dehydroergosterol and ergosterol, respectively) with latitude (Figs. 3.4, 3.5) suggest greater fungal biomass at the northern end of the transect, as the latter is produced almost exclusively by fungi (Djajakirana et al., 1996). These trends suggest that SOM degradation may be constrained by climatic conditions at northern locations along the climosequence, and may account for the slight decrease in SON compounds along this gradient.

3.6.2 Effects of land use on soil organic matter chemistry

Like trends with latitude, differences in surface SOM chemistry attributable to land use were small. No differences between land uses were detectable in C and N *K*-edge XANES spectra (Figs. 3.2, 3.3), suggesting that land use only modestly affects SOM chemistry. This supports previous findings that broad land use categories are poor predictors of SOM chemistry, having undetectable (Grandy et al., 2009) or only minor (Guggenberger et al., 1995) effects on SOM composition.

Despite the small magnitude of land use effects, C and N *K*-edge XANES peak heights revealed minor differences in SOM chemistry of surface soils (Table 3.2), suggesting that shifts from aspen forest to grassland or cultivated land use will alter SOM chemistry in different directions. Forest soils had greater proportions of ketones and carboxyls than grassland and cultivated soils, respectively, but had the lowest carboxyl:ketone ratios, suggesting that forest soils are relatively biodegraded (Gillespie et al., 2014b; a). In contrast, grassland soils had high proportions of carboxyls and amides as well as the highest carboxyl:ketone ratios, indicating that they contain primarily labile SOM. Nitrogen *K*-edge XANES peak heights (Table 3.5) and Py-FIMS (Table 3.6) of land use depth profiles were consistent with this finding, revealing higher proportions of amide in the grassland profile than forest or cultivated profiles. Finally, the relatively low proportions of carboxyls and amides in cultivated soils (Tables 3.2, 3.5) suggest that tillage results in their depletion. Findings of land use effects on SOM chemistry have thus far been inconsistent (e.g., proportion of amides in grassland and cultivated soils; c.f. Schnitzer et al., 2006; Leinweber et al., 2009b) or from incomparable land uses (e.g., Fernandez et al., 2012; Pisani et al., 2013). Notably, our findings did not support previous evidence that cultivation increases the proportion of heterocyclic-N (Schnitzer et al., 2006; Leinweber et al., 2009b; Gillespie et al., 2011).

3.6.3 Soil organic matter chemistry in soil depth profiles

Carbon and N *K*-edge XANES and Py-FIMS revealed that depth more strongly influences SOM chemistry than land use or climate. This is evident in the clear ordering of samples by depth in the ordinations (Figs. 3.8, 3.10), as well as the higher variability in C and N *K*-edge XANES peak heights and Py-FIMS compound classes across depth increments than across land use types (Tables 3.5, 3.6) or length of the transect (Tables 3.2, 3.3). This supports previous findings that SOM chemistry shows marked changes with depth (e.g., Djukic et al., 2010; Vancampenhout et al., 2012) and that subsoil SOM is highly influenced by pedogenic processes such as eluviation (e.g., Rumpel et al., 2002, 2004; Feng and Simpson, 2007).

Increasing proportions of labile SOM components (e.g., increasing carboxyl:ketone ratios, carbohydrates; Tables 3.5, 3.6) and plant-derived compounds (e.g., decreasing hexose:pentose ratios; Table 3.6) indicate that the degree of microbial processing decreases with depth. This may be at least partially attributable to increasing proportions of SOM in organo-mineral associations with depth as indicated by increasing thermostability, particularly in cultivated and grassland profiles (Fig. 3.9), as the proportion of mineral-bound OM typically increases with depth and differs in SOM chemistry from particulate OM (Kögel-Knabner et al., 2008). For example, carboxyl-C is often enriched in mineral-associated OM, reflecting increased oxidation of SOM (Kögel-Knabner et al., 2008) or stabilization of labile carboxylic acids mobilized as DOM and rapidly adsorbed in subsoils (van Hees et al., 2003).

Evidence from both Py-FIMS (Fig. 3.8; Table 3.6) and C and N *K*-edge XANES (Figs. 3.6, 3.7; Table 3.5) suggests that cultivated and grassland soil profiles are more homogenous with depth than the forest profile. The vertical distribution of SOM components is influenced by both subsoil OM inputs, including plant roots and exudates, DOM, bioturbation, and translocation of free or bound OM, as well as by pedological processes (Rumpel and Kögel-Knabner, 2011). The clear ordering of grassland increments in the PCA ordination (Fig. 3.8) suggests relatively homogenous SOM chemistry and may arise from bioturbation, a common process in prairie soils of the region (Pennock et al., 2011). In contrast, bioturbating animals (Zaitlin and Hayashi, 2012) are generally absent from forest soils in the boreal region of Saskatchewan, enhancing horizonation and consequently, the vertical stratification of various SOM constituents, visible in the relatively wide spread of forest soil increments (Figs. 3.8, 3.10). The separation of the two upper increments of the cultivated profile from the deeper two (Figs.

3.8, 3.10) coincides with the depth of tillage in this profile (11 cm), implying that cultivation has homogenized and altered surface soil SOM chemistry.

Characteristics of the cultivated profile suggest a lasting influence of historical vegetative inputs on SOM chemistry. In the PCA ordination (Fig. 3.8), the uppermost increment of the cultivated profile is located adjacent to the forest and grassland litter samples, suggesting the incorporation of litter into the tillage profile upon land use conversion. Further support for the preservation of SOM constituents following conversion to cultivated land use is the intensity of the *m/z* signal for ergosterol in the two plowed increments, which decreases in the order of forest > cultivated > grassland at these depths. Ergosterol content of cultivated soils is typically lower than that of either grassland or forest soils (Djajakirana et al., 1996), suggesting that the relatively high proportion of ergosterol in the cultivated soil profile may be a remnant of previous vegetation. Indeed, the influence of historical vegetation on SOM chemical composition has been reported in studies of different land use types (Dümig et al., 2009; Pisani et al., 2013), including cultivated soils (Sleutel et al., 2008, 2011).

3.7 Conclusions

The joint application of C and N *K*-edge XANES and Py-FIMS to a climosequence of native grassland, native aspen forest, and cultivated soils revealed that differences in land use and climate lead to only modest differences in SOM chemistry, despite controlling for confounding pedogenic processes such as parent material, topography, and soil age. Remarkably, soil depth profiles showed greater variability in SOM chemistry over 20 cm than was apparent in surface soils across the 46-km climosequence and despite broad differences in land use, with the vertical stratification of SOM components reflecting land use specific processes (e.g., bioturbation, tillage). Our findings suggest that within-profile dynamics have a greater effect on SOM chemistry than processes operating on landscape (e.g., land use) and regional (e.g., climate) scales.

The observed similarity of SOM chemistry in soils regardless of latitude or land use indicates that SOM chemistry at the prairie-forest ecotone in Saskatchewan is largely unresponsive to changes in MAT on the scale of those predicted to occur with climate change (~0.7 °C) and associated shifts in land use. We found little evidence for the evolution of SOM chemistry with latitudinal changes in climate and land use, suggesting a uniform metabolism of

different biochemical compounds regardless of their intrinsic stability, with no indication that relatively labile SOM components are preferentially degraded. This suggests that any reductions in SOM along the latitudinal gradient are controlled by factors other than biochemical composition, in line with emerging views of SOM turnover (Marschner et al., 2008; Kleber et al., 2011; Schmidt et al., 2011; Dungait et al., 2012).

Limitations of individual analytical techniques necessitate a multi-methodological approach when examining SOM chemistry (Leinweber et al., 2009a, 2013). Here we successfully combine complementary C and N *K*-edge XANES and Py-FIMS techniques to elucidate the chemical nature of SOM from a climosequence of soils in Saskatchewan, interpreting agreements between the techniques as strong evidence of SOM chemical quality. We attributed discrepancies between C and N *K*-edge XANES and Py-FIMS to both their fundamentally different perspectives of SOM chemistry (i.e., electronic structure of molecules vs. nominal masses of ionized molecules) as well as their limitations. For example, soft X-rays used in C and N *K*-edge XANES are inherently surface-sensitive (Sham and Rivers, 2002), and overlapping resonances make unambiguous assignment of spectral features difficult (Leinweber et al., 2007). Likewise, the sensitivity of Py-FIMS is limited due to the soft nature of field ionization required to reduce fragmentation (Schulten and Leinweber, 1996), and, while the step-wise heating process utilized in Py-FIMS transfers less energy to samples than flash-pyrolysis methods, there is nevertheless a possibility for pyrolytic formation of heterocyclic-N artifacts (Leinweber et al., 2013). Clearly, limitations of various analytical techniques highlight the need for multiple methods to obtain a more comprehensive understanding of SOM chemistry, as results from a single analytical technique may be misleading and provide only a limited understanding of SOM chemical quality.

4. BIOLOGICAL STABILITY OF SOIL ORGANIC MATTER AND RELATION TO ORGANIC MATTER CHEMISTRY ALONG AN ECOTONAL CLIMOSEQUENCE[1]

4.1 Preface

The previous chapter demonstrated that only minor variations in SOM chemistry occurred with differences in climate and land use along a latitudinal transect in north-central Saskatchewan. However, SOM persistence is also influenced by organo-mineral interactions and accessibility. As such, despite a similar chemistry, variations in the biological stability of SOM along the climosequence may occur nonetheless. In this chapter, we aim to relate SOM chemistry to the biological stability of SOM as measured in a long-term aerobic laboratory incubation. Assays of biological stability directly measure the persistence of SOM, regardless of the mechanisms influencing its stability. As such, this study examines the 'real-world' differences in SOM pools as affected by climate and land use to improve predictions of changes in soil C storage and N supply at the grassland-forest ecotone in Saskatchewan.

[1] This manuscript is currently in preparation for publication. Coauthors include Dan Pennock, Peter Leinweber, and Fran Walley, all of whom provided invaluable contributions to the funding of research, assistance in facilitation of laboratory analyses and data interpretation, as well as editing this manuscript. Both Dan Pennock and Fran Walley conceptualized the study design.

4.2 Abstract

Understanding the relationship between SOM decomposition dynamics and climate change is essential to predicting future SOM stocks and potential climate change feedbacks. Here, we employ a space-for-time substitution to explore the effects of climate change on the susceptibility of SOM to degradation. Using a 24-wk laboratory incubation, we examine C and N mineralization in native grassland, native trembling aspen, and cultivated soils along a latitudinal climosequence at the grassland-forest ecotone in central Canada to evaluate the effect of climate shifts and associated land use changes on SOM biological stability. Furthermore, we investigate the role of SOM chemistry, measured using XANES spectroscopy and pyrolysis-field ionization mass spectrometry (Py-FIMS), on SOM stabilization.

Despite a MAT gradient of only ~0.7 °C along the transect, laboratory incubation revealed large changes in SOM stability with latitude along the climosequence. Soils from cooler, moister sites at the northern end of the transect contained a greater proportion of labile SOM: from the southernmost to the northernmost site along the climosequence, proportions of C mineralized ranged from 10.7 to 42.3% and proportions of N mineralized ranged from 0.9 to 10.3%. Furthermore, land use differences in SON stability were revealed, and tended to decrease in the order of grassland < cultivated < forest soils. Finally, SOM chemistry did not vary predictably with measures of biological stability, and did not evolve consistently across soils and litter from different land uses throughout the incubation. These findings suggest the biological stability of SOM is influenced by climate, and to a lesser degree, land use, with SOM in forests from the northern end of the climosequence being the most susceptible to degradation with climate change. Our exploration of SOM chemistry as a regulation on decomposition indicates that biochemical recalcitrance alone does not determine SOM stability at the boreal forest ecotone, suggesting that other stabilization mechanisms such as physico-chemical protection are involved.

4.3 Introduction

Understanding the response of soil C and N dynamics to climate change is essential to predicting future SOM stocks. Changes in global MAT, predicted to be 0.3–0.7 °C for the period of 2016–2035 (relative to 1986–2005; IPCC, 2013), may alter SOM pools by increasing C (Raich and Schlesinger, 1992) and N mineralization (MacDonald et al., 1995). However, while

soils represent a large SOC pool—containing 2000 Pg C (Janzen, 2004)—various chemical components of SOM may be differently susceptible to biodegradation, making predictions of future SOM stocks difficult. Accordingly, there is a need to determine the proportion of SOM susceptible to degradation in a warmer climate, particularly in regions sensitive to climate change.

The climate-driven ecotone at the prairie-forest boundary in central Canada is one such vulnerable region (Hogg, 1994; Williams et al., 2009). Here, MAT is expected to increase 2 °C by 2020 (relative to 1961–1990; Sauchyn and Kulshreshtha, 2008). Accompanying increases in evapotranspiration (Hogg and Hurdle, 1995; Sauchyn and Kulshreshtha, 2008; Barrow, 2009) may lead to rapid shifts in dominant plant species, as evidenced by paleoclimate records (Williams et al., 2009). Likewise, a northern shift in plant hardiness zones (McKenney et al., 2014) and ongoing deforestation (Fitzsimmons, 2002) in the region indicate that native lands will continue to be converted to agricultural production at the southern boundary of the boreal forest.

Both climate and land use may affect SOM decomposition and consequently, future SOM stocks. Climate can alter decomposition directly, as microbial decomposition of SOM is temperature dependent (Davidson and Janssens, 2006; Conant et al., 2011), and indirectly, with temperature influencing rates of chemical processes involved in SOM protection and stabilization. Temperature controls the adsorption of SOM to mineral surfaces and regulates enzyme production, which is involved in aggregate formation (Davidson and Janssens, 2006; Conant et al., 2011). However, findings of climatic effects on mineralization pool size and dynamics are conflicting (e.g., MacDonald et al., 1995; Douglas et al., 1998; Giardina and Ryan, 2000; Franzluebbers et al., 2001; Dalias et al., 2001; Paré et al., 2006; Meyer et al., 2006; Bolinder et al., 2007; Hilli et al., 2008; Dessureault-Rompré et al., 2010). Land use can also influence SOM stabilization (John et al., 2005; Kögel-Knabner et al., 2008) through differences in inputs and disturbances (Six et al., 2002). Consequently, differences in land use may also affect SOM mineralization in soils from different vegetation types (Raich and Tufekcioglu, 2000; Arevalo et al., 2012), land uses (Ajwa et al., 1998; Arevalo et al., 2012), or tree species (Giardina et al., 2001).

However, SOM decomposition is regulated not only by physical protection and chemical stabilization, but is also modified by biochemical quality (Conant et al., 2011). While the notion that inherent biochemical recalcitrance determines SOM persistence has recently been

questioned (Marschner et al., 2008; Kleber, 2010; Schmidt et al., 2011; Dungait et al., 2012), SOM chemistry remains important as it can influence other stabilization mechanisms (von Lützow et al., 2006). For example, peptides may play an important role in the formation of organo-mineral associations (Knicker, 2011), and SON chemistry may limit or enhance SOC decomposition (Hessen et al., 2004; Craine et al., 2007; Knicker, 2011). However, linking changes in climate and land use to SOM chemistry and biological stability remains to be fully explored. Climate may affect SOM chemistry (e.g., Amelung et al., 1997, 1999a; b, 2006; Sjögersten et al., 2003; Glaser and Amelung, 2003; Dalmolin et al., 2006; Montané et al., 2007; Djukic et al., 2010; Xu et al., 2010), which in turn may alter biological stability. Vegetation changes may also alter SOM chemistry via inheritance of chemical compounds from plant inputs (Filley et al., 2008; Stewart et al., 2011), while cultivation may lead to the selective enrichment of stable compounds such as heterocyclic N (Schnitzer et al., 2006; Leinweber et al., 2009b; Gillespie et al., 2011).

Our goal was to assess the effects of latitude and land use on the susceptibility of SOM to degradation, using grassland, forest, and cultivated soils across a climosequence at the grassland-forest ecotone in Saskatchewan, Canada as an analogue for the future effects of climate change. We accomplished this by characterizing the biological stability of SOM using readily mineralizable C and potentially mineralizable N—evaluated during a 24-wk incubation—as indicators of labile SOM stocks (Haynes, 2005). Additionally, we aimed to relate SOM stability to its chemistry using synchrotron-based XANES spectroscopy and Py-FIMS. Finally, we evaluated changes in SOM chemistry during incubation to further explore the link between lability and substrate chemistry.

4.4 Materials and Methods

4.4.1 Sites and sampling design

The study area comprises a 46-km climosequence in west-central Saskatchewan described by Purton et al. (2015). Briefly, MAP ranges from 418 to 443 mm and MAT ranges from 0.9 to 0.2 °C from the southern to northern end of the climosequence (Hijmans et al., 2005). Dominant vegetation in this region has been relatively static since deglaciation, aside from a period of forest encroachment from 6–2 ka (Williams et al., 2009). To control for confounding effects of other pedogenic factors, sites were located on a uniform glacial till

deposit ('Ice Stream 1' described by Ó Cofaigh et al., 2009) and soils were sampled from midslope positions. In twelve locations (Fig. 3.1) mineral surface soils (0–5 cm) were sampled from paired native trembling aspen forest and cultivated sites, with paired native grassland sites (n = 4) sampled where available. At native sites, litter material was collected separately. To further explore land use differences, soils were collected in 5-cm increments to a depth of 30 cm at adjacent location 3 sites. Soils were classified according to the Canadian System of Soil Classification (Soil Classification Working Group, 1998).

4.4.2 Soil properties

Samples were air-dried and ground prior to determination of soil properties. Total and organic C contents were determined by combustion using a LECO CR-12 (LECO Corp, St. Joseph, MI); prior to analysis of OC content, samples were acidified with vapors from concentrated HCl. Total N was determined using a LECO CNS-2000 (LECO Corp, St. Joseph, MI). Soil pH was measured in $CaCl_2$ (Hendershot et al., 2008). Particle size distributions of mineral samples were assessed using the modified pipette method (Indorante et al., 1990), after samples were pretreated with 30% H_2O_2 to remove OM.

4.4.3 Readily mineralizable C

Readily mineralizable C was assessed on a subset of grassland and forest surface soils (n = 4, and 10, respectively) and litter samples (n = 1, 5, respectively) in triplicate, using the procedure described by Hopkins (2008). Three empty vials were included in the assay as blanks. Briefly, 15 g dry-weight equivalent of field-moist soil was sieved to 2 mm and 5 g dry-weight equivalent of litter was sieved to 4 mm before being placed in a 110 mL plastic vial. Samples were adjusted to 22.5% moisture (w/w) with deionized H_2O, covered with a perforated plastic lid, and incubated at 25 °C and 85-90% relative humidity. Samples were preincubated for 14 d to allow equilibration to occur. Once weekly throughout the 24-wk incubation, lids were removed and vials were placed into 1 L glass jars containing a vial of 10 mL deionized H_2O to prevent sample drying. Jars were sealed with airtight lids fitted with rubber septa. Background gas samples were taken immediately before incubation in the sealed jars, and gas samples from each jar were taken after 6 h during the first two samplings and after 24 h for all subsequent sampling dates. During sampling, the headspace of each jar was thoroughly mixed and ~20 mL of gas was extracted using a polypropylene syringe and injected into an 12 mL evacuated glass vial

(Exetainer®, Labco Ltd.) containing approximately 2 mg of $Mg(ClO_4)_2$ and fitted with silicon and rubber septa. Carbon dioxide concentrations were analyzed using a Varian CP-4900 Micro Gas Chromatograph (Varian Inc.) using 400 ppm and 2000 ppm CO_2 standards for calibration. Moisture was adjusted weekly with deionized H_2O.

Concentrations of CO_2 were converted from ppm to mg CO_2-C using the ideal gas law, with pressure considered constant at 101.3 kPa. Cumulative respiration over the 24-wk incubation was calculated from weekly respiration rates according to Paré et al. (2006), with the equation:

$$C_t = C_{t-1} + (k_p + k_{p-1})/2 \times (JJ_p - JJ_{p-1}) \quad \text{Eq. 4.1}$$

where C_t is mineralized C (mg kg^{-1}) at time t (d), k is the daily respiration rate (mg kg^{-1} d^{-1}), p is the incubation period (1–24), and JJ is the Julian day.

4.4.4 Potentially mineralizable N

Following the procedure described by Curtin and Campbell (2008), potentially mineralizable N was determined for grassland, forest, and cultivated samples in triplicate, including climosequence surface soils (n = 4, 11, and 8, respectively), litter (n = 2, 7, and 0, respectively), and location 3 subsoils (n = 5, 5, and 5, respectively). Briefly, soil and litter samples were sieved and weighed as described for the C mineralization assay, then were mixed in a 1:1 ratio with acid-washed sand (GRANUSIL®, GHP Systems, Inc.) to facilitate drainage. Six sand blanks were included in the incubation. Samples were incubated in Buchner funnels containing a glass microfiber pad (type GF/B, Whatman®, GE Co.) placed between 30 µm nylon mesh. Glass microfiber pads were also placed on sample surfaces to reduce soil disturbance during leaching. Samples were preleached prior to incubation. Samples were brought to 22.5% moisture (w/w) with deionized H_2O, covered with perforated parafilm and incubated at the same conditions described in the C mineralization assay to facilitate direct comparison of estimated parameters. Sample moisture was adjusted weekly with deionized H_2O. Samples were extracted with 100 mL 0.01 *M* $CaCl_2$ followed by 25 mL N-free nutrient solution at wk 2, 4, 6, 8, 12, 16, 20, and 24. During extraction, vacuum suction was used to reduce samples to 15% moisture (w/w). Leachates were collected and sample moisture was adjusted to 22.5% (w/w) with

deionized H_2O before being replaced in the incubation chamber. Leachates were analyzed for NO_3^- and NH_4^+ using a Technicon AutoAnalyzer (Technicon Industrial Systems).

4.4.5 Model parameterization

Model parameterization was performed using R statistical software (v. 3.0.2; R Core Team, 2013), using package nlrwr (Ritz and Streibig, 2008). For both C and N mineralization data, various kinetic models (Table 4.1) were fit using least squares nonlinear regression. Model fits were tested to determine which model best described the data using the procedure outlined by Ritz and Streibig (2008), with the aim of utilizing a common equation for all samples to enable comparison of parameters while minimizing residuals. Data from three subsamples was used to parameterize cumulative C and N mineralization curves for each sample.

Table 4.1 Kinetic models tested for goodness-of-fit in describing mineralization data (adapted from Nieder and Benbi, 2008).

Eq.	Model	Formula†	Reference(s)
4.2	Zero-order (ZO)	$N_t = K_t$	Tabatabai and Al-Khafaji (1980); Addiscott (1983)
4.3	First order single compartment (FOSC)	$N_t = N_0(1\text{-}e^{-kt})$	Stanford and Smith (1972)
4.4	First order double compartment (FODC)	$N_t = N_d(1\text{-}e^{-k_d t}) + N_r(1\text{-}e^{-k_r t})$	Molina et al. (1980); Nuske and Richter (1981); Deans et al. (1986)
4.5	First order plus zero order (FOZO)	$N_t = N_d(1\text{-}e^{-k_d t}) + K_t$	Bonde and Rosswall (1987); Lindemann et al. (1988); Seyfried and Rao (1988)

† where N_t = cumulative N mineralized (mg kg^{-1}) at time t (d); K = zero-order rate constant (d^{-1}); N_0 = N mineralization potential (mg kg^{-1}); k = first order rate constant (d^{-1}); N_d = readily decomposable organic N fraction (mg kg^{-1}); k_d = first order rate constant of N_d (d^{-1}); N_r = recalcitrant organic N fraction (mg kg^{-1}); k_r = first order rate constant of N_r (d^{-1}).

4.4.6 Carbon and N K-edge X-ray absorption near edge structure

Three surface soils (location 2) and two litter samples (location 1) from the N mineralization assay were subsampled at weeks 0, 2, 4, and 8 of the incubation. Subsamples were frozen at -80 °C prior to being lyophilized and pulverized with a ball mill. Spectra were collected at the spherical grating monochromator (SGM) beamline 11ID-1 at the CLS (Saskatoon, SK, Canada). At the C and N *K*-edges, this beamline has a resolving power ($E/\Delta E$) greater than 10^4 and delivers 10^{11} photons s^{-1} (Regier et al., 2007a; b). Prior to acquisition, ~1 mg of each sample was mixed with deionized H_2O, deposited on a freshly Au-coated Si wafer, and air-dried. Conductive C tape (SGE, Toronto, ON, Canada) affixed wafers to sample plates.

Spectra were acquired in fast-scanning mode with the exit slit set at 25 μm (e.g., Gillespie et al., 2014b; a). Partial fluorescence yield scans of a subset of climosequence surface soils (n = 8) and litter (n = 3) were collected using a silicon drift detector (SDD) in February 2014. Total fluorescence yield N *K*-edge scans of soils and litter subsampled during the incubation were collected in May 2013 using a two-stage micro channel plate detector; C *K*-edge PFY scans of these samples were collected using a SDD in September 2013. Each scan was collected for 20 s (Gillespie et al., 2014a; b) from a fresh location to reduce X-ray exposure (Leinweber et al., 2007). Carbon and N *K*-edge energies were calibrated using the $1s \rightarrow \pi^*_{C=O}$ transition at 288.6 eV (Kim et al., 2003) of citric acid and the $1s \rightarrow \pi^*$ vibrational manifold of N_2 gas evolved from $(NH_4)_2SO_4$ at 400.8 eV (Gillespie et al., 2008), respectively.

Spectra were processed using custom macros in Igor Pro (ver. 6.2, WaveMetrics Inc., Lake Oswego, OR, USA) and using the Athena software package (Ravel and Newville, 2005). Spectra were normalized to the incident flux (I_0) using measurements of a Au-coated Si wafer. To account for C contamination of beamline optics (Watts et al., 2006), I_0 measurements at the C *K*-edge were scaled and offset prior to normalization. Data from a minimum of 15 (TFY) or 30 (PFY) scans produced the averaged spectra of each sample. Averaged spectra were background corrected with a linear regression fit through the pre-edge region and were scaled to an edge step of unity. Features at the C and N *K*-edges were assigned according to the literature (Myneni, 2002; Urquhart and Ade, 2002; Dhez et al., 2003; Cooney and Urquhart, 2004; Hardie et al., 2007; Leinweber et al., 2007; Solomon et al., 2009; Kruse et al., 2011). A background arctangent function parameterized as $f(x) = a_1 * \text{atan}[(x - a_2) * a_3] + a_4$ (Rovezzi et al., 2009) and a series of Gaussian peaks were fitted to the normalized XANES spectral features using the Fityk software package (version 1.2.1; Wojdyr, 2010). Curve parameters were constrained to ensure equal width of all $1s \rightarrow \pi^*$ features. Ratios of peak heights were calculated to determine the relative abundance of carboxyls-to-ketones (carboxyl:ketone), thought to be related to mineralization potential (Gillespie et al., 2014b).

4.4.7 Pyrolysis-field ionization mass spectrometry

Approximately 5 mg of location 3 soil increments (to a depth of 20 cm) were air-dried and pulverized prior to being pyrolyzed in the ion source (emitter: 4.7 kV, counter electrode -5.5 kV) of a double-focusing Finnigan MAT 95. Samples were heated from 50 °C to 650 °C, in 10

°C steps over 15 minutes in a 10^{-4} Pa vacuum. To prevent pyrolysis product residues, the emitter was flash heated between magnetic scans. For each sample, 65 spectra were recorded over the mass range 15–900 *m/z*. Ion intensities were normalized to 1 mg of the sample. Marker signals (*m/z*) were assigned to relevant substance classes according to the literature (Hempfling et al., 1988; Schnitzer and Schulten, 1992; Schulten and Leinweber, 1996; van Bochove et al., 1996; Leinweber et al., 2009a, 2013). Compound classes used in data amalgamation were: carbohydrates, phenols and lignin monomers, lignin dimers, lipids (lipids, alkanes, alkenes, fatty acids and n-alkyl esters), alkylaromatics, heterocyclic N (and nitriles), sterols, amides (amino acids, peptides and amino sugars), suberin, and free fatty acids. Additionally, Py-FIMS analyses yielded information on ratios of hexoses-to-pentoses (hexose:pentose), interpreted as a measure of microbial origin of SOM (Cheshire et al., 1990). Thermostability, a measure predicting resistance to microbial degradation (Leinweber et al., 2008), was calculated as mass loss over 400–650 °C relative to mass loss over the whole temperature range.

4.4.8 Statistics

Statistical analyses were conducted using the R software package (ver. 3.0.2, R Core Team, 2013). Variables were tested for normality using Shapiro-Wilk's test and homogeneity of variance between land uses was assessed using Levene's test. Non-normally distributed variables were transformed prior to analysis. Relationships between response variables and both latitude and depth were tested using linear regression. Univariate ANOVA was used to test for land use effects, with Tukey's range tests used for post-hoc comparisons. Mixed-effects models were used when analyzing samples from depth profiles. In surface soils, Pearson correlations between C and N mineralization parameters and XANES (n = 7, 9, respectively) and Py-FIMS (n = 5, 6, respectively) variables were calculated and tested for significance. Likewise, correlations between N mineralization parameters and SOM chemistry variables were calculated (n = 12) for soil depth profiles.

4.5 Results

4.5.1 General soil characteristics

General characteristics of climosequence surface soils have been described previously (Purton et al., 2015). Briefly, our aim was to select sites located on a uniform glacial till deposit. The similarity in particle size distributions (Table 4.2) at all locations support their genesis on the

same glacial ice stream unit (Ó Cofaigh et al., 2009) with the exception of the forest site at location 1, which was not included in the mineralization assays. Clay content decreased with latitude ($p < 0.001$, $r = -0.62$), in accordance with the flow direction of the ice-stream. Additionally, TC ($p < 0.01$, $r = -0.51$), OC ($p < 0.05$, $r = -0.45$), and TN ($p < 0.001$, $r = -0.67$) decreased with latitude while log OC:TN increased with latitude in surface soils ($p < 0.01$, $r = 0.55$) and in litter samples ($p < 0.01$, $r = 0.71$; Tables 4.2, 4.3).

Table 4.2 Locations and properties of climosequence surface soils used in incubation.

Land use	Location	Latitude	Longitude	TC	OC	TN	OC:TN	pH	Sand	Silt	Clay	— Soil classification —		
		°N	°W	— g kg^{-1} —					— % —			Canadian†	WRB‡	USDA§
Grassland	1	53.294	108.760	49.7	43.8	4.2	10.4	5.7	49	26	25	O.BLC	CH-cc	C.Haplocryoll
Grassland	2	53.321	108.777	44.5	39.0	4.2	9.3	7.0	69	12	19	CA.BLC	CL-ha	T.Calcicryoll
Grassland	3	53.341	108.764	45.5	45.4	4.1	11.1	6.1	68	17	15	O.BLC	CH-cc	C.Haplocryoll
Grassland	6	53.438	108.765	29.6	25.2	2.5	10.1	7.0	81	6	13	O.BLC	CH-cc	C.Haplocryoll
Forest	2	53.319	108.776	63.8	55.8	5.4	10.3	5.4	64	17	19	D.GL	LV-ct-hu	T.Haplocryalf
Forest	3	53.341	108.765	57.6	55.9	4.2	13.3	4.9	62	21	17	D.GL	LV-ct-hu	T.Haplocryalf
Forest	4	53.365	108.775	13.2	12.6	1.2	10.5	5.1	84	6	10	BR.GL	LV-ct-ap	T.Haplocryalf
Forest	5	53.394	108.785	25.9	27.6	2.6	10.6	5.1	58	28	13	D.GL	LV-ct-hu	T.Haplocryalf
Forest	6	53.438	108.764	78.9	71.3	4.8	14.9	5.2	56	31	13	BR.GL	LV-ct-ap	T.Haplocryalf
Forest	7	53.449	108.772	23.1	21.5	2.0	10.8	5.7	50	36	14	D.GL	LV-ct-hu	T.Haplocryalf
Forest	8	53.489	108.809	30.9	32.1	2.1	15.3	5.5	65	20	15	D.GL	LV-ct-hu	T.Haplocryalf
Forest	9	53.509	108.755	18.8	19.2	1.5	12.8	5.4	69	24	7	BR.GL	LV-ct-ap	T.Haplocryalf
Forest	10	53.565	108.801	36.9	31.9	1.8	17.7	4.5	51	40	9	O.GL	LV-ct	T.Haplocryalf
Forest	11	53.628	108.765	20.8	20.4	1.2	17.0	5.4	64	31	5	O.GL	LV-ct	T.Haplocryalf
Forest	12	53.707	108.805	6.1	5.9	0.4	14.8	4.9	67	28	5	D.GL	LV-ct-hu	T.Haplocryalf
Cultivated	3	53.347	108.782	41.5	24.9	3.0	8.3	4.7	64	23	14	O.BLC	CH-cc	C.Haplocryoll
Cultivated	5	53.397	108.812	28.5	27.6	2.4	11.5	6.1	61	29	10	O.BLC	CH-cc	C.Haplocryoll
Cultivated	7	53.448	108.777	23.3	23.3	2.1	11.1	5.8	59	29	13	O.BLC	CH-cc	C.Haplocryoll
Cultivated	10	53.542	108.803	18.4	18.9	1.5	12.6	6.3	70	20	10	D.GL	LV-ct-hu	T.Haplocryalf

† Soil Classification Working Group (1998). O.BLC = Orthic Black Chernozem; CA.BLC = Calcarous Black Chernozem; D.GL = Dark Gray Luvisol; BR.GL = Brunisolic Gray Luvisol; O.GL = Orthic Gray Luvisol.

‡ IUSS Working Group WRB (2014). CH-cc = Calcic Chernozem; CL-ha = Haplic Calcisol; LV-ct-hu = Cutanic Luvisol (Humic); LV-ct-ap = Cutanic Luvisol (Abruptic); LV-ct = Cutanic Luvisol.

§ Soil Survey Staff (2014). C = Calcic; T = Typic.

Differences between land use were also evident. Soil pH was lowest ($p < 0.01$; grassland 6.4 ± 0.6; forest: 5.3 ± 0.5; cultivated: 6.0 ± 0.7) and OC:TN ratios were highest ($p < 0.01$; grassland: 10.2 ± 0.7; forest: 13.4 ± 2.6; cultivated: 10.7 ± 2.1) in forest surface soils. Forest litter had the highest amount of TC ($p < 0.001$; grassland: 76.3 ± 16.1 g kg^{-1}; forest: 244.1 ± 61.5 g kg^{-1}), OC ($p < 0.001$; grassland: 66.6 ± 22.0 g kg^{-1}; forest: 226.9 ± 66.5 g kg^{-1}), and TN ($p < 0.01$; grassland: 6.4 ± 3.0 g kg^{-1}; forest: 14.1 ± 3.5 g kg^{-1}), while pH was highest in grassland litter ($p < 0.01$; grassland: 6.4 ± 0.5; forest: 5.8 ± 0.3). In the location 3 soil profiles, OC:TN ratios and texture differed between land uses (Table 4.4).

Soil profiles also revealed trends in soil properties with depth (Table 4.4). Clay content ($p < 0.05$, $r = 0.53$) increased with depth while log TC ($p < 0.001$, $r = -0.87$), log OC ($p < 0.001$, $r = -0.90$), log TN ($p < 0.001$, $r = -0.91$), and OC:TN ($p < 0.05$, $r = -0.58$) decreased with depth.

Table 4.3 Locations and properties of climosequence litter samples used in incubation.

Land use	Location	Latitude	Longitude	TC	OC	TN	OC:TN	pH	— Soil classification —		
		°N	°W	— g kg^{-1} —					Canadian[†]	WRB[‡]	USDA[§]
Grassland	1	53.293	108.760	98.3	92.8	10.0	9.3	5.9	O.BLC	CH-cc	C.Haplocryoll
Forest	1	53.293	108.763	185.0	179.3	13.5	13.3	6.4	O.LG	GL-ha.lv	A.Cryaquoll
Forest	5	53.394	108.785	226.0	173.1	15.7	11.0	5.9	D.GL	LV-ct-hu	T.Haplocryalf
Forest	9	53.509	108.755	140.6	139.0	12.1	11.5	5.9	BR.GL	LV-ct-ap	T.Haplocryalf
Forest	11	53.628	108.765	224.1	214.5	10.6	20.2	5.5	O.GL	LV-ct	T.Haplocryalf
Forest	12	53.707	108.805	279.1	259.0	12.3	21.1	5.7	D.GL	LV-ct-hu	T.Haplocryalf

† Soil Classification Working Group (1998). O.BLC = Orthic Black Chernozem; O.LG = Orthic Luvic Gleysol; D.GL = Dark Gray Luvisol; BR.GL = Brunisolic Gray Luvisol; O.GL = Orthic Gray Luvisol.

‡ IUSS Working Group WRB (2014). CH-cc = Calcic Chernozem; GL-ha.lv = Haplic Luvic Gleysol; LV-ct-hu = Cutanic Luvisol (Humic); LV-ct-ap = Cutanic Luvisol (Abruptic); LV-ct = Cutanic Luvisol.

§ Soil Survey Staff (2014). C = Calcic; A = Argic; T = Typic.

Table 4.4 Properties of location 3 soil depth profiles used in incubation.

Land use	Depth	Horizon†	TC	OC	TN	OC:TN	pH	Sand	Silt	Clay
	cm			— g kg^{-1} —					— % —	
Grassland	0–5	Ah	45.5	45.4	4.1	11.1	6.1	68	17	15
Grassland	5–10	Ah	24.7	24.4	2.1	11.6	6.1	68	15	17
Grassland	10–15	Ah/Bm1	22.9	20.2	1.8	11.2	6.2	66	13	21
Grassland	15–20	Bm1	13.4	13.3	1.0	13.3	6.5	74	7	18
Grassland	20–25	Bm1	13.8	13.7	1.1	12.5	7.2	64	20	16
Grassland	25–30	Bm1/Bm2	9.5	7.4	0.9	8.2	6.8	62	21	17
Forest	0–5	Ah	57.6	55.9	4.2	13.3	4.9	62	21	17
Forest	5–10	Ah/Aej	24.6	23.3	2.1	11.1	5.0	63	21	16
Forest	10–15	Aej	11.5	11.0	1.1	10.0	5.0	61	28	11
Forest	15–20	Aej/Bt	7.9	8.2	0.7	11.7	5.5	61	25	14
Forest	20–25	Bt	5.9	6.1	0.7	8.7	4.5	53	29	17
Forest	25–30	Bt	ND‡	5.6	0.7	8.0	5.2	59	20	21
Cultivated	0–5	Ap	41.5	24.9	3.0	8.3	4.7	64	23	14
Cultivated	5–10	Ap	21.4	23.4	2.4	9.8	4.7	61	25	14
Cultivated	10–15	Ap/Bt	13.1	12.1	1.5	8.1	3.1	52	29	19
Cultivated	15–20	Bt	4.6	4.4	0.9	4.9	6.2	45	34	22
Cultivated	20–25	Bt	5.4	ND	ND	ND	6.5	48	26	26
Cultivated	25–30	Bt	4.8	6.9	0.8	8.6	6.7	48	25	28
Summary statistics of soil profiles by land use§										
Grassland			21.6 ± 13.1	19.2 ± 14.9	1.8 ± 1.2	11.3 ± 1.7 a	6.5 ± 0.4 a	67 ± 4 a	15 ± 5 b	17 ± 2
Forest			21.5 ± 21.5	20.4 ± 21.1	1.6 ± 1.4	10.5 ± 2.0 a	5.0 ± 0.3 b	60 ± 3 ab	24 ± 4 a	16 ± 3
Cultivated			15.1 ± 14.5	13.3 ± 9.5	1.7 ± 1.0	7.9 ± 1.8 b	5.3 ± 1.4 ab	53 ± 8 b	27 ± 4 a	20 ± 6
ANOVA			ns	ns	ns	$p < 0.05$	$p < 0.05$	$p < 0.01$	$p < 0.01$	ns

† Soil Classification Working Group (1998).

‡ Not determined due to limited sample quantity.

§ Values are means of mineral soil increments of each land use ± standard deviation; values with different lowercase letters are significantly different according to Tukey's HSD test ($p < 0.05$).

4.5.2 Readily mineralizable C

A subset of grassland and forest surface soils (Table 4.5) and forest litter samples (Table 4.6) were incubated and parameters for the proportion of potentially mineralizable C (C_0/OC) and C mineralization rates (k_C) were extracted. Cultivated surface soils and location 3 soil depth profiles excluded from the assay as the investigation of the effects of cultivation on the susceptibility of SOC to degradation was outside the scope of this study.

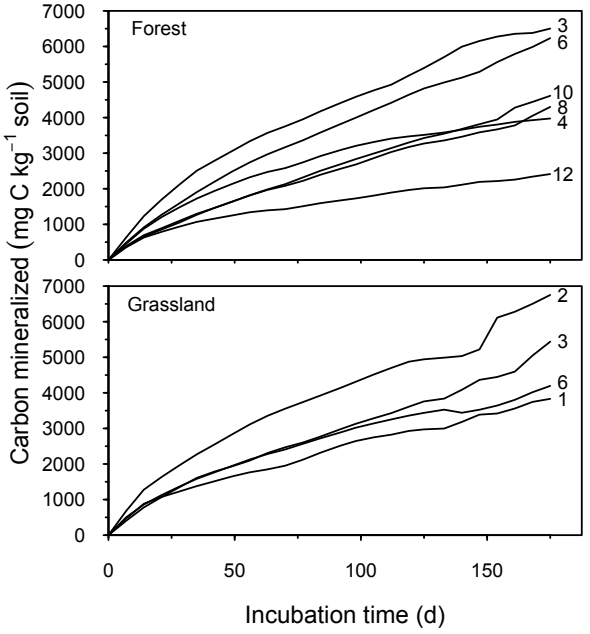

Fig. 4.1 Cumulative C mineralized in grassland and forest surface soils throughout 24-wk incubation. Lines represent means of three subsamples at each weekly gas sampling, with numbers referring to specific sampling locations.

The amount of C mineralized (C_m) in surface soils throughout the 24-wk incubation decreased with latitude (Fig. 4.1; $p < 0.05$, $r = -0.60$), reflecting concomitant decreases in OC (Table 4.2). However, when normalized to initial OC content, no trends with latitude were discernible in the proportion of C mineralized (log C_m/OC). Neither C_m nor log C_m/OC differed between land uses (Table 4.5). In litter samples, both C_m and C_m/OC were unrelated to latitude (Table 4.6). While the FOZO model generally provided the best fit for C mineralization data, FOSC parameters also described the data well, with model convergence occurring within 25 iterations, suggesting the existence of a single pool of SOC in climosequence soils. Although

assumptions of the FOSC model have recently been brought into question (Curtin et al., 2012), these parameters are presented (Tables 4.5, 4.6) to allow comparison with the literature as well as with N mineralization data from the current study.

Table 4.5 Amount of mineralized C (C_m) and N (N_m) in 24-wk incubation and associated parameters estimated using the first-order single compartment (FOSC) kinetic model of climosequence surface soils used in incubation.

Land use	Location	C_m	C_m/OC	C_0	C_0/OC	k_C	N_m	N_m/TN	N_0	N_0/TN	k_N
		g C kg^{-1} soil	%	g C kg^{-1} soil	%	d^{-1}	mg N kg^{-1} soil	%	mg N kg^{-1} soil	%	d^{-1}
Grassland	1	3.8	8.7	4.7	10.7	0.0086	40	0.9	–‡	–	–
Grassland	2	6.8	17.3	7.1	18.1	0.0101	79	1.9	394	9.4	0.0013
Grassland	3	5.4	12.0	9.0	19.8	0.0046	49	1.2	–	–	–
Grassland	6	4.2	16.6	4.5	17.8	0.0116	49	1.9	–	–	–
Forest	2	ND†	ND	ND	ND	ND	115	2.1	1522	28.2	0.0004
Forest	3	6.5	11.6	8.0	14.3	0.0094	158	3.8	1954	46.5	0.0005
Forest	4	4.0	31.6	4.3	34.1	0.0140	59	5.0	170	14.2	0.0026
Forest	5	3.6	13.2	4.3	15.6	0.0088	74	2.8	127	4.9	0.0050
Forest	6	6.2	8.7	9.0	12.7	0.0062	134	2.8	180	3.7	0.0074
Forest	7	3.5	16.3	4.4	20.3	0.0077	45	2.2	88	4.4	0.0043
Forest	8	4.3	13.4	6.3	19.6	0.0059	62	2.9	234	11.1	0.0017
Forest	9	4.2	21.8	4.4	22.7	0.0136	58	3.9	97	6.5	0.0056
Forest	10	4.6	14.5	7.4	23.1	0.0050	91	5.1	–	–	–
Forest	11	3.1	15.2	4.1	20.2	0.0077	42	3.5	153	12.8	0.0018
Forest	12	2.4	40.9	2.5	42.3	0.0136	41	10.3	75	18.8	0.0050
Cultivated	1	ND	ND	ND	ND	ND	79	2.0	–	–	–
Cultivated	2	ND	ND	ND	ND	ND	65	2.2	–	–	–
Cultivated	3	ND	ND	ND	ND	ND	97	3.2	207	6.9	0.0036
Cultivated	4	ND	ND	ND	ND	ND	74	2.1	–	–	–
Cultivated	5	ND	ND	ND	ND	ND	58	2.4	205	8.5	0.0018
Cultivated	7	ND	ND	ND	ND	ND	50	2.4	112	5.3	0.0032
Cultivated	8	ND	ND	ND	ND	ND	76	3.5	–	–	–
Cultivated	10	ND	ND	ND	ND	ND	60	4.0	430	28.7	0.0009

(continued on next page)

Table 4.5 - continued

Land use	C_m	C_m/OC	C_0	C_0/OC	k_C	N_m	N_m/TN	N_0	N_0/TN	k_N
	g C kg^{-1} soil	%	g C kg^{-1} soil	%	d^{-1}	mg N kg^{-1} soil	%	mg N kg^{-1} soil	%	d^{-1}
Summary statistics of surface soils by land use§										
Grassland	5.1 ± 1.3	13.7 ± 4.1	6.3 ± 2.1	16.6 ± 4.0	0.0087 ± 0.0030	54 ± 17	1.5 ± 0.5 b	394	9.4	0.0013
Forest	4.2 ± 1.3	18.7 ± 10.1	5.5 ± 2.1	22.5 ± 9.2	0.0092 ± 0.0034	80 ± 40	4.0 ± 2.3 a	460 ± 683	15 ± 13	0.0034 ± 0.0024
Cultivated	ND	ND	ND	ND	ND	70 ± 15	2.7 ± 0.7 a	239 ± 135	12 ± 11	0.0024 ± 0.0013
ANOVA	ns	ns	ns	ns	ns	ns	$p < 0.01$	ns	ns	ns

† Samples were not selected for analysis due to limited sample quantity.

‡ FOSC model did not fit the data.

§ Values are means of surface soils of each land use ± standard deviation; values with different lowercase letters are significantly different according to Tukey's HSD test ($p < 0.05$).

In surface soils, calculated FOSC parameters describing the proportion of readily mineralizable C (log C_0/OC) and k_C did not differ between land use types. However, log C_0/OC (Fig. 4.2, $p < 0.05$, $r = 0.60$), but not k_C, was related to latitude. No latitudinal trends were found in FOSC parameters of litter samples (Table 4.6).

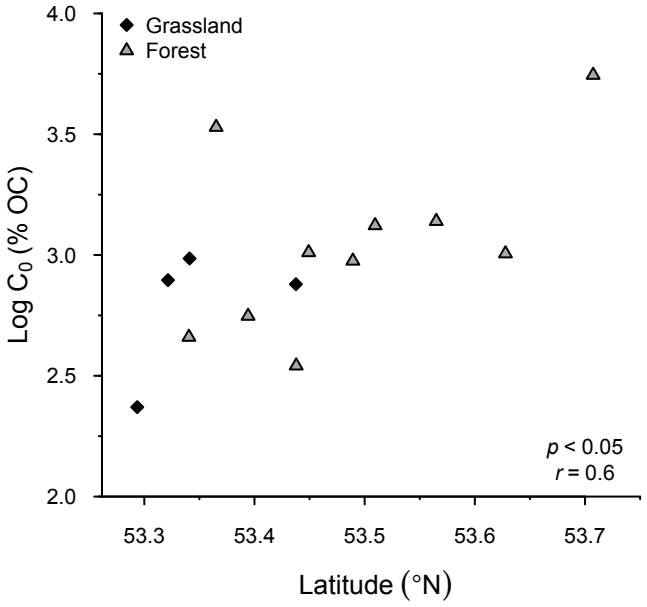

Fig. 4.2 Pearson's correlation between readily mineralizable C and latitude in a 24-wk incubation for grassland and forest surface soils.

Table 4.6 Amount of mineralized C (C_m) and N (N_m) in 24-wk incubation and associated parameters estimated using the first-order single compartment (FOSC) kinetic model of climosequence litter samples used in incubation.

Land use	Location	C_m	C_m/OC	C_0	C_0/OC	k_C	N_m	N_m/TN	N_0	N_0/TN	k_N
		g C kg^{-1} litter	%	g C kg^{-1} litter	%	d^{-1}	mg N kg^{-1} litter	%	mg N kg^{-1} litter	%	d^{-1}
Grassland	1	12.2	13.2	14.7	15.8	0.0086	186	1.9	–‡	–	–
Grassland	3	ND†	ND	ND	ND	ND	119	1.7	1034	14.6	0.0007
Forest	1	21.4	11.9	23.5	13.1	0.0111	181	1.3	–	–	–
Forest	3	ND	ND	ND	ND	ND	463	2.2	–	–	–
Forest	5	19.9	11.5	26.7	15.4	0.0070	217	1.4	–	–	–
Forest	9	28.9	20.8	29.4	21.1	0.0174	249	2.1	2697	22.3	0.0006
Forest	11	19.3	9.0	20.1	9.4	0.0140	217	2.0	393	3.7	0.0045
Forest	12	20.5	7.9	21.9	8.4	0.0144	248	2.0	407	3.3	0.0054

† Samples were not selected for analysis due to limited sample quantity.

‡ FOSC model did not fit the data.

4.5.3 Potentially mineralizable N

The amount of N mineralized (log N_m) in surface soils was not significantly related to latitude or land use (Fig. 4.3); however, trends followed those in C mineralization (Fig. 4.1). In contrast, the proportion of N mineralized (log N_m/TN) in surface soils increased with latitude ($p < 0.001$, $r = 0.72$) and was lowest in grassland soils (Table 4.5). In agreement with C mineralization results, litter N_m and N_m/TN were not related to latitude (Table 4.6). In location 3 soil depth profiles, log N_m decreased with depth (Fig. 4.4; $p < 0.001$, $r = -0.84$), reflecting decreases in TN with depth (Table 4.4); no differences between land uses were discernible (Table 4.7). In contrast, N_m/TN did not vary with depth and was significantly higher in the forest soil profile than grassland or cultivated profiles (Table 4.7).

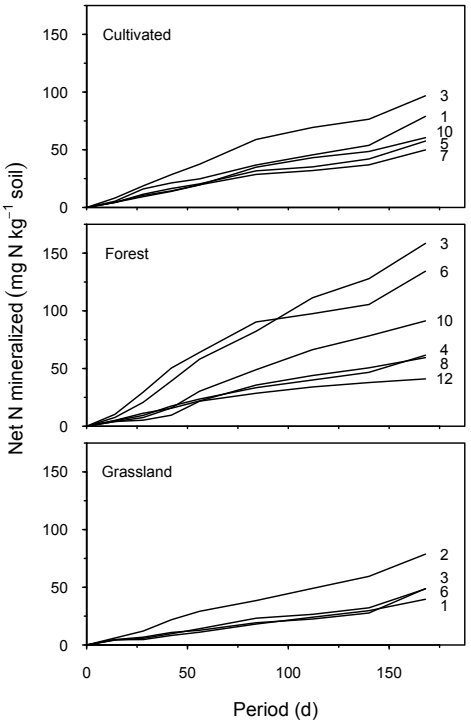

Fig. 4.3 Cumulative net N mineralized in cultivated, grassland, and forest surface soils throughout 24-wk incubation. Lines represent means of three subsamples at each leaching date, with numbers referring to specific sampling locations.

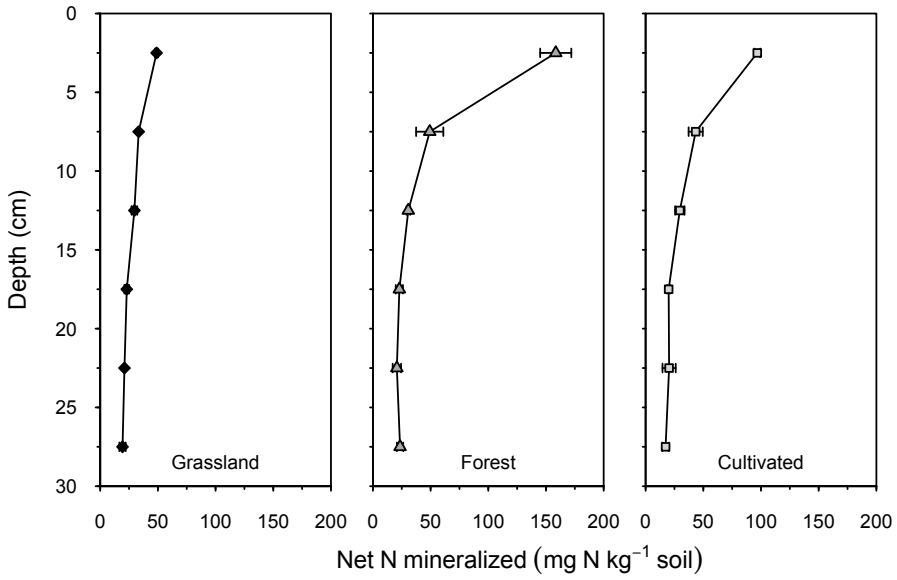

Fig. 4.4 Net N mineralized throughout 24-wk incubation in grassland, forest, and cultivated soil depth profiles from location 3. Error bars represent standard deviation of three subsamples.

In the majority of samples—particularly in surface soils—N mineralization data conformed best to the FOSC kinetic model, suggesting the existence of a single pool of mineralizable SON. Notably, the ZO kinetic model outperformed the FOSC model when describing litter samples, while the FOZO kinetic model best described subsurface soils. Given the model's superior performance, FOSC parameters for the proportion of potentially mineralizable N (N_0/TN) and N mineralization rates (k_N) were calculated (Tables 4.5–4.7). Strong mineralization lags prevented FOSC model convergence in 12 samples (8 surface soils and 4 litter samples), which were excluded from further analysis.

Table 4.7 Amount of mineralized N (N_m) in 24-wk incubation and associated parameters estimated using the first-order single compartment (FOSC) kinetic model of location 3 soil depth profiles used in incubation.

Land use	Depth	N_m	N_m/TN	N_0	N_0/TN	k_N
	cm	mg N kg^{-1} soil	%	mg N kg^{-1} soil	%	d^{-1}
Grassland	0–5	49	1.2	–‡	–	–
Grassland	5–10	33	1.6	129	6.1	0.0017
Grassland	10–15	30	1.6	72	4.0	0.0028
Grassland	15–20	23	2.3	13	1.3	0.0268
Grassland	20–25	21	1.9	11	1.0	0.0304
Grassland	25–30	19	2.2	22	2.5	0.0092
Forest	0–5	158	3.8	1954	46.5	0.0005
Forest	5–10	49	2.3	145	6.9	0.0025
Forest	10–15	31	2.8	115	10.4	0.0018
Forest	15–20	23	3.3	31	4.5	0.0072
Forest	20–25	21	3.0	30	4.3	0.0057
Forest	25–30	24	3.4	47	6.8	0.0038
Cultivated	0–5	97	3.2	207	6.9	0.0036
Cultivated	5–10	43	1.8	134	5.6	0.0023
Cultivated	10–15	30	2.0	55	3.7	0.0043
Cultivated	15–20	20	2.2	25	2.8	0.0078
Cultivated	20–25	20	ND†	28	ND	0.0066
Cultivated	25–30	17	2.2	19	2.3	0.0118
Summary statistics of soil profiles by land use§						
Grassland		29 ± 11	1.8 ± 0.4 b	50 ± 51 b	3.0 ± 2.1 b	0.0142 ± 0.0135
Forest		51 ± 54	3.1 ± 0.5 a	387 ± 769 a	13.2 ± 16.4 a	0.0036 ± 0.0025
Cultivated		38 ± 30	2.3 ± 0.5 b	78 ± 76 b	4.3 ± 1.9 b	0.0061 ± 0.0035
ANOVA		ns	$p < 0.01$	$p < 0.05$	$p < 0.01$	ns

† Nitrogen content not determined due to limited sample quantity.
‡ FOSC model did not fit the data.
§ Values are means of all depth increments of each land use ± standard deviation; values with different lowercase letters are significantly different according to Tukey's HSD test ($p < 0.05$).

The FOSC parameters describing N mineralization were not related to latitude or land use in surface soils or litter samples. However, analysis of soil depth profiles revealed that both log N_0/TN ($p < 0.05$, $r = -0.61$) and log k_N ($p < 0.01$, $r = 0.69$) varied with depth. Additionally, N_0/TN was highest in forest soils (Fig. 4.5a, Table 4.7).

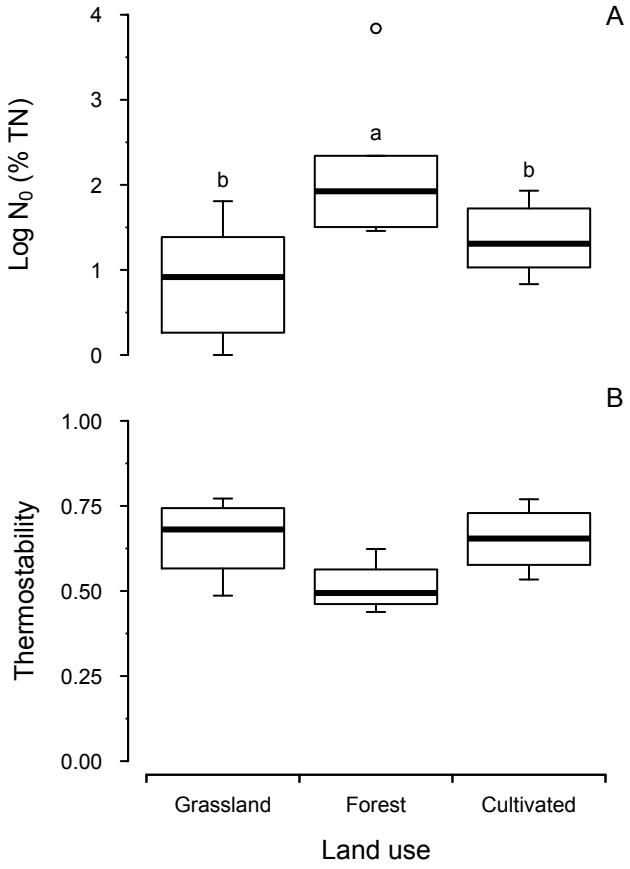

Fig. 4.5 Boxplots of (A) potentially mineralizable N pools, and (B) thermostability by land use in soil depth profiles from location 3.

4.5.4 Soil organic matter chemistry

Features in C *K*-edge XANES spectra (Fig. 4.6) were assigned as: a) C=C in protonated/alkylated aromatics and alkenes at 285.0 eV (aromatic-C); b) aliphatic-C in nitriles, carbonyl-C in ketones and aldehydes, and C bound in aromatic heterocycles at 286.5 eV (ketone); and c) carbonyl-C in carboxyl and amide at 288.5 eV (carboxyl). At the N *K*-edge (Fig. 4.7), dominant features were assigned as a) aromatic N in 6-membered rings at 398.8 eV (heterocyclic-N); b) amidic-N with possible contributions from pyrrolic-N at 401.4 eV (amide); and c) alkyl-N, inorganic NH_4^+, and the $1s \rightarrow \sigma^*$ feature at 405.5 eV (alkyl-N).

In a subset of surface soils from the mineralization assay, Py-FIMS but not XANES analysis revealed latitudinal trends in SOM chemistry. Carbohydrates ($p < 0.05$, $r = -0.90$), phenols and lignin monomers ($p < 0.05$, $r = -0.88$), lipids ($p < 0.01$, $r = 0.96$), heterocyclic N (p

< 0.05, r = -0.85), sterols (p < 0.001, r = 0.99), and amide (p < 0.05, r = -0.88) all varied with latitude. Additionally, thermostability decreased with increasing latitude (p < 0.05, r = -0.81).

While too few observations were present to examine contrasts between forest, grassland, and cultivated surface soils, soil depth profiles revealed differences in SOM chemistry with land use. The forest profile had a greater proportion of lipids (p < 0.05; grassland: 4.7 ± 0.3%; forest: 7.5 ± 2.7%; cultivated: 5.5 ± 0.8%) and sterols (p < 0.05; grassland: 1.2 ± 0.5%; forest: 7.1 ± 6.0%; cultivated: 3.0 ± 1.5%) than the grassland profile. While not significant, the forest profile also had higher hexose:pentose ratios (p = 0.05; grassland: 2.1 ± 0.2%; forest: 2.6 ± 0.4%; cultivated: 2.1 ± 0.2%) and lower thermostability (p = 0.07; grassland: 0.66 ± 0.12%; forest: 0.51 ± 0.08%; cultivated: 0.65 ± 0.10%) than grassland or cultivated soils. Nitrogen *K*-edge XANES of soil depth profiles revealed differences in amide, which was highest in the grassland profile (p < 0.01; grassland: 0.37 ± 0.04; forest: 0.32 ± 0.03; cultivated: 0.32 ± 0.05; normalized absorbance, arbitrary units [a.u.]). Though not significant, the grassland profile tended to have higher proportions of carboxyl than the cultivated profile (p = 0.08; grassland: 0.53 ± 0.03; forest: 0.50 ± 0.01; cultivated: 0.47 ± 0.04; a.u.).

Depth trends were revealed by Py-FIMS measurements, with alkylaromatics (p < 0.05, r = 0.60), suberin (p < 0.05, r = -0.63), and thermostability varying with depth (p < 0.05, r = 0.62). While not significant, heterocyclic N (p = 0.06, r = 0.56) and log free fatty acids (p = 0.09, r = -0.51) also tended to vary with depth. Additionally, XANES features for aromatic-C (p < 0.01, r = -0.79), ketone (p < 0.01, r = -0.78), and amide (p < 0.01, r = -0.77) decreased with depth while log carboxyl:ketone increased with depth (p < 0.01, r = 0.77).

4.5.5 Correlations of mineralization parameters with soil properties and soil organic matter chemistry

In surface soils, mineralization parameters tended to be negatively correlated with TC, OC, TN, and sand content (Table 4.8). While few parameters were correlated with measures of SOM chemistry, lipids were correlated with both log C_m/OC and log N_m/TN. Few correlations were found between litter samples and measured variables, though SOM chemistry (i.e., XANES, Py-FIMS) was not measured. In soil depth profiles, a number of correlations were found between N mineralization parameters and soil properties, XANES, and Py-FIMS variables. Log N_0/TN and log k_N values tended to be correlated with these variables in opposing

directions. This is likely related to the inverse correlation between N_0/TN and log k_N ($p < 0.001$, $r = -0.94$), which resulted from fitting the FOSC model in samples that lack a distinct plateau (Campbell et al., 1993). Given the interdependence of these parameters, we interpret only the former.

Table 4.8 Pearson correlations between measures of SOM mineralization, soil properties, and SOM chemistry in surface soils, litter samples, and soil depth profiles. Only significant correlations are reported[†].

	Correlation (*r*)										
Mineralization parameter	TC	OC	TN	OC:TN	pH	Sand	Silt	Clay	XANES[‡]	Py-FIMS[§]	Thermo-stability
	Surface soils										
Log C_m/OC	-0.82***	-0.83***	-0.81***	ns	ns	0.58*	ns	-0.63*	(ketone) -0.77*	(lipids) 0.90*	ns
Log C_0/OC	-0.78**	-0.78***	-0.83***	ns	ns	ns	ns	-0.72**	ns	ns	ns
k_C	-0.55*	-0.58*	ns	ns	ns	0.60*	ns	ns	ns	ns	ns
Log N_m/TN	-0.48*	-0.49*	-0.65***	0.56**	-0.56**	ns	ns	-0.76***	ns	(lipids) 0.83* (sterols) 0.85*	ns
Log N_0/TN	ns	ns	ns	ns	ns	ns	ns	ns	ns	ns	ns
k_N	ns	ns	ns	ns	ns	ns	ns	ns	(amide) 0.92**	(alkyl) -0.95*	ns
	Litter samples										
C_m/OC	ns	ns	ns	ns	ns	NA[#]	NA	NA	ND[††]	ND	ND
C_0/OC	ns	ns	ns	-0.84*	ns	NA	NA	NA	ND	ND	ND
k_C	ns	ns	ns	ns	ns	NA	NA	NA	ND	ND	ND
N_m/TN	ns	ns	ns	ns	-0.74*	NA	NA	NA	ND	ND	ND
N_0/TN	ns	ns	ns	ns	ns	NA	NA	NA	ND	ND	ND
k_N	ns	ns	ns	ns	ns	NA	NA	NA	ND	ND	ND

(continued on next page)

Table 4.8 - continued

Mineralization parameter	Correlation (*r*)										
	TC	OC	TN	OC:TN	pH	Sand	Silt	Clay	XANES‡	Py-FIMS§	Thermo-stability
	Soil depth profiles¶										
N_m/TN	ns	ns	ns	ns	ns	ns	ns	ns	ns	ns	ns
Log N_0/TN	0.59*	0.68*	0.66**	ns	-0.55*	ns	ns	ns	(aromatic) 0.76** (ketone) 0.82** (het-N) 0.65* (carb:ket) -0.71*	(hex:pent) 0.76** (ncomp) -0.67* (sterols) 0.61* (fatty) 0.68*	-0.75**
Log k_N	-0.61*	-0.74**	-0.72**	ns	0.55*	ns	ns	ns	(aromatic) -0.86*** (ketone) -0.82** (het-N) -0.73* (carb:ket) 0.81**	(hex:pent) -0.70* (ncomp) 0.65*	0.64*

† Significant correlations at 0.05 (*), 0.01 (**), and 0.001 (***) probability levels.
‡ Correlated X-ray absorption near edge structure (XANES) features in brackets; aromatic = aromatic-C; het-N = heterocyclic-N; carb:ket = carboxyl:ketone.
§ Correlated pyrolysis-field ionization mass spectrometry (Py-FIMS) compound classes in brackets; alkyl = alkylaromatics; hex:pent = hexose:pentose; ncomp = heterocyclic-N; fatty = free fatty acids.
¶ TC, OC, TN, lipids, sterols, fatty, and carb:ket were log-transformed prior to correlation in soil depth profiles.
# Particle size only determinable in mineral soils.
†† Samples were not selected for analysis due to limited sample quantity.

4.5.6 Trends in soil organic matter chemistry during incubation

To determine the role of SOM chemistry as a control on stability, the evolution of SOM chemistry throughout the first 8 wk of the 24-wk incubation was measured by C (Fig. 4.6) and N (Fig. 4.7) *K*-edge XANES of surface soils (location 2), and litter samples (location 1) from different land uses. Prior to incubation (wk 0), SOM chemistry of litter and mineral samples did not differ significantly. Additionally, differences between land uses were minor, with forest samples having the greatest proportion of ketones ($p < 0.05$; grassland: 0.20 ± 0.02; forest: 0.28 ± 0.02; cultivated: 0.18; a.u.).

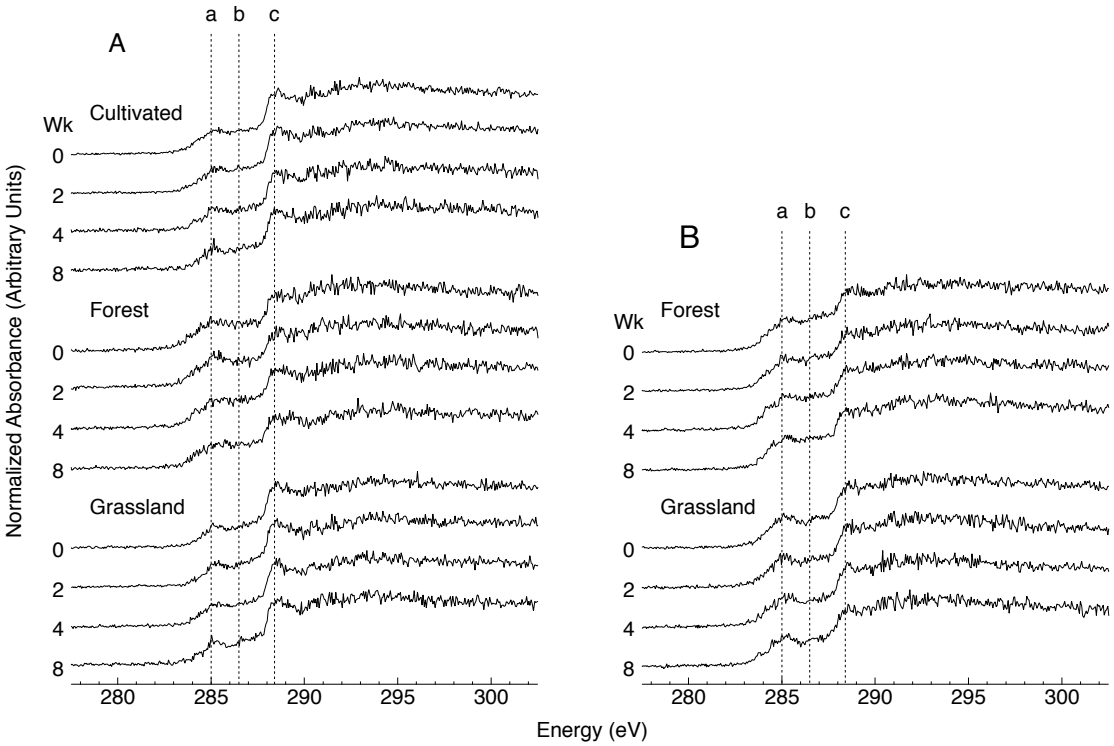

Fig. 4.6 Carbon *K*-edge X-ray absorption near edge structure (XANES) spectra of (A) grassland, forest, and cultivated surface soils, and (B) forest and grassland litter samples throughout the first 8 wk of incubation. Carbon features are assigned as (a) aromatic-C at 285.0 eV; (b) ketone at 286.5 eV; and (c) carboxyl at 288.5 eV.

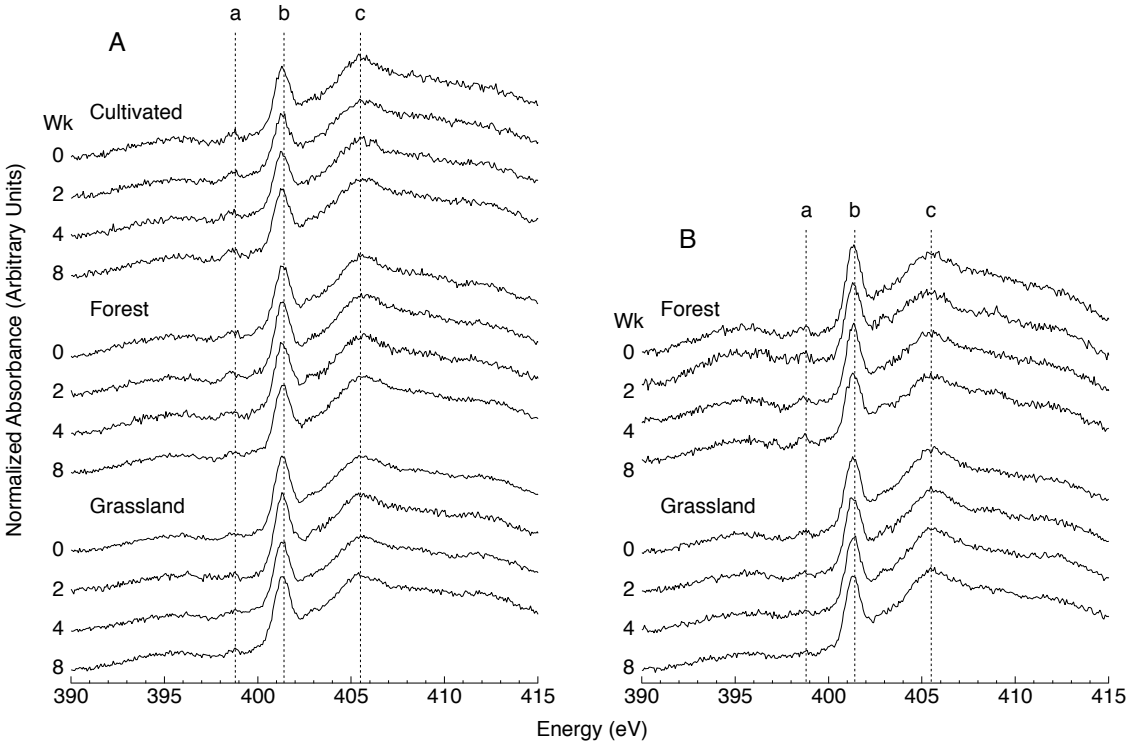

Fig. 4.7 Nitrogen *K*-edge X-ray absorption near edge structure (XANES) spectra of (A) grassland, forest, and cultivated surface soils, and (B) forest and grassland litter samples throughout the first 8 wk of incubation. Nitrogen features are assigned as (a) heterocyclic-N at 398.8 eV; (b) amide at 401.4 eV; and (c) alkyl-N at 405.5 eV.

Differences in SOM chemistry between subsampling periods (i.e., wk 0, 2, 4, and 8) were difficult to discern by visual inspection of spectra (Figs. 4.6, 4.7). For all samples, Pearson's correlations of XANES features with subsampling period were not significant. Likewise, no trends in SOM chemistry over time were found when mineral and litter samples were analyzed separately. Only when samples were separated by both type (mineral surface soil or litter) and land use were trends with incubation time revealed. In the grassland soil, the proportion of alkyl-N decreased with incubation period ($p < 0.05$, $r = -0.99$), while in the forest soil the proportion of ketones declined over time ($p < 0.05$, $r = -0.99$). In the cultivated soil, proportions of aromatic-C increased throughout the incubation ($p < 0.05$, $r = 0.99$). No changes in grassland or forest litter chemistry occurred during the incubation.

4.6 Discussion

Generally, C and N mineralization results agree with previous findings from similar land uses (e.g., Ajwa et al., 1998; Côté et al., 2000; Arevalo et al., 2012). Net amounts of N

mineralized throughout the incubation, expressed on a TN basis, ranged from 0.9–10.3%, 1.3–2.2%, and 1.2–3.8% in surface soils, litter samples, and depth profiles, respectively. The proportion of C_m/OC ranged to a greater extent: from 8.7–40.9% in surface soils and 6.7–20.8% in litter samples.

4.6.1 Climatic trends in C and N mineralization

Predicted increases in MAT and evapotranspiration in the study region (Sauchyn and Kulshreshtha, 2008; Barrow, 2009) suggests current climate norms, and subsequently vegetation, will shift northward. As such, climatic and vegetation differences with decreasing latitude along the climosequence can serve as a surrogate for future characteristics at the northern end. The ~0.7 °C gradient in MAT along the climosequence lead to two discernible trends in surface soil mineralization parameters. First, log N_m/TN increased with increasing latitude, and log C_m/OC, while not significant, showed an increasing trend with latitude (p = 0.07, r = 0.50), indicating that greater proportions of SOM were mineralized in samples from the northern end of the climosequence during the incubation. Second, increasing log C_0/OC with latitude (Fig. 4.2) reveal that the proportion of biologically stable SOC is greatest at the southern end of the transect. Indeed, values derived from the sites at the two endpoints of the transect (site 1 grassland – site 12 forest) represent both extremes of N_m/TN, C_m/OC, and C_0/OC values (Table 4.5). The wide range in these parameters across the climosequence (9.4, 32.2, and 31.6%, respectively) suggests a strong climatic effect on SOM mineralization.

While increases in log C_0/OC with latitude suggest the pool of stable SOC was influenced by climate, the absence of this trend in log N_0/TN may indicate that SON is less susceptible to climatic changes. However, potentially mineralizable C and N are not analogous measurements: while C mineralization reflects the gross heterotrophic activity of soil microorganisms, N mineralization represents the net flux of mineral N released from the soil (Haynes, 2005). As such, differences between C and N mineralization parameters may result from the incorporation of immobilization processes into N, but not C, mineralization measurements. Alternatively, although log C_m/OC and log C_0/OC values were highly correlated ($p < 0.001$, r = 0.93), log N_m/TN and log N_0/TN values were not, suggesting that the FOSC model better described the C mineralization data. This may be due, in part, to the increase in net N mineralization near the end of the incubation (Fig. 4.3), causing deviations from the FOSC model. Likewise, an initial lag

phase in net N mineralization, most evident in forest soils (Fig. 4.3), may reflect a predominance of immobilization during this period (Scott et al., 1998) due to the significantly higher OC:TN ratios of forest surface soils and the relatively low incubation temperature (Campbell et al., 1993). This lag may also have contributed to deviations from the FOSC model. As such, while the absence of correlation between N_0/TN and latitude—despite the relationship between C_0/OC and latitude—may reflect the greater responsiveness of mineralizable C concentrations (Haynes, 2005), it may also indicate difficulties in modeling N mineralization in climosequence surface soils.

Soil organic matter chemistry is one of the dominant controls defining its resistance to degradation (Stevenson, 1994; Christensen, 1996; Sollins et al., 1996). Despite recent controversy surrounding its importance (Marschner et al., 2008; Kleber, 2010; Schmidt et al., 2011; Dungait et al., 2012), it remains a key component of conceptual models of SOM decomposition (Conant et al., 2011). However, we found little evidence that biochemical recalcitrance dominates SOM stability in climosequence surface soils. Indeed, neither C_0/OC nor N_0/TN were correlated to measures of SOM chemistry (Table 4.8). Additionally, while both C_m/OC and N_m/TN were correlated with XANES and Py-FIMS measures of chemistry, the only shared trend was a positive relationship with the proportion of soil lipids, which also increased with latitude. Notably, C_m/OC was inversely related to the C *K*-edge XANES ketone feature, in agreement with Gillespie et al. (2014b). As ketones are indicators of biologically transformed SOM (Gillespie et al., 2014a) and can be produced via fatty acid oxidation (Dent et al., 2004), the gradient in SOM chemistry with stability may reflect a continuum of SOM degradation. This, in turn, may result from differences in climate, in agreement with findings that warmer temperatures encourage the accumulation of stable SOM (Dalias et al., 2001; Paré et al., 2006; Hilli et al., 2008). However, while lipids were correlated with latitude ($p < 0.01$, $r = 0.96$), ketones were not, suggesting that climate may not be responsible for the observed ketone-lipid continuum. Additionally, given that lipids comprised only 4.5–13.1% of SOM in the subset of climosequence surface soils under study (Purton et al., 2015), it is unlikely that variation in lipids could lead to the comparatively large ranges in C (32.3%) and N (9.4%) mineralization across the climosequence (Table 4.5).

While the current study explicitly focused on biochemical recalcitrance as a SOM stabilization mechanism, we found indirect evidence suggesting an important role of physico-

chemical protection along the climosequence. All mineralization variables exhibiting a latitudinal trend were also negatively correlated with clay content (Table 4.8), which decreased by ~20% with latitude (Table 4.2). Like climate, clay content influences SOM adsorption (Baldock and Skjemstad, 2000), and can increase physical protection of OM (Six et al., 2002; von Lützow et al., 2006), making it difficult to disentangle the effects of climate from those of clay on mineralization dynamics across the climosequence. Furthermore, the role of a dominant stabilization mechanism other than biochemical recalcitrance is supported by the absence of a latitudinal trend in litter mineralization parameters (Table 4.6), suggesting organo-mineral interactions may be responsible for SOM stabilization in surface soils. Notably, thermostability—often interpreted as representing differences in bond type and strength (Schulten and Leinweber, 1999; Sleutel et al., 2011) as well as indicating resistance to further microbial degradation (Leinweber et al., 2008)—was not correlated with mineralization parameters in surface soils (Table 4.8), suggesting physical protection may play a key role in stabilization of climosequence SOM at the soil surface.

4.6.2 Land use effects on C and N mineralization

Despite broad differences in vegetation and land use, observed differences in SOM mineralization were relatively small. While no differences were found in surface SOC mineralization parameters, when expressed on a TN unit basis, biological stability of SON tended to follow the order of grassland > cultivated > forest soils in both surface soils (Table 4.5) and soil profiles (Table 4.7). Notably, N_m/TN of grassland surface soils was significantly lower than that of forest and cultivated soils. As grassland sites were located at the southern end of the climosequence (Table 4.2), their apparent stability may reflect the influence of latitude, rather than land use. However, results from adjacent soil profiles revealed land use differences in both N_m/TN and N_0/TN (Table 4.7), indicating that land use does influence SOM stability. These findings are inconsistent with others from this region: Arevalo et al. (2012) found C_m/OC to be lower in a native trembling aspen forest soil than in paired agricultural and non-native grassland soils. However, C_m/OC and N_m/TN are not analogous measurements, with CO_2 respired measuring the total activity of heterotrophic soil microorganisms while N leachates represent the net flux of inorganic N released from the soil (Haynes, 2005). Furthermore, the dominance of different stabilization mechanisms may explain incongruities with previous studies.

The detection of few differences in SOM chemistry between land use profiles indicates that biochemical recalcitrance is not the dominant stabilization mechanism resulting in observed differences in SON lability. Of the SOM chemistry variables measured, only Py-FIMS lipid and sterol compound classes and the N *K*-edge XANES amide feature differed significantly between land use types. However, aside from sterols, SOM chemistry variables correlated with N mineralization parameters (Table 4.8) were not the same as those that differed between land uses. Yet, sterols have been found to be negatively correlated with SON mineralization in sandy arable soils from NW Germany (Heumann et al., 2011), and can exhibit an anti-microbial effect specific to microorganisms actively involved in N cycling (Heumann et al., 2013), and thus remain unlikely to lead to the increase in SOM lability as observed here. Likewise, while N mineralization parameters in surface soils and soil profiles were correlated with soil pH, which was found to be significantly lower in forests, Curtin (1998) found differences in pH to be unrelated to N_0 in cultivated soils in Saskatchewan, suggesting pH is not responsible for the observed land use differences in SON lability.

Notably, while not significantly different between land use profiles ($p = 0.07$), thermostability was inversely correlated with log N_0/TN, and tended to mirror land use differences in N_0/TN (Fig. 4.5a, b). Unlike compound classes, each of which represent only a portion of SOM, thermostability incorporates information from the entire range of *m/z* measured, and thus is a broad measure of SOM stability. As such, thermostability is a more plausible influence on SOM lability than individual compound classes, suggesting that decreased organo-mineral association may be responsible for the observed lability of SON in the forest soil profile. Indeed, all Py-FIMS compound classes correlated with N_0/TN in soil profiles were also correlated with thermostability ($p < 0.01$, $|r| > 0.75$), suggesting that correlations between these variables and log N_0/TN may reflect the influence of thermostability—rather than biochemical recalcitrance—on the resistance of SON to degradation. Furthermore, though potentially the result of mineralization-immobilization dynamics, some correlations of SOM chemistry variables with log N_0/TN ran counter to expectation. For example, as measured by N *K*-edge XANES, heterocyclic-N was positively correlated with N_0/TN, suggesting that this feature contributes to SOM lability. However, heterocyclic forms of N are thought to be resistant to decomposition (Mengel, 1996; Kögel-Knabner, 2002; Jokic et al., 2004), particularly relative to other forms of N (Gärdenäs et al., 2011), and thus it would be expected that this XANES feature be negatively

correlated with N_0/TN. As such, trends in SOM chemistry remain difficult to reconcile with observed differences in SON lability, suggesting another mechanism is responsible for SOM stabilization.

4.6.3 Dynamics of soil organic matter chemistry during decomposition

Carbon and N *K*-edge XANES revealed that SOM chemistry does not evolve predictably during decomposition. Despite the view of some chemical features as biochemically labile or recalcitrant, we did not find trends in the relative depletion or enrichment of XANES features throughout the first 8 wk of the incubation that were consistent across sample type (surface soil or litter) or land use. This suggests SOM mineralization is not controlled by biochemical recalcitrance, with losses in SOC and SON reflecting relatively uniform depletion of all chemical features, in accordance with the existence of a single pool of mineralizable SOM as indicated by conformation of climosequence soil C and N mineralization to the FOSC kinetic model. Modest trends in SOM chemistry over time were only discernible when correlations were performed on individual samples, despite similarity in initial XANES chemistry (Figs. 4.6, 4.7). Specifically, alkyl-N and ketones were depleted in grassland and forest surface soils, respectively, while aromatic-C was enriched in cultivated soils. Such changes, along with the static SOM chemistry of litter samples, suggest the existence of land use- or soil-specific interactions between SOM chemical features and other stabilization mechanisms, such as the association of OM with minerals.

4.7 Conclusions

Assessment of SOM along a climosequence of grassland, forest, and cultivated soils with a similar pedogenic history revealed both latitudinal trends and land use differences in the biological stability of SOM. The susceptibility of SOM to degradation was greatest at the northern end of the climosequence and in forest soils. As such, cooler, moister climates may promote the accumulation of labile SOM that may be lost with climate change. Likewise, the conversion of forests to cultivated soils and vegetation shifts from forest to grassland may trigger the loss of this labile pool of SOM. However, despite a MAT gradient of only ~0.7 °C, differences in the biological stability of SOM attributable to land use were small relative to the magnitude of differences associated with latitude, suggesting that climatic processes may affect SOM stabilization mechanisms to a greater extent than land use.

Our findings suggest that SOM chemistry does not strongly influence its biological stability. While lipids were correlated with C and N mineralization in surface soils, only sterols were consistently correlated with measures of N mineralization in both surface soils and soil depth profiles. Furthermore, negative correlations of mineralization measures with clay content in climosequence surface soils and with thermostability in depth profiles suggests a greater influence of other stabilization mechanisms on the biological stability of SOM. Finally, our assessment of SOM chemistry evolution throughout the incubation revealed that changes in SOM chemistry are not consistent across land uses, indicating that biochemical recalcitrance alone did not control the preservation of SOM.

5. SYNTHESIS AND CONCLUSIONS

The response of SOM and terrestrial C stocks to global climate change has been the focus of much research, yet key questions remain. The magnitude and direction of the response of SOC stocks to predicted changes in climate (e.g., Kirschbaum, 2000; Friedlingstein et al., 2006; Heimann and Reichstein, 2008; Janssens and Vicca, 2010), remains uncertain, due to the complex nature of SOM decomposition dynamics. Indeed, while it is well known that SOM decomposition is temperature-dependent, biological and chemical constraints to SOM decay are themselves affected by temperature, and potentially other climatic factors (Thornley and Cannell, 2001; Davidson and Janssens, 2006). Of these constraining factors, the role of biochemical recalcitrance in determining SOM stability is particularly uncertain, and has recently been brought into question (Marschner et al., 2008; Kleber, 2010; Schmidt et al., 2011; Dungait et al., 2012). These important knowledge gaps highlight the need to enhance our understanding of SOM decomposition and constraints on SOM decay, particularly as they relate to environmental changes that can be expected to occur during this period of global climate change.

The research presented in this thesis addresses these gaps in our collective understanding by examining and attempting to reconcile the response of SOM chemistry and SOM biological stability to differences in climate and land use along a pedogenically defensible climosequence at the grassland-forest ecotone in west-central Saskatchewan. Using paired trembling aspen forest, grassland, and cultivated soils developed on the same glacial ice stream unit and controlling for topographic differences allowed us to study changes in SOM chemistry and persistence resulting from differences in climate and land use. This rigorous study design allowed us to use latitudinal variations in these properties as a surrogate for changes that are likely to occur in the region with global climate change, elucidating relationships that may otherwise have remained obscured.

5.1 Summary of findings

Our study of the effects of climate and land use on SOM chemistry (Chapter 3) demonstrated that SOM chemistry was relatively insensitive to changes in climate and land use

on the magnitude of those predicted to occur with climate change in the near future. We found SOM chemistry to be remarkably similar despite a climatic gradient of 0.7 °C MAT and broad differences in land use. In contrast, SOM chemistry varied more markedly within 20-cm depth profiles than across the entire 46-km transect. Additionally, these depth trends were modified by land use, revealing that pedon-scale processes (e.g., bioturbation, tillage) have a greater impact on SOM chemistry than landscape- or regional-scale processes.

In Chapter 4, the examination of SOM biological stability using a 24-wk incubation revealed trends that diverged from those found in SOM chemistry across the climosequence. The biological stability of SOM tended to vary most greatly with latitude. Despite the intent of our study design to control for other pedogenic factors, confounding effects of soil texture impeded the attribution of latitudinal variation in biological stability solely to climatic differences. Nonetheless, SOM tended to be least stable in cooler, moister sites at the northern end of the climosequence, though this observation may also be due, in whole or in part, to concomitant decreases in clay content. Biological stability also varied with land use, being least stable in forest soils. Measures of SOM biological stability were generally not well correlated with measures of SOM chemistry, and individual SOM chemical moieties were not selectively preserved—or preferentially depleted—across samples from different land uses during decomposition. These findings suggest that biochemical recalcitrance does not control SOM persistence in the soils studied. Instead, correlations with clay content and thermostability suggest that organo-mineral association may play a greater role in SOM stabilization in these soils, with land use and—potentially—climate modifying the operation or effectiveness of this stabilization mechanism, thereby leading to the observed differences in SOM biological stability.

The finding that SOM chemistry has a relatively homogenous composition across land uses and climates is consistent with the 'Chemical Convergence Hypothesis' (Wickings et al., 2012) of SOM chemical transformations, supporting the existence of a common decomposition sequence that serves to homogenize SOM despite differences in initial litter input chemistry (Grandy and Neff, 2008). The model of Grandy and Neff (2008) proposes that decomposition leads to consistent and predictable changes in SOM chemistry as well as concomitant physical and biological breakdown of particulate fractions. As such, SOM chemistry converges during decomposition, and various particulate fractions are linked to SOM in different stages of decomposition, with silt and clay fractions being more decomposed than sand-associated and

particulate SOM (Grandy and Neff, 2008). Given that our study design explicitly sampled soils from the same parent material, differences in particle size, though present, may not have been great enough to yield differences in SOM chemistry, thereby potentially explaining the similarity in SOM chemistry across the climosequence. Also consistent with this model, trends in SOM chemistry within soil depth profiles may be attributable to variation in organo-mineral association, which studies in other environments have shown increases with depth (von Lützow et al., 2008; Rumpel and Kögel-Knabner, 2011). However, as no explicit measures of the microbial biomass were examined in the research described in this thesis, the contribution of the microbial community composition to the observed similarity in SOM chemistry along the climosequence remains unknown. Relatively homogenous edaphic properties across the climosequence may have led to similarities in decomposer communities (Lauber et al., 2008), which may have also led to the convergence of SOM chemistry.

Observations that SOM chemistry and SOM biological stability are largely unlinked is consistent with the recent paradigm shift which suggests biochemical recalcitrance is not an important determinant of SOM preservation (Marschner et al., 2008; Kleber, 2010; Schmidt et al., 2011; Dungait et al., 2012). Latitudinal and depth trends as well as land use differences in SOM chemistry and biological stability were often mutually exclusive: SOM chemistry was relatively homogenous across climosequence surface soils but varied markedly with depth, while SOM biological stability varied with latitude and differed between land uses but exhibited only minor variation with depth. Moreover, the relatively uniform depletion of SOM chemical moieties during long-term incubations supported our finding that a single compartment model of SOM mineralization tended to best describe decomposition, further indicating that SOM persistence is not controlled by various chemical 'pools' of differing biochemical recalcitrance, as is assumed in many SOC cycling models (e.g., CENTURY, RothC). Examinations of the evolution of SOM chemistry during decomposition revealed only sample-specific trends as decomposition proceeded. As biochemically recalcitrant compounds, by definition, must be stable regardless of the environment in which they are placed (Kleber, 2010), such sample-specific trends must be reflective of soil- or land use-specific interactions between different SOM chemical components and other stabilization mechanisms (i.e., organo-mineral association, microbial inaccessibility). Together, these findings indicate that biochemical recalcitrance is not the dominant SOM stabilization mechanism in these soils.

5.2 Future research directions

While the research presented in this thesis examined the influence of climate and climate-induced land use differences on SOM chemistry and biological stability, future investigations should expand their scope to determine if these findings are broadly applicable regardless of parent material, or if responses are different in soils of different mineralogy or texture. Indeed, soil texture has been observed to influence SOM chemistry (Grandy et al., 2009), particularly in subsoil horizons (Vancampenhout et al., 2012). Since both the physical and chemical breakdown of SOM occur simultaneously, SOM chemistry and degree of microbial processing varies with soil particle size (Grandy and Neff, 2008). As such, SOM in relatively fine-textured soils—such as those found along the climosequence examined in this research—is often highly degraded, and as such it is more likely to have already converged to a common chemistry (Grandy and Neff, 2008). As coarser soils may be associated with less processed SOM (Grandy and Neff, 2008), initial differences in plant litter chemistry may persist and be reflected in SOM chemistry. Likewise, soil texture is a strong predictor of microbial biomass, diversity, and community composition, with fine-textured soils buffering against land use effects (Crowther et al., 2014). As virtually all SOC is processed by the microbial biomass at some point (Grandy and Neff, 2008), diminished differences in microbial dynamics may have potentially led to the observed uniformity in SOM chemistry along the climosequence. While we found SOM biological stability to be largely unrelated to SOM chemistry, it remains to be investigated whether this holds true in other soil types. Sandy soils are of particular interest, as the relative importance of biochemical recalcitrance in SOM stabilization may be enhanced (Six et al., 2002), the chemistry of SOM is more likely to be divergent (Grandy and Neff, 2008), and the buffering effect of clay on microbial dynamics is diminished (Crowther et al., 2014) in coarse-textured soils.

Our finding that biochemical recalcitrance does not significantly control SOM biological stability suggests that future inquiries into the response of SOM persistence to changes in climate and land use should explicitly examine the roles of organo-mineral association and microbial inaccessibility in SOM stabilization. Notably, these stabilization mechanisms may be more responsive to environmental changes than SOM biochemical recalcitrance. While the production of biochemically recalcitrant SOM is controlled by environmental factors (e.g., plant litter inputs), by definition its decomposition is not (Kleber, 2010). An important caveat to this is that kinetic theory implies that the decomposition of stable SOM—regardless of the stabilization

mechanism(s) involved in its protection (von Lützow and Kögel-Knabner, 2010)—is more temperature sensitive (Bosatta and Ågren, 1999; Fierer et al., 2005; Davidson and Janssens, 2006; Craine et al., 2010). Nonetheless, organo-mineral association and microbial inaccessibility may be influenced by environmental changes to a greater extent than biochemical recalcitrance: both the formation and destruction of soil aggregates (modifying microbial accessibility) as well as the adsorption and desorption of SOM to minerals are regulated by temperature (Davidson and Janssens, 2006). As such, SOM protected by organo-mineral association and microbial inaccessibility may become a readily available substrate as soon as these protection mechanisms cease to operate (Kleber, 2010), highlighting the need for future investigations into the controls on these constraints to SOM decomposition.

6. REFERENCES

Addiscott, T. 1983. Kinetics and temperature relationships of mineralization and nitrification in Rothamsted soils with differing histories. J. Soil Sci. 34: 343–353.

Ajwa, H.A., C.W. Rice, and D. Sotomayor. 1998. Carbon and nitrogen mineralization in tallgrass prairie and agricultural soil profiles. Soil Sci. Soc. Am. J. 62: 942–951.

Amelung, W., S. Brodowski, A. Sandhage-Hofmann, and R. Bol. 2008. Combining biomarker with stable isotope anlyses for assessing the transformation and turnover of soil organic matter. Adv. Agron. 100: 155–250.

Amelung, W., K.W. Flach, and W. Zech. 1997. Climatic effects on soil organic matter composition in the Great Plains. Soil Sci. Soc. Am. J. 61: 115–123.

Amelung, W., K.-W. Flach, and W. Zech. 1999a. Lignin in particle-size fractions of native grassland soils as influenced by climate. Soil Sci. Soc. Am. J. 63: 1222–1228.

Amelung, W., X. Zhang, and K.W. Flach. 2006. Amino acids in grassland soils: climatic effects on concentrations and chirality. Geoderma 130: 207–217.

Amelung, W., X. Zhang, K.W. Flach, and W. Zech. 1999b. Amino sugars in native grassland soils along a climosequence in North America. Soil Sci. Soc. Am. J. 63: 86–92.

Amundson, R. 2001. The carbon budget in soils. Annu. Rev. Earth Planet. Sci. 29: 535–562.

Angers, D.A., and G.R. Mehuys. 1990. Barley and alfalfa cropping effects on carbohydrate contents of a clay soil and its size fractions. Soil Biol. Biochem. 22: 285–288.

Arevalo, C.B.M., S.X. Chang, J.S. Bhatti, and D. Sidders. 2012. Mineralization potential and temperature sensitivity of soil organic carbon under different land uses in the parkland region of Alberta, Canada. Soil Sci. Soc. Am. J. 76: 241–251.

Arnarson, T.S., and R.G. Keil. 2000. Mechanisms of pore water organic matter adsorption to montmorillonite. Mar. Chem. 71: 309–320.

Bachmann, J., G. Guggenberger, T. Baumgartl, R.H. Ellerbrock, E. Urbanek, M.-O. Goebel, K. Kaiser, R. Horn, and W.R. Fischer. 2008. Physical carbon-sequestration mechanisms under special consideration of soil wettability. J. Plant Nutr. Soil Sci. 171: 14–26.

Baldock, J.A., and K. Broos. 2011. Soil organic matter. p. 11.1–11.52. *In* Huang, P.M., Li, Y., Sumner, M.E. (eds.), Handbook of Soil Sciences: Properties and Processes. 2nd ed. Handbook of Soil Science. CRC Press, Boca Raton, FL.

Baldock, J.A., and J.O. Skjemstad. 2000. Role of the soil matrix and minerals in protecting natural organic materials against biological attack. Org. Geochem. 31: 697–710.

Barrett, J.E., and I.C. Burke. 2000. Potential nitrogen immobilization in grassland soils across a soil organic matter gradient. Soil Biol. Biochem. 32: 1707–1716.

Barrow, E. 2009. Climate scenarios for Saskatchewan. Prairie Adaptation Research Collaborative, Regina, SK.

Baum, C., K.-U. Eckhardt, and J. Hahn. 2013. Impact of poplar on soil organic matter quality and microbial communities in arable soils. Plant, Soil Environ. 59: 95–100.

Berg, B., and C. McClaugherty. 2014. Plant litter. Decomposition, humus formation, carbon sequestration. 3rd ed. Springer, Heidelberg, DE.

van Bochove, E., D. Couillard, M. Schnitzer, and H.-R. Schulten. 1996. Pyrolysis-field ionization mass spectrometry of the four phases of cow manure composting. Soil Sci. Soc. Am. J. 60: 1781–1786.

Bolinder, M.A., O. Andrén, T. Kätterer, R. de Jong, A.J. VandenBygaart, D.A. Angers, L.-E. Parent, and E.G. Gregorich. 2007. Soil carbon dynamics in Canadian Agricultural Ecoregions: Quantifying climatic influence on soil biological activity. Agric. Ecosyst. Environ. 122: 461–470.

Bonde, T.A., and T. Rosswall. 1987. Seasonal variation of potentially mineralizable nitrogen in four cropping systems. Soil Sci. Soc. Am. J. 51: 1508–1514.

Bosatta, E., and G.I. Ågren. 1999. Soil organic matter quality interpreted thermodynamically. Soil Biol. Biochem. 31: 1889–1891.

Callesen, I., K. Raulund-Rasmussen, C.J. Westman, and L. Tau-Strand. 2007. Nitrogen pools and C:N ratios in well-drained Nordic forest soils related to climate and soil texture. Boreal Environ. Res. 12: 681–692.

Campbell, C.A., B.H. Ellert, and Y.W. Jame. 1993. Nitrogen mineralization potential in soils. p. 341–349. *In* Carter, M.R. (ed.), Soil Sampling and Methods of Analysis. 1st ed. Lewis Publishers, Boca Raton, FL.

Cheshire, M.V., B.T. Christensen, and L.H. Sørensen. 1990. Labelled and native sugars in particle-size fractions from soils incubated with ^{14}C straw for 6 to 18 years. J. Soil Sci. 41: 29–39.

Christensen, B.T. 1996. Carbon in primary and secondary organomineral complexes. p. 97–166. *In* Carter, M.R., Stewart, B.A. (eds.), Structure and Organic Matter Storage in Agricultural Soils. CRC Press, Inc., Boca Raton, FL.

Conant, R.T., M.G. Ryan, G.I. Ågren, H.E. Birge, E.A. Davidson, P.E. Eliasson, S.E. Evans, S.D. Frey, C.P. Giardina, F.M. Hopkins, R. Hyvönen, M.U.F. Kirschbaum, J.M. Lavallee, J. Leifeld, W.J. Parton, J.M. Steinweg, M.D. Wallenstein, J.Å. Martin Wetterstedt, and M.A. Bradford. 2011. Temperature and soil organic matter decomposition rates - synthesis of current knowledge and a way forward. Glob. Chang. Biol. 17: 3392–3404.

Cookson, W.R., M. Osman, P. Marschner, D.A. Abaye, I. Clark, D.V. Murphy, E.A. Stockdale, and C.A. Watson. 2007. Controls on soil nitrogen cycling and microbial community composition across land use and incubation temperature. Soil Biol. Biochem. 39: 744–756.

Cooney, R.R., and S.G. Urquhart. 2004. Chemical trends in the near-edge X-ray absorption fine structure of monosubstituted and para-bisubstituted benzenes. J. Pysical Chem. B 108: 18185–18191.

Côté, L., S. Brown, D. Paré, J. Fyles, and J. Bauhus. 2000. Dynamics of carbon and nitrogen mineralization in relation to stand type, stand age and soil texture in the boreal mixedwood. Soil Biol. Biochem. 32: 1079–1090.

Craine, J.M., N. Fierer, and K.K. McLauchlan. 2010. Widespread coupling between the rate and temperature sensitivity of organic matter decay. Nat. Geosci. 3: 854–857.

Craine, J.M., C. Morrow, and N. Fierer. 2007. Microbial nitrogen limitation increases decomposition. Ecology 88: 2105–2113.

Crowther, T.W., D.S. Maynard, J.W. Leff, E.E. Oldfield, R.L. McCulley, N. Fierer, and M.A. Bradford. 2014. Predicting the responsiveness of soil biodiversity to deforestation: a cross-biome study. Glob. Chang. Biol. 20: 2983–94.

Curtin, D., M.H. Beare, and G. Hernandez-Ramirez. 2012. Temperature and moisture effects on microbial biomass and soil organic matter mineralization. Soil Sci. Soc. Am. J. 76: 2055–2067.

Curtin, D., and C.A. Campbell. 2008. Mineralizable nitrogen. p. 599–606. *In* Carter, M.R., Gregorich, E.G. (eds.), Soil Sampling and Methods of Analysis. 2nd ed. Taylor & Francis Group, Boca Raton, FL.

Curtin, D., C. Campbell, and A. Jalil. 1998. Effects of acidity on mineralization: pH-dependence of organic matter mineralization in weakly acidic soils. Soil Biol. Biochem. 30: 57–64.

Dalias, P., J.. Anderson, P. Bottner, and M.-M. Coûteaux. 2001. Long-term effects of temperature on carbon mineralisation processes. Soil Biol. Biochem. 33: 1049–1057.

Dalmolin, R.S.D., C.N. Gonçalves, D.P. Dick, H. Knicker, E. Klamt, and I. Kögel-Knabner. 2006. Organic matter characteristics and distribution in Ferralsol profiles of a climosequence in southern Brazil. Eur. J. Soil Sci. 57: 644–654.

Davidson, E.A., and I.A. Janssens. 2006. Temperature sensitivity of soil carbon decomposition and feedbacks to climate change. Nature 440: 165–173.

Deans, J.R., J.A.E. Molina, and C.E. Clapp. 1986. Models for predicting potentially mineralizable nitrogen and decomposition rate constants. Soil Sci. Soc. Am. J. 50: 323–326.

Demanèche, S., L. Jocteur-Monrozier, H. Quiquampoix, and P. Simonet. 2001. Evaluation of biological and physical protection against nuclease degradation of clay-bound plasmid DNA. Appl. Environ. Microbiol. 67: 293–299.

Dent, B.B., S.L. Forbes, and B.H. Stuart. 2004. Review of human decomposition processes in soil. Environ. Geol. 45: 576–585.

Derenne, S., and C. Largeau. 2001. A review of some important families of refractory macromolecules: composition, origin, and fate in soils and sediments. Soil Sci. 166: 833–847.

Dessureault-Rompré, J., B.J. Zebarth, D.L. Burton, M. Sharifi, J. Cooper, C.A. Grant, and C.F. Drury. 2010. Relationships among mineralizable soil nitrogen, soil properties, and climatic indices. Soil Sci. Soc. Am. J. 74: 1218–1227.

Dhez, O., H. Ade, and S.G. Urquhart. 2003. Calibrated NEXAFS spectra of some common polymers. J. Electron Spectros. Relat. Phenomena 128: 85–96.

Djajakirana, G., R.G. Joergensen, and B. Meyer. 1996. Ergosterol and microbial biomass relationship in soil. Biol. Fertil. Soils 22: 299–304.

Djukic, I., F. Zehetner, M. Tatzber, and M.H. Gerzabek. 2010. Soil organic-matter stocks and characteristics along an Alpine elevation gradient. J. Plant Nutr. Soil Sci. 173: 30–38.

Doerr, S.H., R. a. Shakesby, and R.P.D. Walsh. 2000. Soil water repellency: its causes, characteristics and hydro-geomorphological significance. Earth-Science Rev. 51: 33–65.

Douglas, C.L.J., P.E. Rasmussen, H.P. Collins, and S.L. Albrecht. 1998. Nitrogen mineralization across a climosequence in the Pacific Northwest. Soil Biol. Biochem. 30: 1765–1772.

Dümig, A., H. Knicker, P. Schad, C. Rumpel, M.-F. Dignac, and I. Kögel-Knabner. 2009. Changes in soil organic matter composition are associated with forest encroachment into grassland with long-term fire history. Eur. J. Soil Sci. 60: 578–589.

Dungait, J.A.J., D.W. Hopkins, A.S. Gregory, and A.P. Whitmore. 2012. Soil organic matter turnover is governed by accessibility not recalcitrance. Glob. Chang. Biol. 18: 1781–1796.

Elliot, E.T. 1986. Aggregate structure and carbon, nitrogen, and phosphorus in native and cultivated soils. Soil Sci. Soc. Am. J. 50: 627–633.

Eusterhues, K., C. Rumpel, M. Kleber, and I. Kögel-Knabner. 2003. Stabilisation of soil organic matter by interactions with minerals as revealed by mineral dissolution and oxidative degradation. Org. Geochem. 34: 1591–1600.

Feng, X., and M.J. Simpson. 2007. The distribution and degradation of biomarkers in Alberta grassland soil profiles. Org. Geochem. 38: 1558–1570.

Feng, X., A.J. Simpson, and M.J. Simpson. 2005. Chemical and mineralogical controls on humic acid sorption to clay mineral surfaces. Org. Geochem. 36: 1553–1566.

Feng, X., A.J. Simpson, K.P. Wilson, D.D. Williams, and M.J. Simpson. 2008. Increased cuticular carbon sequestration and lignin oxidation in response to soil warming. Nat. Geosci. 1: 836–839.

Fernandez, I., B. Carrasco, and A. Cabaneiro. 2012. Evolution of soil organic matter composition and edaphic carbon effluxes following oak forest clearing for pasture: climate change implications. Eur. J. For. Res. 131: 1681–1693.

Fierer, N., J.M. Craine, K. Mclauchlan, and J.P. Schimel. 2005. Litter quality and the temperature sensitivity of decomposition. Ecology 86: 320–326.

Fierer, N., A.S. Grandy, J. Six, and E.A. Paul. 2009. Searching for unifying principles in soil ecology. Soil Biol. Biochem. 41: 2249–2256.

Filley, T.R., T.W. Boutton, J.D. Liao, J.D. Jastrow, and D.E. Gamblin. 2008. Chemical changes to nonaggregated particulate soil organic matter following grassland-to-woodland transition in a subtropical savanna. J. Geophys. Res. 113: G03009.

Fitzsimmons, M. 2002. Estimated rates of deforestation in two boreal landscapes in central Saskatchewan, Canada. Can. J. For. Res. 32: 843–851.

Fontaine, S., S. Barot, P. Barré, N. Bdioui, B. Mary, and C. Rumpel. 2007. Stability of organic carbon in deep soil layers controlled by fresh carbon supply. Nature 450: 277–280.

Franzluebbers, A.J., R.L. Haney, C.W. Honeycutt, M.A. Arshad, H.H. Schomberg, and F.M. Hons. 2001. Climatic influences on active fractions of soil organic matter. Soil Biol. Biochem. 33: 1103–1111.

Frey, S.D., R. Drijber, H. Smith, and J. Melillo. 2008. Microbial biomass, functional capacity, and community structure after 12 years of soil warming. Soil Biol. Biochem. 40: 2904–2907.

Friedlingstein, P., P. Cox, and R. Betts. 2006. Climate–carbon cycle feedback analysis: Results from the C4MIP model intercomparison. J. Clim. 19: 3337–3353.

Gärdenäs, A.I., G.I. Ågren, J. a. Bird, M. Clarholm, S. Hallin, P. Ineson, T. Kätterer, H. Knicker, S.I. Nilsson, T. Näsholm, S. Ogle, K. Paustian, T. Persson, and J. Stendahl. 2011. Knowledge gaps in soil carbon and nitrogen interactions – from molecular to global scale. Soil Biol. Biochem. 43: 702–717.

Giardina, C.P., and M.G. Ryan. 2000. Evidence that decomposition rates of organic carbon in mineral soil do not vary with temperature. Nature 404: 858–861.

Giardina, C.P., M.G. Ryan, R.M. Hubbard, and D. Binkley. 2001. Tree species and soil textural controls on carbon and nitrogen mineralization rates. Soil Sci. Soc. Am. J. 65: 1272–1279.

Gillespie, A.W., A. Diochon, B.L. Ma, M.J. Morrison, L. Kellman, F.L. Walley, T.Z. Regier, D. Chevrier, J.J. Dynes, and E.G. Gregorich. 2014a. Nitrogen input quality changes the biochemical composition of soil organic matter stabilized in the fine fraction: a long-term study. Biogeochemistry 117: 337–350.

Gillespie, A.W., H. Sanei, A. Diochon, B.H. Ellert, T.Z. Regier, D. Chevrier, J.J. Dynes, C. Tarnocai, and E.G. Gregorich. 2014b. Perennially and annually frozen soil carbon differ in their susceptibility to decomposition: analysis of Subarctic earth hummocks by bioassay, XANES and pyrolysis. Soil Biol. Biochem. 68: 106–116.

Gillespie, A.W., F.L. Walley, R.E. Farrell, P. Leinweber, K.-U. Eckhardt, T.Z. Regier, and R.I.R. Blyth. 2011. XANES and pyrolysis-FIMS evidence of organic matter composition in a hummocky landscape. Soil Sci. Soc. Am. J. 75: 1741–1755.

Gillespie, A.W., F.L. Walley, R.E. Farrell, P. Leinweber, A. Schlichting, K.-U. Eckhardt, T.Z. Regier, and R.I.R. Blyth. 2009. Profiling rhizosphere chemistry: Evidence from carbon and nitrogen K-edge XANES and pyrolysis-FIMS. Soil Sci. Soc. Am. J. 73: 2002–2012.

Gillespie, A.W., F.L. Walley, R.E. Farrell, T.Z. Regier, and R.I.R. Blyth. 2008. Calibration method at the N *K*-edge using interstitial nitrogen gas in solid-state nitrogen-containing inorganic compounds. J. Synchrotron Radiat. 15: 532–534.

Glaser, B., and W. Amelung. 2003. Pyrogenic carbon in native grassland soils along a climosequence in North America. Global Biogeochem. Cycles 17: 331–338.

Goh, K.M. 2011. Carbon sequestration and stabilization in soils: Implications for soil productivity and climate change. Soil Sci. Plant Nutr. 50: 467–476.

Grandy, A.S., and J.C. Neff. 2008. Molecular C dynamics downstream: the biochemical decomposition sequence and its impact on soil organic matter structure and function. Sci. Total Environ. 404: 297–307.

Grandy, A.S., M.S. Strickland, C.L. Lauber, M.A. Bradford, and N. Fierer. 2009. The influence of microbial communities, management, and soil texture on soil organic matter chemistry. Geoderma 150: 278–286.

de Groot, F.M.F., M.A. Arrio, P. Sainctavit, C. Cartier, and C.T. Chen. 1994. Fluorescence yield detection: why it does not measure the X-ray absorption cross section. Solid State Commun. 92: 991–995.

Guggenberger, G., W. Zech, L. Haumaier, and B.T. Christensen. 1995. Land-use effects on the composition of organic matter in particle-size separates of soils: II. CPMAS and solution ^{13}C NMR analysis. Eur. J. Soil Sci. 46: 147–158.

Hardie, A.G., J.J. Dynes, L.M. Kozak, and P.M. Huang. 2007. Influence of polyphenols on the integrated polyphenol-Maillard reaction humification pathway as catalyzed by birnessite. Ann. Environ. Sci. 1: 91–110.

Haynes, R.J. 2005. Labile organic matter fractions as central components of the quality of agricultural soils: an overview. Adv. Agron. 85: 221–268.

Hedges, J.I., G. Eglinton, P.G. Hatcher, D.L. Kirchman, C. Arnosti, S. Derenne, R.P. Evershed, I. Kögel-Knabner, J.W. de Leeuw, R. Littke, W. Michaelis, and J. Rullkötter. 2000. The molecularly-uncharacterized component of nonliving organic matter in natural environments. Org. Geochem. 31: 945–958.

van Hees, P.A.W., S.I. Vinogradoff, A.C. Edwards, D.L. Godbold, and D.L. Jones. 2003. Low molecular weight organic acid adsorption in forest soils: effects on soil solution concentrations and biodegradation rates. Soil Biol. Biochem. 35: 1015–1026.

Heimann, M., and M. Reichstein. 2008. Terrestrial ecosystem carbon dynamics and climate feedbacks. Nature 451: 289–92.

Hempfling, R., W. Zech, and H.-R. Schulten. 1988. Chemical composition of the organic matter in forest soils: 2. Moder profile. Soil Sci. 146: 262–276.

Hendershot, W.H., H. Lalande, and M. Duquette. 2008. Soil reaction and exchangeable acidity. p. 173–178. *In* Carter, M.R., Gregorich, E.G. (eds.), Soil Sampling and Methods of Analysis. 2nd ed. CRC Press, Boca Raton, FL.

Hessen, D., G. Ågren, and T. Anderson. 2004. Carbon sequestration in ecosystems: the role of stoichiometry. Ecology 85: 1179–1192.

Heumann, S., D.L. Rimmer, A. Schlichting, G.D. Abbott, P. Leinweber, and J. Böttcher. 2013. Effects of potentially inhibiting substances on C and net N mineralization of a sandy soil - a case study. J. Plant Nutr. Soil Sci. 176: 35–39.

Heumann, S., A. Schlichting, J. Böttcher, and P. Leinweber. 2011. Sterols in soil organic matter in relation to nitrogen mineralization in sandy arable soils. J. Plant Nutr. Soil Sci. 174: 576–586.

Hijmans, R.J., S.E. Cameron, J.L. Parra, P.G. Jones, and A. Jarvis. 2005. Very high resolution interpolated climate surfaces for global land areas. Int. J. Climatol. 25: 1965–1978.

Hilli, S., S. Stark, and J. Derome. 2008. Carbon quality and stocks in organic horizons in boreal forest soils. Ecosystems 11: 270–282.

Hogg, E.H. 1994. Climate and the southern limit of the western Canadian boreal forest. Can. J. For. Res. 24: 1835–1845.

Hogg, E.H., and P.A. Hurdle. 1995. The aspen parkland in western Canada: a dry-climate analogue for the future boreal forest? Water. Air. Soil Pollut. 82: 391–400.

Homann, P.S., J.S. Kapchinske, and A. Boyce. 2007. Relations of mineral-soil C and N to climate and texture: regional differences within the conterminous USA. Biogeochemistry 85: 303–316.

Hopkins, D.W. 2008. Carbon mineralization. p. 589–598. *In* Carter, M.R., Gregorich, E.G. (eds.), Soil Sampling and Methods of Analysis. 2nd ed. Taylor & Francis Group, Boca Raton, FL.

Indorante, S.J., L.R. Follmer, R.D. Hammer, and P.G. Koenig. 1990. Particle-size analysis by a modified pipette procedure. Soil Sci. Soc. Am. J. 54: 560–563.

IPCC. 2013. Climate Change 2013: The Physical Science Basis. Contribution of Working Group I to the Fifth Assessment Report of the Intergovernmental Panel on Climate Change. Cambridge University Press, New York, NY.

IPCC. 2014. Climate Change 2014: Impacts, Adaptation, and Vulnerability. Part A: Global and Sectoral Aspects. Contribution of Working Group II to the Fifth Assessment Report of the Intergovernmental Panel on Climate Change. Cambridge University Press, Cambridge, UK.

IUSS Working Group WRB. 2014. World Reference Base for Soil Resources 2014. International soil classification system for naming soils and creating legends for soil maps. World Soil Resources Reports No. 106. FAO, Rome.

Jackson, R.B., J. Canadell, J.R. Ehleringer, H.A. Mooney, O.E. Sala, and E.D. Schulze. 1996. A global analysis of root distributions for terrestrial biomes. Oecologia 108: 389–411.

Jandl, G., P. Leinweber, H.-R. Schulten, and K. Ekschmitt. 2005. Contribution of primary organic matter to the fatty acid pool in agricultural soils. Soil Biol. Biochem. 37: 1033–1041.

Jandl, G., P. Leinweber, H.-R. Schulten, and K. Eusterhues. 2004. The concentrations of fatty acids in organo-mineral particle-size fractions of a Chernozem. Eur. J. Soil Sci. 55: 459–470.

Janssens, I.A., and S. Vicca. 2010. Biogeochemistry: soil carbon breakdown. Nat. Geosci. 3: 823–824.

Janzen, H.H. 2004. Carbon cycling in earth systems—a soil science perspective. Agric. Ecosyst. Environ. 104: 399–417.

Janzen, H.H. 2006. The soil carbon dilemma: shall we hoard it or use it? Soil Biol. Biochem. 38: 419–424.

Janzen, H.H., P.E. Fixen, A.J. Franzluebbers, J. Hattey, R.C. Izaurralde, Q.M. Ketterings, D.A. Lobb, and W.H. Schlesinger. 2011. Global prospects rooted in soil science. Soil Sci. Soc. Am. J. 75: 1–8.

Jobbágy, E.G., and R.B. Jackson. 2000. The vertical distribution of soil organic carbon and its relation to climate and vegetation. Ecol. Appl. 10: 423–436.

John, B., T. Yamashita, B. Ludwig, and H. Flessa. 2005. Storage of organic carbon in aggregate and density fractions of silty soils under different types of land use. Geoderma 128: 63–79.

Jokic, A., J.N. Cutler, D.W. Anderson, and F.L. Walley. 2004. Detection of heterocyclic N compounds in whole soils using N-XANES spectroscopy. Can. J. Soil Sci. 84: 291–293.

Jokic, A., J.N. Cutler, E. Ponomarenko, G. van der Kamp, and D.W. Anderson. 2003. Organic carbon and sulphur compounds in wetland soils: insights on structure and transformation processes using K-edge XANES and NMR spectroscopy. Geochim. Cosmochim. Acta 67: 2585–2597.

Jones, C., and P. Falloon. 2009. Sources of uncertainty in global modelling of future soil organic carbon storage. p. 283–315. *In* Baveye, P.C., Laba, M., Mysiak, J. (eds.), Uncertainties in Environmental Modelling and Consequences for Policy Making. NATO Science for Peace and Security Series C: Environmental Security. Springer, Dordrecht, NL.

Kalbitz, K., J. Schmerwitz, D. Schwesig, and E. Matzner. 2003a. Biodegradation of soil-derived dissolved organic matter as related to its properties. Geoderma 113: 273–291.

Kalbitz, K., D. Schwesig, J. Rethemeyer, and E. Matzner. 2005. Stabilization of dissolved organic matter by sorption to the mineral soil. Soil Biol. Biochem. 37: 1319–1331.

Kalbitz, K., D. Schwesig, J. Schmerwitz, K. Kaiser, L. Haumaier, B. Glaser, R. Ellerbrock, and P. Leinweber. 2003b. Changes in properties of soil-derived dissolved organic matter induced by biodegradation. Soil Biol. Biochem. 35: 1129–1142.

Kawahigashi, M., K. Kaiser, K. Kalbitz, A. Rodionov, and G. Guggenberger. 2004. Dissolved organic matter in small streams along a gradient from discontinuous to continuous permafrost. Glob. Chang. Biol. 10: 1576–1586.

Kennedy, M.J., D.R. Pevear, and R.J. Hill. 2002. Mineral surface control of organic carbon in black shale. Science 295: 657–660.

Kiem, R., H. Knicker, M. Körschens, and I. Kögel-Knabner. 2000. Refractory organic carbon in C-depleted arable soils, as studied by ^{13}C NMR spectroscopy and carbohydrate analysis. Org. Geochem. 31: 655–668.

Kiersch, K., J. Kruse, K.-U. Eckhardt, A. Fendt, T. Streibel, R. Zimmermann, G. Broll, and P. Leinweber. 2012a. Impact of grassland burning on soil organic matter as revealed by a synchrotron- and pyrolysis–mass spectrometry-based multi-methodological approach. Org. Geochem. 44: 8–20.

Kiersch, K., J. Kruse, T.Z. Regier, and P. Leinweber. 2012b. Temperature resolved alteration of soil organic matter composition during laboratory heating as revealed by C and N XANES spectroscopy and Py-FIMS. Thermochim. Acta 537: 36–43.

Kim, J.-S., M. Ree, S.W. Lee, W. Oh, S. Baek, B. Lee, T.J. Shin, K.J. Kim, B. Kim, and J. Lüning. 2003. NEXAFS spectroscopy study of the surface properties of zinc glutarate and its reactivity with carbon dioxide and propylene oxide. J. Catal. 218: 386–395.

Kinyangi, J., D. Solomon, B. Liang, M. Lerotic, S. Wirick, and J. Lehmann. 2006. Nanoscale biogeocomplexity of the organomineral assemblage in soil. Soil Sci. Soc. Am. J. 70: 1708–1718.

Kirschbaum, M.U.F. 2000. Will changes in soil organic carbon act as a positive or negative feedback on global warming? Biogeochemistry 48: 21–51.

Kleber, M. 2010. What is recalcitrant soil organic matter? Environ. Chem. 7: 320–332.

Kleber, M., and M.G. Johnson. 2010. Advances in understanding the molecular structure of soil organic matter: implications for interactions in the environment. Adv. Agron. 106: 77–142.

Kleber, M., P.S. Nico, A. Plante, T. Filley, M. Kramer, C. Swanston, and P. Sollins. 2011. Old and stable soil organic matter is not necessarily chemically recalcitrant: implications for modeling concepts and temperature sensitivity. Glob. Chang. Biol. 17: 1097–1107.

Kleber, M., P. Sollins, and R. Sutton. 2007. A conceptual model of organo-mineral interactions in soils: self-assembly of organic molecular fragments into zonal structures on mineral surfaces. Biogeochemistry 85: 9–24.

Knicker, H. 2004. Stabilization of N-compounds in soil and organic-matter-rich sediments—what is the difference? Mar. Chem. 92: 167–195.

Knicker, H. 2011. Soil organic N - an under-rated player for C sequestration in soils? Soil Biol. Biochem. 43: 1118–1129.

Knicker, H., R. Fründ, and H.-D. Lüdemann. 1993. The chemical nature of nitrogen in native soil organic matter. Naturwissenschaften 80: 219–221.

Knicker, H., and I. Kögel-Knabner. 1998. Soil organic nitrogen formation examined by means of NMR spectroscopy. p. 339–356. *In* Stankiewicz, B.A., van Bergen, P.F. (eds.), Nitrogen-Containing Macromolecules in the Bio- and Geosphere. ACS Symposium Series 707. ACS Symposium Series. American Chemical Society, Washington, DC.

Knicker, H., A.W. Scaroni, and P.G. Hatcher. 1996. ^{13}C and ^{15}N NMR spectroscopic investigation on the formation of fossil algal residues. Org. Geochem. 24: 661–669.

Koch, A.L. 1990. Growth and form of the bacterial cell wall. Am. Sci. 78: 327–341.

Kögel, I., R. Hempfling, W. Zech, P.G. Hatcher, and H.-R. Schulten. 1988. Chemical composition of the organic matter in forest soils: 1. Forest litter. Soil Sci. 146: 124–136.

Kögel-Knabner, I. 2002. The macromolecular organic composition of plant and microbial residues as inputs to soil organic matter. Soil Biol. Biochem. 34: 139–162.

Kögel-Knabner, I., G. Guggenberger, M. Kleber, E. Kandeler, K. Kalbitz, S. Scheu, K. Eusterhues, and P. Leinweber. 2008. Organo-mineral associations in temperate soils:

integrating biology, mineralogy, and organic matter chemistry. J. Plant Nutr. Soil Sci. 171: 61–82.

Kononova, M.M. 1961. Soil organic matter: its nature, its role in soil formation and in soil fertility. Pergamon Press Inc., New York, NY.

Krull, E.S., J.A. Baldock, and J.O. Skjemstad. 2003. Importance of mechanisms and processes of the stabilisation of soil organic matter for modelling carbon turnover. Funct. Plant Biol. 30: 207.

Kruse, J., K.-U. Eckhardt, T. Regier, and P. Leinweber. 2011. TG–FTIR, LC/MS, XANES and Py-FIMS to disclose the thermal decomposition pathways and aromatic N formation during dipeptide pyrolysis in a soil matrix. J. Anal. Appl. Pyrolysis 90: 164–173.

Kruse, J., A. Schlichting, J. Siemens, T. Regier, and P. Leinweber. 2010. Pyrolysis-field ionization mass spectrometry and nitrogen *K*-edge XANES spectroscopy applied to bulk soil leachates—a case study. Sci. Total Environ. 408: 4910–4915.

Lauber, C.L., M.S. Strickland, M.A. Bradford, and N. Fierer. 2008. The influence of soil properties on the structure of bacterial and fungal communities across land-use types. Soil Biol. Biochem. 40: 2407–2415.

Legendre, P., and L. Legendre. 2012. Numerical Ecology. 3rd ed. Elsevier, Boston.

Lehmann, J., B. Liang, D. Solomon, M. Lerotic, F. Luizão, J. Kinyangi, T. Schäfer, S. Wirick, and C. Jacobsen. 2005. Near-edge X-ray absorption fine structure (NEXAFS) spectroscopy for mapping nano-scale distribution of organic carbon forms in soil: application to black carbon particles. Global Biogeochem. Cycles 19: GB1013.

Lehmann, J., D. Solomon, J. Kinyangi, L. Dathe, S. Wirick, and C. Jacobsen. 2008. Spatial complexity of soil organic matter forms at nanometre scales. Nat. Geosci. 1: 238–242.

Leinweber, P., G. Jandl, C. Baum, K.-U. Eckhardt, and E. Kandeler. 2008. Stability and composition of soil organic matter control respiration and soil enzyme activities. Soil Biol. Biochem. 40: 1496–1505.

Leinweber, P., G. Jandl, K.-U. Eckhardt, J. Kruse, F.L. Walley, M.J. Khan, R.I.R. Blyth, and T. Regier. 2010. Nitrogen speciation in fine and coarse clay fractions of a Cryoboroll - new evidence from pyrolysis-mass spectrometry and nitrogen *K*-edge XANES. Can. J. Soil Sci. 90: 309–318.

Leinweber, P., G. Jandl, K.-U. Eckhardt, A. Schlichting, and H.-R. Schulten. 2009a. Analytical pyrolysis and soft-ionization mass spectrometry. p. 539–588. *In* Senesi, N., Xing, B., Huang, P.M. (eds.), Biophysico-Chemical Processes Involving Natural Nonliving Organic Matter in Environmental Systems. John Wiley & Sons, Inc., Hoboken, NJ, England.

Leinweber, P., J. Kruse, C. Baum, M. Arcand, J.D. Knight, R. Farrell, K.-U. Eckhardt, K. Kiersch, and G. Jandl. 2013. Advances in understanding of organic nitrogen chemistry in soils using state-of-the-art analytical techniques. Adv. Agron. 119: 83–151.

Leinweber, P., J. Kruse, F.L. Walley, A. Gillespie, K.-U. Eckhardt, R.I.R. Blyth, and T. Regier. 2007. Nitrogen *K*-edge XANES - an overview of reference compounds used to identify unknown organic nitrogen in environmental samples. J. Synchrotron Radiat. 14: 500–511.

Leinweber, P., and H.-R. Schulten. 1995. Composition, stability and turnover of soil organic matter: investigations by off-line pyrolysis and direct spectrometry. J. Anal. Appl. Pyrolysis 32: 91–110.

Leinweber, P., F. Walley, J. Kruse, G. Jandl, K.-U. Eckhardt, R.I.R. Blyth, and T. Regier. 2009b. Cultivation affects soil organic nitrogen: pyrolysis-mass spectrometry and nitrogen K-edge XANES spectroscopy evidence. Soil Sci. Soc. Am. J. 73: 82–92.

Lindemann, W., G. Connell, and N. Urquhart. 1988. Previous sludge addition effects on nitrogen mineralization in freshly amended soil. Soil Sci. Soc. Am. J. 52: 109–112.

Lombi, E., and J. Susini. 2009. Synchrotron-based techniques for plant and soil science: opportunities, challenges and future perspectives. Plant Soil 320: 1–35.

Lorenz, K., R. Lal, C.M. Preston, and K.G.J. Nierop. 2007. Strengthening the soil organic carbon pool by increasing contributions from recalcitrant aliphatic bio(macro)molecules. Geoderma 142: 1–10.

von Lützow, M., and I. Kögel-Knabner. 2010. Opinion response to the concept paper: "What is recalcitrant soil organic matter ?" by Markus Kleber. Environ. Chem. 7: 333–335.

von Lützow, M., I. Kögel-Knabner, K. Ekschmitt, E. Matzner, G. Guggenberger, B. Marschner, and H. Flessa. 2006. Stabilization of organic matter in temperate soils: mechanisms and their relevance under different soil conditions - a review. Eur. J. Soil Sci. 57: 426–445.

von Lützow, M., I. Kögel-Knabner, B. Ludwig, E. Matzner, H. Flessa, K. Ekschmitt, G. Guggenberger, B. Marschner, and K. Kalbitz. 2008. Stabilization mechanisms of organic matter in four temperate soils: Development and application of a conceptual model. J. Plant Nutr. Soil Sci. 171: 111–124.

MacDonald, N.W., D.R. Zak, and K.S. Pregitzer. 1995. Temperature effects on kinetics of microbial respiration and net nitrogen and sulfur mineralization. Soil Sci. Soc. Am. J. 59: 233–240.

Marín-Spiotta, E., C.W. Swanston, M.S. Torn, W.L. Silver, and S.D. Burton. 2008. Chemical and mineral control of soil carbon turnover in abandoned tropical pastures. Geoderma 143: 49–62.

Marschner, B., S. Brodowski, A. Dreves, G. Gleixner, A. Gude, P.M. Grootes, U. Hamer, A. Heim, G. Jandl, R. Ji, K. Kaiser, K. Kalbitz, C. Kramer, P. Leinweber, J. Rethemeyer, A. Schäffer, M.W.I. Schmidt, L. Schwark, and G.L.B. Wiesenberg. 2008. How relevant is recalcitrance for the stabilization of organic matter in soils? J. Plant Nutr. Soil Sci. 171: 91–110.

McGill, W. 2007. The physiology and biochemistry of soil organisms. p. 231–256. *In* Paul, E.A. (ed.), Microbiology, Ecology, and Biochemistry. 3rd ed. Academic Press, New York, NY.

McKenney, D.W., J.H. Pedlar, K. Lawrence, P. Papadopol, K. Campbell, and M.F. Hutchinson. 2014. Change and evolution in the plant hardiness zones of Canada. Bioscience 64: 341–350.

Mengel, K. 1996. Turnover of organic nitrogen in soils and its availability to crops. Plant Soil: 83–93.

Meyer, H., C. Kaiser, and C. Biasi. 2006. Soil carbon and nitrogen dynamics along a latitudinal transect in Western Siberia, Russia. Biogeochemistry 81: 239–252.

Mikutta, R., C. Mikutta, K. Kalbitz, T. Scheel, K. Kaiser, and R. Jahn. 2007. Biodegradation of forest floor organic matter bound to minerals via different binding mechanisms. Geochim. Cosmochim. Acta 71: 2569–2590.

Miller, A.J., R. Amundson, I.C. Burke, and C. Yonker. 2004. The effect of climate and cultivation on soil organic C and N. Biogeochemistry 67: 57–72.

Miltner, A., R. Kindler, H. Knicker, H.-H. Richnow, and M. Kästner. 2009. Fate of microbial biomass-derived amino acids in soil and their contribution to soil organic matter. Org. Geochem. 40: 978–985.

Molina, J.A.E., C.E. Ciapp, and W.E. Larson. 1980. Potentially mineralizable nitrogen in soil: the simple exponential model does not apply for the first 12 weeks of incubation. Soil Sci. Soc. Am. J. 44: 442–443.

Montané, F., P. Rovira, and P. Casals. 2007. Shrub encroachment into mesic mountain grasslands in the Iberian peninsula: Effects of plant quality and temperature on soil C and N stocks. Global Biogeochem. Cycles 21: GB4016.

Myneni, S.C.B. 2002. Soft X-ray spectroscopy and spectromicroscopy studies of organic molecules in the environment. Rev. Mineral. Geochemistry 49: 485–579.

Nieder, R., and D.K. Benbi. 2008. Modeling carbon and nitrogen dynamics in the soil-plant-atmosphere system. p. 307–342. *In* Nieder, R., Benbi, D.K. (eds.), Carbon and Nitrogen in the Terrestrial Environment. Springer, Heidelberg, DE.

Nuske, A., and J. Richter. 1981. N-mineralization in löss-parabrownearthes: incubation experiments. Plant Soil 59: 237–247.

Ó Cofaigh, C., D.J.A. Evans, and I.R. Smith. 2009. Large-scale reorganization and sedimentation of terrestrial ice streams during late Wisconsinan Laurentide Ice Sheet deglaciation. Geol. Soc. Am. Bull. 122: 743–756.

Oksanen, J., F.G. Blanchet, R. Kindt, P. Legendre, P.R. Minchin, R.B. O'Hara, G.L. Simpson, P. Solymos, M. Stevens, H. Henry, and H. Wagner. 2013. vegan: Community Ecology Package.

Olk, D.C. 2008. Improved analytical techniques for carbohydrates, amino compounds, and phenols: tools for understanding soil processes. Soil Sci. Soc. Am. J. 72: 1672–1682.

Otto, A., and M.J. Simpson. 2005. Degradation and preservation of vascular plant-derived biomarkers in grassland and forest soils from Western Canada. Biogeochemistry 73: 377–409.

Otto, A., and M.J. Simpson. 2006. Sources and composition of hydrolysable aliphatic lipids and phenols in soils from western Canada. Org. Geochem. 37: 385–407.

Paré, D., R. Boutin, G.R. Larocque, and F. Raulier. 2006. Effect of temperature on soil organic matter decomposition in three forest biomes of eastern Canada. Can. J. Soil Sci. 86: 247–256.

Parsons, S.A., R.A. Congdon, and I.R. Lawler. 2014. Determinants of the pathways of litter chemical decomposition in a tropical region. New Phytol. 203: 873–82.

Peberdy, J.F. 1990. Fungal cell walls-a review. p. 5–30. *In* Kuhn, P.J., Trinci, A.P.J., Jung, M.J., Goosey, M.W., Copping, L.G. (eds.), Biochemistry of Cell Walls and Membranes in Fungi. Springer, Berlin.

Pennock, D., A. Bedard-Haughn, and V. Viaud. 2011. Chernozemic soils of Canada: genesis, distribution, and classification. Can. J. Soil Sci. 91: 719–747.

Piccolo, A. 2001. The supramolecular structure of humic substances. Soil Sci. 166: 810–832.

Piccolo, A., and J. Mbagwu. 1999. Role of hydrophobic components of soil organic matter in soil aggregate stability. Soil Sci. Soc. Am. J. 63: 1801–1810.

Pisani, O., K.M. Hills, D. Courtier-Murias, A.J. Simpson, N.J. Mellor, E.A. Paul, S.J. Morris, and M.J. Simpson. 2013. Molecular level analysis of long term vegetative shifts and relationships to soil organic matter composition. Org. Geochem. 62: 7–16.

Purton, K.N., D.J. Pennock, P. Leinweber, and F.L. Walley. 2015. Will changes in climate and land use affect soil organic matter composition? Evidence from an ecotonal climosequence. Geoderma (*in review*).

R Core Team. 2013. R: A language and environment for statistical computing.

Raich, J.W., and W.H. Schlesinger. 1992. The global carbon dioxide flux in soil respiration and its relationship to vegetation and climate. Tellus 44: 81–99.

Raich, J.W., and A. Tufekcioglu. 2000. Vegetation and soil respiration: correlations and controls. Biogeochemistry 48: 71–90.

Rasse, D.P., C. Rumpel, and M.-F. Dignac. 2005. Is soil carbon mostly root carbon? Mechanisms for a specific stabilisation. Plant Soil 269: 341–356.

Ravel, B., and M. Newville. 2005. ATHENA, ARTEMIS, HEPHAESTUS: data analysis for X-ray absorption spectroscopy using IFEFFIT. J. Synchrotron Radiat. 12: 537–541.

Regier, T. 2012. Limitations and advancements in soft x-ray spectroscopy. Ph.D. diss. University of Saskatchewan, Saskatoon, SK.

Regier, T., J. Krochak, T.K. Sham, Y.F. Hu, J. Thompson, and R.I.R. Blyth. 2007a. Performance and capabilities of the Canadian Dragon: the SGM beamline at the Canadian Light Source. Nucl. Instruments Methods Phys. Res. A 582: 93–95.

Regier, T., J. Paulsen, G. Wright, I. Coulthard, K. Tan, T.K. Sham, and R.I.R. Blyth. 2007b. Commissioning of the spherical grating monochromator soft X-ray spectroscopy beamline at the Canadian Light Source. AIP Conf. Proc. 879: 473–476.

Rillig, M.C., B.A. Caldwell, H.A.B. Wösten, and P. Sollins. 2007. Role of proteins in soil carbon and nitrogen storage: controls on persistence. Biogeochemistry 85: 25–44.

Ritz, C., and J.C. Streibig. 2008. Nonlinear regression with R. Springer, New York, NY.

Rogers, H.J., H.R. Perkins, and J.B. Ward. 1980. Microbial cell walls and membranes. Chapman and Hall, London.

Rovezzi, M., F. D'Acapito, A. Navarro-Quezada, B. Faina, T. Li, A. Bonanni, F. Filippone, A.A. Bonapasta, and T. Dietl. 2009. Local structure of (Ga,Fe)N and (Ga,Fe)N:Si investigated by X-ray absorption fine structure spectroscopy. Phys. Rev. B 79: 195209.

Rumpel, C., K. Eusterhues, and I. Kögel-Knabner. 2004. Location and chemical composition of stabilized organic carbon in topsoil and subsoil horizons of two acid forest soils. Soil Biol. Biochem. 36: 177–190.

Rumpel, C., and I. Kögel-Knabner. 2011. Deep soil organic matter—a key but poorly understood component of the terrestrial C cycle. Plant Soil 338: 143–158.

Rumpel, C., I. Kögel-Knabner, and F. Bruhn. 2002. Vertical distribution, age, and chemical composition of organic carbon in two forest soils of different pedogenesis. Org. Geochem. 33: 1131–1142.

Saggar, S., A. Parshotam, G.P. Sparling, C.W. Feltham, and P.B.S. Hart. 1996. ^{14}C-labelled ryegrass turnover and residence time in soils varying in clay content and mineralogy. Soil Biol. Biochem. 28: 1677–1686.

Sauchyn, D., and S. Kulshreshtha. 2008. Prairies. p. 275–328. *In* Lemmen, D.S., Warren, F.J., Lacroix, J., Bush, E. (eds.), From impacts to adaptation: Canada in a changing climate 2007. Government of Canada, Ottawa, ON.

Schaumann, G.E., and S. Thiele-Bruhn. 2011. Molecular modeling of soil organic matter: Squaring the circle? Geoderma 166: 1–14.

Scheel, T., C. Dörfler, and K. Kalbitz. 2007. Precipitation of dissolved organic matter by aluminum stabilizes carbon in acidic forest soils. Soil Sci. Soc. Am. J. 71: 64–74.

Schimel, J.P., and J. Bennett. 2004. Nitrogen mineralization: challenges of a changing paradigm. Ecology 85: 591–602.

Schmidt, M.W.I., M.S. Torn, S. Abiven, T. Dittmar, G. Guggenberger, I.A. Janssens, M. Kleber, I. Kögel-Knabner, J. Lehmann, D.A.C. Manning, P. Nannipieri, D.P. Rasse, S. Weiner, and S.E. Trumbore. 2011. Persistence of soil organic matter as an ecosystem property. Nature 478: 49–56.

Schnitzer, M., D.F.E. McArthur, H.-R. Schulten, L.M. Kozak, and P.M. Huang. 2006. Long-term cultivation effects on the quantity and quality of organic matter in selected Canadian prairie soils. Geoderma 130: 141–156.

Schnitzer, M., and H.-R. Schulten. 1992. The analysis of soil organic matter by pyrolysis-field ionization mass spectrometry. Soil Sci. Soc. Am. J. 56: 1811–1817.

Schulten, H.-R. 1987. Pyrolysis and soft ionization mass spectrometry of aquatic/terrestrial humic substances and soils. J. Anal. Appl. Pyrolysis 12: 149–186.

Schulten, H.-R. 1996. Direct pyrolysis-mass spectrometry of soils: a novel tool in agriculture, ecology, forestry, and soil science. p. 373–436. *In* Boutton, T.W., Yamasaki, S. (eds.), Mass Spectrometry of Soils. Marcel Dekker, Inc., New York, NY.

Schulten, H.-R., and P. Leinweber. 1996. Characterization of humic and soil particles by analytical pyrolysis and computer modeling. J. Anal. Appl. Pyrolysis 38: 1–53.

Schulten, H.-R., and P. Leinweber. 1999. Thermal stability and composition of mineral-bound organic matter in density fractions of soil. Eur. J. Soil Sci. 50: 237–248.

Schulten, H.-R., and M. Schnitzer. 1998. The chemistry of soil organic nitrogen: a review. Biol. Fertil. Soils 26: 1–15.

Schumacher, M., I. Christl, A.C. Scheinost, C. Jacobsen, and R. Kretzschmar. 2005. Chemical heterogeneity of organic soil colloids investigated by scanning transmission X-ray microscopy and C-1s NEXAFS microspectroscopy. Environ. Sci. Technol. 39: 9094–9100.

Schwesig, D., K. Kalbitz, and E. Matzner. 2003. Effects of aluminium on the mineralization of dissolved organic carbon derived from forest floors. Eur. J. Soil Sci. 54: 311–322.

Scott, N.A., R.L. Parfitt, D.J. Ross, and G.J. Salt. 1998. Carbon and nitrogen transformations in New Zealand plantation forest soils from sites with different N status. Can. J. For. Res. 28: 967–976.

Seyfried, M., and P.S.C. Rao. 1988. Kinetics of nitrogen mineralization in Costa Rican soils: model evaluation and pretreatment effects. Plant Soil 106: 159–169.

Sham, T.K., and M.L. Rivers. 2002. A brief overview of synchrotron radiation. Rev. Mineral. Geochemistry 49: 117–147.

Simpson, M.J., and A.J. Simpson. 2012. The chemical ecology of soil organic matter molecular constituents. J. Chem. Ecol. 38: 768–84.

Sinsabaugh, R., M. Carreiro, and D. Repert. 2002. Allocation of extracellular enzymatic activity in relation to litter composition, N deposition, and mass loss. Biogeochemistry 60: 1–24.

Six, J., R. Conant, E. Paul, and K. Paustian. 2002. Stabilization mechanisms of soil organic matter: implications for C-saturation of soils. Plant Soil 241: 155–176.

Six, J., E.. Elliott, and K. Paustian. 2000. Soil macroaggregate turnover and microaggregate formation: a mechanism for C sequestration under no-tillage agriculture. Soil Biol. Biochem. 32: 2099–2103.

Sjögersten, S., B.L. Turner, N. Mahieu, L.M. Condron, and P.A. Wookey. 2003. Soil organic matter biochemistry and potential susceptibility to climatic change across the forest-tundra ecotone in the Fennoscandian mountains. Glob. Chang. Biol. 9: 759–772.

Sleutel, S., P. Leinweber, S.A. Begum, M.A. Kader, P. Van Oostveldt, and S. De Neve. 2008. Composition of organic matter in sandy relict and cultivated heathlands as examined by pyrolysis-field ionization MS. Biogeochemistry 89: 253–271.

Sleutel, S., P. Leinweber, E. Van Ranst, M.A. Kader, and K. Jegajeevagan. 2011. Organic matter in clay density fractions from sandy cropland soils with differing land-use history. Soil Sci. Soc. Am. J. 75: 521.

Smith, P., and P.D. Falloon. 2000. Modelling refractory soil organic matter. Biol. Fertil. Soils 30: 388–398.

Šnajdr, J., T. Cajthaml, V. Valášková, V. Merhautová, M. Petránková, P. Spetz, K. Leppänen, and P. Baldrian. 2011. Transformation of *Quercus petraea* litter: successive changes in litter chemistry are reflected in differential enzyme activity and changes in the microbial community composition. FEMS Microbiol. Ecol. 75: 291–303.

Soil Classification Working Group. 1998. The Canadian System of Soil Classification. 3rd ed. Agriculture and Agri-Food Canada, Publ. 1646, Ottawa, ON.

Soil Survey Staff. 2014. Keys to Soil Taxonomy. 12th ed. USDA-Natural Resources Conservation Service, Washington, DC.

Sollins, P., P. Homann, and B.A. Caldwell. 1996. Stabilization and destabilization of soil organic matter: mechanisms and controls. Geoderma 74: 65–105.

Solomon, D., J. Lehmann, J. Kinyangi, B. Liang, K. Heymann, L. Dathe, K. Hanley, S. Wirick, and C. Jacobsen. 2009. Carbon (1s) NEXAFS spectroscopy of biogeochemically relevant reference organic compounds. Soil Sci. Soc. Am. J. 73: 1817–1830.

Solomon, D., J. Lehmann, J. Kinyangi, B. Liang, and T. Schäfer. 2005. Carbon K-edge NEXAFS and FTIR-ATR spectroscopic investigation of organic carbon speciation in soils. Soil Sci. Soc. Am. J. 69: 107–119.

Spielvogel, S., J. Prietzel, and I. Kögel-Knabner. 2008. Soil organic matter stabilization in acidic forest soils is preferential and soil type-specific. Eur. J. Soil Sci. 59: 674–692.

Stanford, G., M.H. Frere, and D.H. Schwaninger. 1973. Temperature coefficient of soil nitrogen mineralization. Soil Sci. 115: 321–323.

Stanford, G., and S.J. Smith. 1972. Nitrogen mineralization potentials of soils. Soil Sci. Soc. Am. J. 36: 465–472.

Steenwerth, K., and L. Jackson. 2002. Soil microbial community composition and land use history in cultivated and grassland ecosystems of coastal California. Soil Biol. Biochem. 34: 1599–1611.

Stevenson, F.J. 1994. Humus Chemistry: Genesis, Composition, Reactions. 2nd ed. John Wiley & Sons, Toronto, ON.

Stewart, C.E., J.C. Neff, K.L. Amatangelo, and P.M. Vitousek. 2011. Vegetation effects on soil organic matter chemistry of aggregate fractions in a Hawaiian forest. Ecosystems 14: 382–397.

Stöhr, J. 1992. NEXAFS Spectroscopy. Springer, New York, NY.

Sutton, R., and G. Sposito. 2005. Molecular structure in soil humic substances: the new view. Environ. Sci. Technol. 39: 9009–9015.

Tabatabai, M., and A. Al-Khafaji. 1980. Comparison of nitrogen and sulfur mineralization in soils. Soil Sci. Soc. Am. J. 44: 1000–1006.

Taylor, J.P., B. Wilson, M.S. Mills, and R.G. Burns. 2002. Comparison of microbial numbers and enzymatic activities in surface soils and subsoils using various techniques. Soil Biol. Biochem. 34: 387–401.

Theng, B.K.G., G.J. Churchman, and R.H. Newman. 1986. The occurence of interlayer clay-organic complexes in two New Zealand soils. Soil Sci. 142: 262–266.

Thiele-Bruhn, S., P. Leinweber, K.-U. Eckhardt, H.K. Siem, and H.-P. Blume. 2014. Chernozem properties of Black Soils in the Baltic region of Germany as revealed by mass-spectrometric fingerprinting of organic matter. Geoderma 213: 144–154.

Thornley, J.H.M., and M.G.R. Cannell. 2001. Soil carbon storage response to temperature: a hypothesis. Ann. Bot. 87: 591–598.

Tisdall, J.M., and J.M. Oades. 1982. Organic matter and water-stable aggregates in soils. J. Soil Sci. 33: 141–163.

Trinsoutrot, I., S. Recous, B. Bentz, M. Linères, D. Chèneby, and B. Nicolardot. 2000. Biochemical quality of crop residues and carbon and nitrogen mineralization kinetics under nonlimiting nitrogen conditions. Soil Sci. Soc. Am. J. 64: 918–926.

Urbanová, M., J. Šnajdr, V. Brabcová, V. Merhautová, P. Dobiášová, T. Cajthaml, D. Vaněk, J. Frouz, H. Šantrůčková, and P. Baldrian. 2014. Litter decomposition along a primary post-mining chronosequence. Biol. Fertil. Soils 50: 827–837.

Urquhart, S.G., and H. Ade. 2002. Trends in the carbonyl core (C 1S, O 1S) $\rightarrow \pi^*_{C=O}$ transition in the near-edge X-ray absorption fine structure spectra of organic molecules. J. Phys. Chem. B 106: 8531–8538.

Vairavamurthy, A., and S. Wang. 2002. Organic nitrogen in geomacromolecules: insights on speciation and transformation with K-edge XANES spectroscopy. Environ. Sci. Technol. 36: 3050–3056.

Vancampenhout, K., B. De Vos, K. Wouters, R. Swennen, P. Buurman, and J. Deckers. 2012. Organic matter of subsoil horizons under broadleaved forest: highly processed or labile and plant-derived? Soil Biol. Biochem. 50: 40–46.

Waksman, S.A. 1936. Humus: origin, chemical composition and importance in nature. Williams and Wilkins, Baltimore, MD.

Wallenstein, M.D., M.L. Haddix, E. Ayres, H. Steltzer, K.A. Magrini-Bair, and E.A. Paul. 2013. Litter chemistry changes more rapidly when decomposed at home but converges during decomposition–transformation. Soil Biol. Biochem. 57: 311–319.

Wang, K., and B. Xing. 2005. Structural and sorption characteristics of adsorbed humic acid on clay minerals. J. Environ. Qual. 34: 342–349.

Wattel-Koekkoek, E.J.W., P.P.L. van Genuchten, P. Buurman, and B. van Lagen. 2001. Amount and composition of clay-associated soil organic matter in a range of kaolinitic and smectitic soils. Geoderma 99: 27–49.

Watts, B., L. Thomsen, and P.C. Dastoor. 2006. Methods in carbon K-edge NEXAFS: experiment and analysis. J. Electron Spectros. Relat. Phenomena 151: 105–120.

Wershaw, R.L. 1986. A new model for humic materials and their interactions with hydrophobic organic chemicals in soil-water or sediment-water systems. J. Contam. Hydrol. 1: 29–45.

Wershaw, R.L. 2004. Evaluation of conceptual models of natural organic matter (humus) from a consideration of the chemical and biochemical processes of humification. Scientific Investigations Report 2004-5121. U.S. Geological Survey, Reston, VA.

Wessels, J.G.H., and J.H. Sietsma. 1981. Fungal cell walls: a survey. p. 352–394. *In* Tanner, W., Loewus, F.A. (eds.), Encyclopedia of Plant Physiology. Plant Carbohydrates II. Springer, Berlin.

Wickings, K., A.S. Grandy, S.C. Reed, and C.C. Cleveland. 2012. The origin of litter chemical complexity during decomposition. Ecol. Lett. 15: 1180–1188.

Wilcken, H., C. Sorge, and H.-R. Schulten. 1997. Molecular composition and chemometric differentiation and classification of soil organic matter in Podzol B-horizons. Geoderma 76: 193–219.

Williams, J.W., B. Shuman, and P.J. Bartlein. 2009. Rapid responses of the prairie-forest ecotone to early Holocene aridity in mid-continental North America. Glob. Planet. Change 66: 195–207.

Wojdyr, M. 2010. Fityk: a general-purpose peak fitting program. J. Appl. Crystallogr. 43: 1126–1128.

Xu, X., Y. Zhou, H. Ruan, Y. Luo, and J. Wang. 2010. Temperature sensitivity increases with soil organic carbon recalcitrance along an elevational gradient in the Wuyi Mountains, China. Soil Biol. Biochem. 42: 1811–1815.

Yannikos, N., P. Leinweber, B.L. Helgason, C. Baum, F.L. Walley, and K.C.J. Van Rees. 2014. Impact of Populus trees on the composition of organic matter and the soil microbial community in Orthic Gray Luvisols in Saskatchewan (Canada). Soil Biol. Biochem. 70: 5–11.

Zaitlin, B., and M. Hayashi. 2012. Interactions between soil biota and the effects on geomorphological features. Geomorphology 157-158: 142–152.

Zang, X., J.D.H. van Heemst, K.J. Dria, and P.G. Hatcher. 2000. Encapsulation of protein in humic acid from a histosol as an explanation for the occurrence of organic nitrogen in soil and sediment. Org. Geochem. 31: 679–695.

Zogg, G.P., D.R. Zak, D.B. Ringelberg, D.C. White, N.W. MacDonald, and K.S. Pregitzer. 1997. Compositional and functional shifts in microbial communities due to soil warming. Soil Sci. Soc. Am. J. 61: 475–481.

APPENDIX

Table A.1 Soil profile descriptions from all sites along study climosequence.

Land Use	Site	Horizon[†]	Depth		Structure[‡]		Colour	pH	D_b	TC	OC	TN	OC:TN	Sand Fractions[‡‡]					Texture		
			Start	End	Class	Kind	(moist)							VCSa	CSa	MSa	FSa	VFSa	Sand	Silt	Clay
			— cm —						g cm^{-1}	— g kg^{-1} —				— % —					— % —		
Grassland	1	LF	-3	0	NA	NA	ND[§]	5.9	0.4	98.3	92.8	10.0	9.3	NA[§§]	NA	NA	NA	NA	NA[¶¶]	NA	NA
Grassland	1	Ah	0	9	C	SBK	10YR2/1	5.7	1.0	49.7	43.8	4.2	10.4	1	7	11	20	10	49	26	25
Grassland	1	AB	9	15	M	PR	10YR2/2	6.0	1.1	31.1	32.8	3.3	9.9	2	10	13	19	10	53	25	21
Grassland	1	Bmu1	15	40	C	SBK	10YR3/3	6.3	1.1	16.8	16.4	1.8	9.1	1	8	11	14	10	43	33	24
Grassland	1	Bmu2	40	54	C	SBK	10YR3/4	6.9	1.6	7.2	6.2	0.9	6.9	3	8	17	25	17	70	15	15
Grassland	1	Cca	54	80	C	SBK	10YR4/3	7.6	ND[¶]	8.5	4.7	0.7	6.7	3	13	18	23	9	65	22	13
Grassland	1	Ckcat1	80	101	NA	MA	10YR4/3	8.2	1.8	16.1	4.1	0.6	6.8	0	2	5	12	13	32	34	34
Grassland	1	Ckcat2	101	115+	C	SBK	2.5Y4/3	7.8	1.6	13.1	5.1	ND[#]	ND	1	7	11	16	6	42	35	23
Grassland	2	LFH	-4	0	NA	NA	ND	6.6	0.4	61.2	42.5	5.4	7.9	NA	NA	NA	NA	NA	NA	NA	NA
Grassland	2	Ah	0	12	C	SBK	10YR2/1	7.2	1.1	36.7	27.8	3.2	8.7	2	7	16	25	9	60	22	18
Grassland	2	Bmk	12	26	C	SBK	10YR3/3	7.6	1.4	27.0	19.4	2.5	7.8	3	13	17	21	5	56	22	22
Grassland	2	Ccak1	26	63	C	SBK	10YR6/3	8.0	1.5	37.0	8.6	1.1	7.8	1	6	13	20	7	46	29	26
Grassland	2	Ccak2	63	94+	C	SBK	2.5Y4/3	7.9	1.2	17.5	2.7	0.5	5.4	1	8	16	22	7	54	30	17
Grassland	3	F	-3	0	NA	NA	ND	6.1	0.5	77.4	75.0	7.1	10.6	NA	NA	NA	NA	NA	NA	NA	NA
Grassland	3	Ah	0	14	F	GR	10YR2/1	6.2	1.2	26.7	25.8	2.3	11.7	3	12	20	26	9	69	13	18
Grassland	3	Bm1	14	28	F	SBK	10YR4/4	7.2	1.8	13.8	13.7	1.1	12.5	3	14	21	20	6	64	20	16
Grassland	3	Bm2	28	44	F	SBK	10YR4/3	7.6	1.5	18.7	12.0	1.0	12.0	1	9	19	24	6	60	24	17
Grassland	3	Cca	44	85	F	SBK	10YR6/3	7.9	1.0	21.2	13.0	0.6	21.7	1	11	19	26	8	62	23	15
Grassland	3	Ck	85	100+	NA	SGR	10YR6/3	7.9	ND	10.1	3.6	0.3	12.0	1	10	29	28	7	74	19	7
Grassland	6	F	-6	0	NA	NA	ND	7.0	0.5	68.2	56.1	2.9	19.3	NA	NA	NA	NA	NA	NA	NA	NA
Grassland	6	Ah	0	14	F	GR	10YR2/2	7.1	1.3	22.3	20.1	2.0	10.1	1	11	25	29	6	73	16	11
Grassland	6	Bm	14	25	F	GR	10YR3/3	7.2	1.2	14.6	11.9	1.3	9.2	2	8	19	25	6	61	26	13
Grassland	6	Cca	25	71	NA	MA	10YR5/3	7.6	1.3	15.8	3.5	0.5	7.0	3	11	20	23	6	63	28	9
Grassland	6	Ck	71	104+	NA	SGR	2.5Y5/4	7.9	ND	10.1	1.4	0.2	7.0	3	14	23	24	5	70	25	5

(continued on next page)

Table A.1 – continued

Land Use	Site	Horizon†	Depth		Structure‡		Colour	pH	D_b	TC	OC	TN	OC:TN	Sand Fractions‡‡					Texture		
			Start	End	Class	Kind	(moist)							VCSa	CSa	MSa	FSa	VFSa	Sand	Silt	Clay
			— cm —						g cm^{-1}	— g kg^{-1} —				— % —					— % —		
Forest	1	LFH	-4	0	NA	NA	ND	6.4	0.4	185.0	179.3	13.5	13.3	NA	NA	NA	NA	NA	NA	NA	NA
Forest	1	Ah	0	6	C	SBK	10YR2/1	6.3	0.6	52.3	53.2	4.3	12.4	2	7	7	9	5	31	57	12
Forest	1	Ahe	6	10	C	ABK	10YR3/2	6.1	0.7	32.6	32.8	2.7	12.1	2	6	6	9	5	28	58	14
Forest	1	Ae	10	14	C	ABK	10YR5/2	5.9	1.0	13.6	13.1	1.3	10.1	2	6	5	8	7	28	61	11
Forest	1	Aeg	14	17	C	ABK	10YR5/2	5.8	0.7	4.6	4.8	0.7	6.9	1	4	4	6	8	23	66	11
Forest	1	Btg1	17	33	C	ABK	10YR4/2	5.8	0.7	7.2	7.5	1.0	7.5	0	2	5	8	7	21	59	20
Forest	1	Btg2	33	57	C	SBK	10YR5/2	5.5	1.1	5.3	5.3	0.9	5.9	0	1	2	5	6	14	55	31
Forest	1	IIBg	57	91	C	SBK	10YR4/2	6.4	ND	4.0	2.4	0.5	4.8	14	24	15	5	1	59	24	17
Forest	1	IIICgcak	91	110+	NA	MA	10YR4/2	7.4	1.6	8.0	2.1	ND	ND	1	5	9	15	5	37	35	28
Forest	2	LFH	-5	0	NA	NA	ND	6.4	0.3	228.4	231.0	14.2	16.3	NA	NA	NA	NA	NA	NA	NA	NA
Forest	2	Ah	0	8	C	SBK	10YR2/1	5.0	0.7	69.0	60.3	5.4	11.1	1	10	16	18	9	54	24	22
Forest	2	Ah/Ahe	8	14	C	SBK	10YR3/1	4.7	0.9	34.9	36.0	3.4	10.6	2	11	13	14	6	48	24	27
Forest	2	Ae	14	18	VC	PL	10YR5/3	6.0	1.4	10.0	9.9	1.4	7.1	1	9	16	18	6	50	36	14
Forest	2	Bt	18	69	C	SBK	10YR4/3	6.0	1.1	6.0	5.8	0.9	6.4	0	3	7	11	7	28	45	27
Forest	2	Ccak	69	120	C	SBK	2.5Y4/3	7.7	ND	13.8	2.3	0.5	4.6	1	8	18	22	6	55	28	16
Forest	2	Ccaktj	120	140+	NA	MA	2.5Y4/2	7.6	1.5	11.5	2.0	ND	ND	2	7	16	25	6	58	28	15
Forest	3	LF	-5	0	NA	NA	ND	5.7	0.2	329.6	305.6	21.5	14.2	NA	NA	NA	NA	NA	NA	NA	NA
Forest	3	Ah	0	8	F	GR	10YR3/2	4.9	1.0	41.1	39.6	3.2	12.8	3	11	17	23	8	63	21	17
Forest	3	Aej	8	16	F	PL	10YR5/3	5.0	1.3	8.5	8.4	0.9	9.3	1	7	15	23	12	58	28	14
Forest	3	Bt	16	36	M	SBK	10YR4/4	6.2	1.6	7.0	4.9	0.6	8.2	2	8	15	23	9	58	25	17
Forest	3	BC	36	48	M	ABK	10YR5/4	7.6	1.5	16.9	5.8	0.7	8.3	0	6	14	24	9	52	29	18
Forest	3	Cca1	48	64	M	ABK	10YR6/3	7.7	ND	22.9	5.1	0.6	8.5	0	3	12	21	9	46	33	22
Forest	3	Cca2	64	89	NA	SGR	10YR6/4	7.8	ND	20.2	3.3	0.4	8.3	0	6	13	21	7	48	31	21
Forest	3	Ck	89	99+	NA	SGR	10YR6/4	7.7	ND	14.4	1.3	0.2	6.5	1	9	17	24	7	57	29	14
Forest	4	F	-4	0	NA	NA	ND	5.9	0.3	189.3	137.5	11.5	12.0	NA	NA	NA	NA	NA	NA	NA	NA
Forest	4	Ahe	0	4.5	NA	SGR	10YR4/2	5.1	1.2	13.2	12.6	1.2	10.5	0	4	22	45	12	84	6	10
Forest	4	Bm	4.5	24.5	NA	SGR	10YR6/3	5.6	1.6	4.5	4.1	0.4	10.3	0	5	20	38	9	73	20	7
Forest	4	Bt	24.5	41.5	M	ABK	10YR4/4	5.2	1.3	3.5	3.3	0.3	11.0	0	5	20	37	8	70	17	13
Forest	4	C	41.5	95+	NA	SG	10YR5/4	5.8	ND	2.4	2.3	0.3	7.7	0	4	18	38	9	68	18	13

(continued on next page)

Table A.1 – continued

Land Use	Site	Horizon†	Depth		Structure‡		Colour	pH	D_b	TC	OC	TN	OC:TN	Sand Fractions‡‡					Texture		
			Start	End	Class	Kind	(moist)							VCSa	CSa	MSa	FSa	VFSa	Sand	Silt	Clay
			— cm —						g cm^{-1}	— g kg^{-1} —				— % —					— % —		
Forest	5	LF	-4	0	NA	NA	ND	5.9	0.2	226.0	173.1	15.7	11.0	NA	NA	NA	NA	NA	NA	NA	NA
Forest	5	Ah	0	4	F	GR	10YR2/1	5.1	1.2	25.9	27.6	2.6	10.6	1	9	16	21	11	58	28	13
Forest	5	Ahe	4	18	F	GR	10YR3/2	5.1	1.7	4.3	4.5	0.6	7.5	0	7	18	24	5	54	35	11
Forest	5	Bt1	18	25	F	PL	10YR5/3	5.3	1.5	4.2	4.1	0.6	6.8	2	11	13	23	6	52	25	24
Forest	5	Bt2	25	44	F	ABK	10YR4/4	5.3	1.6	3.1	2.9	0.5	5.8	1	8	20	27	6	62	19	20
Forest	5	Bm	44	101	F	SBK	10YR4/6	5.6	1.6	1.7	1.6	0.2	8.0	2	18	44	22	1	87	4	9
Forest	5	C	101	107	F	ABK	10YR4/3	6.9	ND	5.8	3.5	0.5	6.8	1	8	11	10	3	33	35	32
Forest	5	Cca	107	124+	F	SBK	10YR5/3	7.5	ND	17.9	3.0	0.5	6.0	0	1	8	17	3	30	35	35
Forest	6	LFH	-9	0	NA	NA	ND	6.0	0.1	302.3	303.1	19.1	15.9	NA	NA	NA	NA	NA	NA	NA	NA
Forest	6	Ahe	0	4	C	SBK	10YR3/1	5.2	0.9	78.9	71.3	4.8	14.9	0	6	16	24	10	56	31	13
Forest	6	Bm	4	20	C	ABK	10YR4/3	4.6	0.9	14.5	15.1	1.2	11.7	1	8	14	21	9	53	40	7
Forest	6	Bt1	20	67.5	M	SBK	10YR4/4	5.4	1.2	3.7	3.5	0.5	7.0	1	8	17	24	7	58	23	20
Forest	6	Bt2	67.5	100	C	SBK	2.5Y4/4	5.3	1.8	2.6	2.7	0.4	6.8	0	7	14	21	9	51	25	25
Forest	6	Cca	100	150+	NA	MA	2.5Y4/3	7.3	ND	14.0	3.4	0.4	8.5	1	7	13	21	8	51	36	14
Forest	7	LF	-4	0	NA	NA	ND	5.8	0.2	270.6	221.8	10.2	21.7	NA	NA	NA	NA	NA	NA	NA	NA
Forest	7	Ah	0	6	F	GR	10YR2/1	5.7	1.2	23.1	21.5	2.0	10.8	0	5	12	21	12	50	36	14
Forest	7	Ahe	6	12	F	GR	10YR3/2	5.6	1.4	9.2	7.1	0.9	7.9	1	8	16	20	4	48	41	10
Forest	7	Bt1	12	20	F	SBK	10YR5/3	5.7	1.6	6.7	6.8	0.7	9.7	1	6	13	19	5	44	42	14
Forest	7	Bt2	20	54	F	ABK	10YR4/4	6.3	1.5	5.1	4.0	0.5	8.0	1	8	14	20	5	48	34	18
Forest	7	BC	54	66	F	SBK	10YR7/3	7.4	1.2	4.9	2.5	0.4	6.3	9	16	22	20	4	73	16	11
Forest	7	Cca	66	95+	NA	SGR	10YR8/2	7.5	ND	6.3	2.3	0.3	6.7	2	13	22	25	6	68	21	11
Forest	8	LF	-7	0	NA	NA	ND	5.2	0.1	211.3	211.9	12.3	17.2	NA	NA	NA	NA	NA	NA	NA	NA
Forest	8	Ah	0	8	F	GR	10YR2/1	5.5	1.0	23.4	24.1	1.7	15.1	1	6	15	25	12	58	27	15
Forest	8	Aej	8	13	F	SBK	10YR3/3	5.6	1.3	9.6	8.7	0.8	10.9	1	17	17	22	7	56	27	17
Forest	8	Bm	13	17	F	SBK	7.5YR3/3	5.6	ND	5.6	4.8	0.6	8.0	2	8	12	17	6	45	37	18
Forest	8	Bt1	17	29	M	SBK	10YR3/4	5.3	1.2	3.3	3.4	0.3	11.3	1	8	14	24	9	55	21	23
Forest	8	Bt2	29	60	M	SBK	10YR4/4	5.8	1.1	2.6	2.5	0.1	25.0	1	9	20	26	7	64	18	18
Forest	8	C	60	105+	NA	MA	10YR5/4	6.3	ND	3.8	2.8	0.1	28.0	4	11	16	20	6	57	24	19

(continued on next page)

Table A.1 – continued

Land Use	Site	Horizon†	Depth		Structure‡		Colour	pH	D_b	TC	OC	TN	OC:TN	Sand Fractions‡‡					Texture		
			Start	End	Class	Kind	(moist)							VCSa	CSa	MSa	FSa	VFSa	Sand	Silt	Clay
			— cm —						g cm^{-1}	— g kg^{-1} —				— % —					— % —		
Forest	9	LFH	-7	0	NA	NA	ND	5.9	0.5	140.6	139.0	12.1	11.5	NA	NA	NA	NA	NA	NA	NA	NA
Forest	9	Ahe	0	2	C	SBK	10YR4/2	5.4	1.3	18.8	19.2	1.5	12.8	1	11	21	25	11	69	24	7
Forest	9	Aej	2	6	C	SBK	10YR5/2	5.3	1.3	6.4	4.7	0.6	7.8	0	7	18	25	7	57	37	6
Forest	9	Bm	6	20	C	SBK	10YR5/3	5.5	1.8	2.9	2.7	0.4	6.8	0	6	19	28	8	63	30	7
Forest	9	Bt	20	90	C	ABK	10YR4/3	5.5	1.7	3.9	3.6	0.5	7.2	1	6	10	19	7	42	30	28
Forest	9	Ccaktj	90	140	NA	MA	10YR4/3	7.4	ND	13.2	5.0	ND	ND	1	6	13	20	6	46	34	20
Forest	10	LF	-5.5	0	NA	NA	ND	5.6	0.2	342.5	346.7	16.5	21.0	NA	NA	NA	NA	NA	NA	NA	NA
Forest	10	Ah	0	2	F	GR	10YR3/2	4.5	1.1	36.9	31.9	1.8	17.7	0	4	12	20	15	51	40	9
Forest	10	Aej	2	11	F	PL	10YR4/2	4.4	1.7	6.6	5.8	0.5	11.6	1	6	13	17	6	43	55	2
Forest	10	Bt1	11	57	F	SBK	10YR5/3	4.9	1.5	3.9	4.3	0.4	10.8	3	8	13	18	8	49	30	20
Forest	10	Bt2	57	116+	F	ABK	10YR5/4	5.0	1.5	2.6	2.6	0.5	5.2	1	6	12	20	9	48	28	24
Forest	11	LFH	-3	0	NA	NA	ND	5.5	0.4	224.1	214.5	10.6	20.2	NA	NA	NA	NA	NA	NA	NA	NA
Forest	11	Ahe	0	2	F	PL	10YR4/1	5.4	1.1	20.8	20.4	1.2	17.0	1	9	16	24	15	64	31	5
Forest	11	Ae	2	13	F	PL	10YR7/1	5.2	1.5	3.0	2.6	0.2	13.0	2	9	15	18	6	50	44	6
Forest	11	Bt	13	73	M	ABK	10YR4/2	5.6	1.5	3.1	2.9	0.2	14.5	3	10	14	18	7	52	26	23
Forest	11	Cca	73	100+	NA	MA	10YR6/3	7.4	ND	5.3	3.8	0.2	19.0	1	8	14	20	9	52	25	22
Forest	12	FH	-7	0	NA	NA	ND	5.7	0.3	279.1	259.0	12.3	21.1	NA	NA	NA	NA	NA	NA	NA	NA
Forest	12	Ahe	0	5	C	SBK	10YR3/2	4.9	1.7	6.1	5.9	0.4	14.8	0	7	18	26	16	67	28	5
Forest	12	Aej	5	7	C	PL	10YR5/3	4.8	1.6	4.5	4.2	0.2	21.0	0	6	13	21	14	55	40	6
Forest	12	Bm1	7	33	C	SBK	10YR5/4	4.9	1.5	4.7	3.1	0.2	15.5	0	7	16	23	14	61	29	10
Forest	12	Bm2	33	48	C	SBK	10YR5/3	4.9	1.6	2.3	1.9	0.1	19.0	0	8	19	29	13	69	21	9
Forest	12	Bt	48	150	C	SBK	10YR4/3	5.4	1.6	3.1	2.7	0.2	13.5	1	8	16	21	8	54	23	23
Forest	12	Ccakjt	150	180+		MA	10YR4/3	7.3	ND	7.9	4.3	ND	ND	0	7	16	20	6	50	25	25
Cultivated	1	Ap	0	11	M	SBK	10YR3/1	6.5	1.3	35.1	32.3	3.4	9.5	13	20	14	8	3	58	26	16
Cultivated	1	Bt1	11	28	F	SBK	10YR3/4	6.2	1.6	7.2	5.5	1.1	4.9	13	20	14	8	4	58	15	28
Cultivated	1	Bt2	28	38	M	SBK	10YR4/3	6.2	1.9	5.3	4.8	0.9	5.3	17	18	9	6	3	52	17	31
Cultivated	1	Bt3	38	42	C	SBK	10YR3/4	6.2	1.7	2.9	3.0	0.8	4.0	12	27	22	7	2	70	9	21
Cultivated	1	Bm	42	52	NA	SGR	10YR5/4	6.5	1.5	2.3	2.3	0.5	4.6	3	20	32	12	4	71	11	18
Cultivated	1	BC	52	70	NA	SGR	10YR5/4	7.0	2.1	4.0	2.3	0.5	5.5	4	21	37	13	2	77	9	14
Cultivated	1	Cca	70	81+	NA	SGR	10YR6/4	7.5	2.2	12.0	1.1	0.4	2.8	34	29	19	7	1	90	6	4

(continued on next page)

Table A.1 – continued

Land Use	Site	Horizon†	Depth		Structure‡		Colour	pH	D_b	TC	OC	TN	OC:TN	Sand Fractions‡‡					Texture		
			Start	End	Class	Kind	(moist)							VCSa	CSa	MSa	FSa	VFSa	Sand	Silt	Clay
			— cm —						g cm^{-1}	— g kg^{-1} —				— % —					— % —		
Cultivated	2	Ap	0	10	F	SBK	10YR3/1	6.9	1.4	31.2	28.5	3.0	9.5	2	10	16	24	10	61	23	15
Cultivated	2	Ahk	10	25	M	SBK	10YR3/2	7.6	1.5	17.2	14.7	1.7	8.6	3	10	14	19	6	52	33	15
Cultivated	2	Bmk1	25	33	F	SBK	10YR4/3	8.0	1.5	17.3	9.1	1.4	6.5	12	13	10	12	5	55	21	24
Cultivated	2	Bmk2	33	42	M	SBK	10YR6/4	8.1	1.4	19.6	3.3	0.7	4.7	31	13	12	16	4	78	11	10
Cultivated	2	Bmk3	42	74	M	SBK	10YR6/3	8.1	1.8	17.7	2.3	0.4	5.8	2	9	15	26	11	61	30	9
Cultivated	2	Ck	74	110+	M	SBK	2.5YR5/3	8.0	2.0	15.1	1.6	0.4	4.0	4	7	13	22	8	56	32	12
Cultivated	3	Ap	0	11	F	SBK	10YR3/2	4.7	1.3	31.5	24.1	2.7	8.9	0	4	15	28	14	62	24	14
Cultivated	3	Bt1	11	40	F	SBK	10YR3/3	6.7	1.5	4.8	4.9	0.9	6.1	1	6	13	20	10	49	25	25
Cultivated	3	Bt2	40	60	F	SBK	10YR4/4	7.5	1.9	17.8	4.4	0.7	6.3	4	12	16	21	6	59	25	16
Cultivated	3	Cca	60	91+	NA	MA	10YR4/2	7.8	1.7	22.8	3.0	0.6	5.0	1	7	13	18	6	45	31	24
Cultivated	4	Ap	0	14	F	GR	10YR2/2	6.0	1.4	34.0	35.6	3.3	10.8	0	4	13	23	10	50	37	12
Cultivated	4	Ae	14	16	F	PL	10YR5/3	6.2	1.8	19.0	16.8	1.9	8.8	1	6	11	16	6	40	50	10
Cultivated	4	Bt1	16	39	M	SBK	10YR4/4	6.6	1.6	4.9	4.9	0.7	7.0	1	3	8	14	6	32	39	29
Cultivated	4	Bt2	39	70	M	SBK	10YR5/5	6.9	1.7	4.8	3.1	0.4	7.8	2	10	13	21	9	55	26	19
Cultivated	4	Cca	70	83+	NA	MA	10YR4/3	7.4	1.7	19.1	4.5	0.6	7.5	4	9	12	19	6	51	29	20
Cultivated	5	Ap	0	10	F	SBK	10YR2/2	6.0	1.5	22.9	21.0	1.9	11.7	1	7	15	23	7	53	37	10
Cultivated	5	Bt1	10	46	M	SBK	10YR3/3	6.5	1.8	3.7	3.7	0.5	7.4	5	12	14	15	5	52	27	22
Cultivated	5	Bt2	46	82	M	SBK	10YR4/4	6.3	1.8	2.7	2.4	0.4	6.0	3	14	21	11	3	52	26	22
Cultivated	5	Cca	82	96+	NA	MA	10YR4/3	7.1	1.8	17.6	2.7	0.3	9.0	0	1	11	23	4	39	33	28
Cultivated	6	Ap	0	14	F	SBK	10YR3/2	5.9	0.9	55.5	51.2	4.8	10.7	1	7	14	19	5	45	37	18
Cultivated	6	Bt	14	49	F	SBK	10YR5/4	6.4	1.6	9.4	8.3	1.0	8.3	1	6	11	16	5	40	39	21
Cultivated	6	Cca	49	85+	F	SBK	10YR7/3	7.9	2.0	22.9	3.4	0.4	8.5	6	14	16	16	4	55	32	13
Cultivated	7	Ap	0	17	F	SBK	10YR2/1	5.7	1.2	26.3	27.1	2.4	11.3	0	6	14	24	9	54	34	12
Cultivated	7	Bt	17	51	M	SBK	10YR4/4	7.0	1.5	7.8	7.5	0.9	9.4	2	9	16	20	5	52	25	23
Cultivated	7	Cca1	51	74	F	SBK	2.5YR5/3	8.2	1.6	18.5	2.9	0.4	7.3	2	13	16	18	4	49	31	20
Cultivated	7	Cca2	74	98+	F	SBK	2.5YR4/2	8.0	2.1	11.2	1.8	0.3	9.0	2	11	18	22	5	58	32	10

(continued on next page)

Table A.1 – continued

Land Use	Site	Horizon†	Depth		Structure‡		Colour	pH	D_b	TC	OC	TN	OC:TN	Sand Fractions‡‡					Texture		
			Start	End	Class	Kind	(moist)							VCSa	CSa	MSa	FSa	VFSa	Sand	Silt	Clay
			— cm —						g cm^{-1}	— g kg^{-1} —				— % —					— % —		
Cultivated	8	Ap	0	16.5	F	SBK	10YR2/2	5.4	1.3	24.0	22.5	2.3	9.8	1	6	12	17	11	47	42	11
Cultivated	8	AB	16.5	22.5	F	SBK	10YR3/3	5.8	1.5	5.5	5.2	0.8	6.5	1	6	8	9	4	29	55	16
Cultivated	8	Bt	22.5	42.5	F	SBK	10YR4/4	5.7	1.6	3.8	3.8	0.6	6.3	0	5	16	28	9	59	23	18
Cultivated	8	IIBm1	42.5	74.5	NA	SGR	10YR4/6	5.6	1.7	1.1	1.1	0.3	5.5	8	23	37	17	1	89	4	7
Cultivated	8	Bm2	74.5	114.5+	NA	SGR	2.5YR5/4	5.6	1.7	1.3	1.2	0.3	6.0	1	12	24	34	9	80	10	10
Cultivated	9	Ap	0	9	F	SBK	10YR3/3	6.3	1.1	23.3	21.6	2.4	9.0	4	8	15	21	10	57	21	22
Cultivated	9	Bt	9	46	M	SBK	10YR3/4	6.3	1.8	4.7	4.3	0.5	8.6	1	5	11	16	9	42	30	28
Cultivated	9	Cca	46	90+	M	SBK	2.5Y5/3	7.4	1.8	12.2	2.6	0.3	8.7	2	8	12	18	7	47	27	26
Cultivated	10	Ap	0	9	F	SBK	10YR3/2	6.4	1.2	18.4	18.9	1.5	12.6	1	9	20	30	11	70	20	10
Cultivated	10	Bt1	9	36	F	SBK	10YR4/4	5.8	1.8	3.2	3.3	0.9	3.7	5	14	18	19	6	61	20	18
Cultivated	10	Bt2	36	63	M	SBK	10YR4/3	6.4	1.9	2.6	3.2	0.1	32.0	2	10	16	20	8	56	23	21
Cultivated	10	Bt3	63	80	C	SBK	10YR4/2	6.2	2.0	2.9	3.5	0.0	–††	1	8	14	22	9	55	25	21
Cultivated	10	Bt4	80	90+	NA	MA	10YR4/4	7.4	1.8	10.1	2.8	0.1	55.0	2	7	14	20	8	52	29	19
Cultivated	11	Ap	0	16	F	SBK	10YR4/3	5.7	1.3	14.1	13.2	1.2	11.0	2	6	11	16	8	43	50	7
Cultivated	11	Ae	16	24	F	SBK	10YR7/3	6.1	2.1	2.9	5.0	0.3	16.7	0	6	16	26	12	60	32	9
Cultivated	11	Bt1	24	47	M	SBK	10YR4/3	5.9	2.0	2.8	2.9	0.2	14.5	4	10	15	18	6	52	22	26
Cultivated	11	Bt2	47	70	C	SBK	10YR5/4	5.1	2.0	2.7	2.7	0.2	13.5	2	12	14	20	7	53	25	22
Cultivated	11	Bt3	70	99	M	SBK	10YR5/3	4.9	1.7	3.1	3.6	0.3	18.0	4	8	13	19	8	53	24	23
Cultivated	11	Cca	99	102+	F	ABK	10YR5/2	7.1	1.6	5.8	3.1	0.2	15.5	0	4	12	19	7	44	32	24
Cultivated	12	Ap	0	10	F	GR	10YR2/2	4.9	1.2	40.3	35.3	2.4	14.7	2	8	17	24	9	60	30	10
Cultivated	12	Bm1	10	43	NA	SGR	10YR4/4	4.8	1.7	6.5	5.4	0.4	13.5	0	5	14	24	8	52	37	11
Cultivated	12	Bm2	43	73+	NA	MA	10YR5/4	5.1	2.0	2.4	2.0	0.1	20.0	2	10	18	27	11	67	22	12

† Soil classifying and soil sampling occurred in separate pits < 5 m apart. Presented here are the horizons and characteristics of the field classification and the physical and chemical properties of corresponding 5- or 10-cm soil increments from the adjacent sampling pit. Where horizons or horizon boundaries from the two pits did not directly correspond, the horizon best fitting the physical and chemical properties of the sample increments was used.

‡ Structure kind: ABK = angular blocky; SBK = subangular blocky; GR = granular; PL = platy; PR = prismatic; SGR = single grained; MA = massive. Structure class: F = fine; M = medium C = coarse; VC = very coarse. Structure class not applicable in SGR or MA kinds. Structure class and kind not applicable to litter samples.

§ Color of litter samples was not determined due to high variability within a single sample.

¶ Bulk density of deep horizons were not determined due to the variable volume of sample collected using a soil Auger.

Nitrogen content of deep horizons was assumed to be negligible and was therefore not determined.

†† Value approaches infinity due to extremely low (< 0.0 g kg^{-1}) nitrogen content.

‡‡ VCSa = very coarse sand; CSa = coarse sand; MSa = medium sand; FSa = fine sand; VFSa = very fine sand. Cumulative values equal the percentage of sand in a sample.

§§ Sand fractions only determinable in mineral soils.

¶¶ Particle size only determinable in mineral soils.